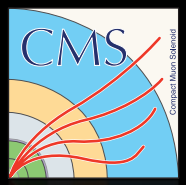

RWTH AACHEN UNIVERSITY

Probing the Higgs-charm Yukawa coupling with the CMS experiment: latest results and future prospects

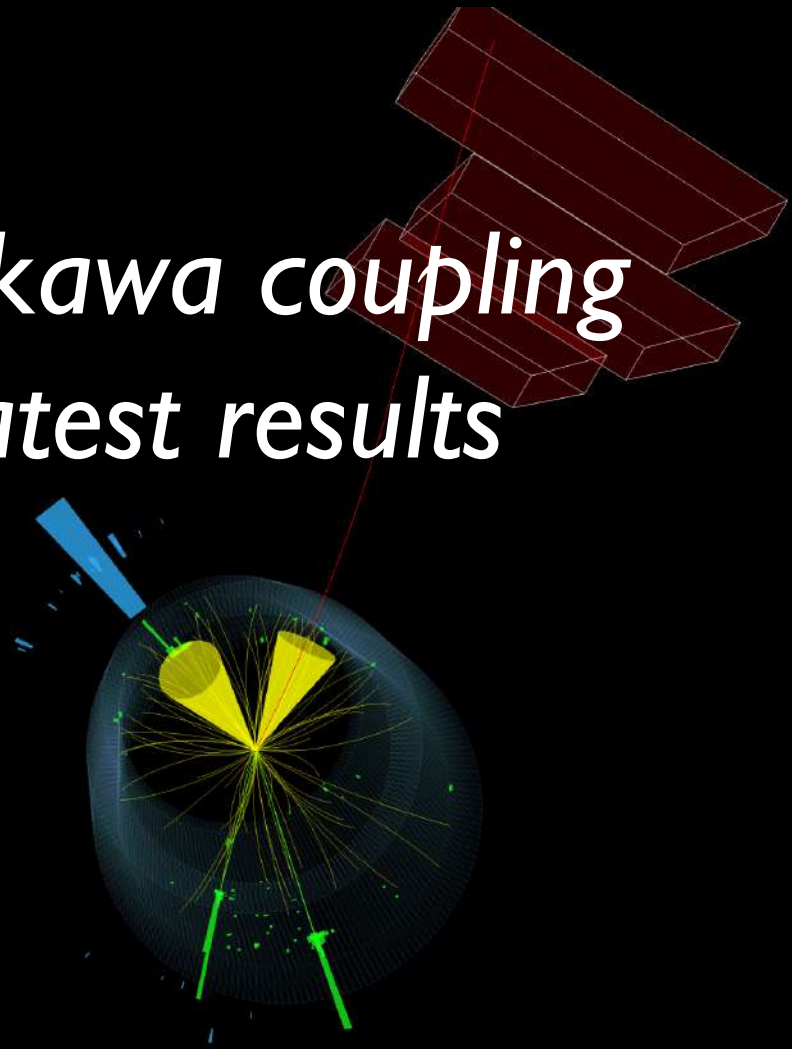

Luca Mastrolorenzo[1]

JETP Seminar
Fermi National Accelerator Laboratory, 29th April 2022

[1] Rheinisch-Westfälische Technische Hochschule (RWTH) Aachen University

The Standard Model of Particle Physics

- The SM is a non-abelian, locally gauge-invariant, quantum field theory (QFT), symmetric under local gauge transformation of the group:

$$U(1)_Y \otimes SU(2)_L \otimes SU(3)$$

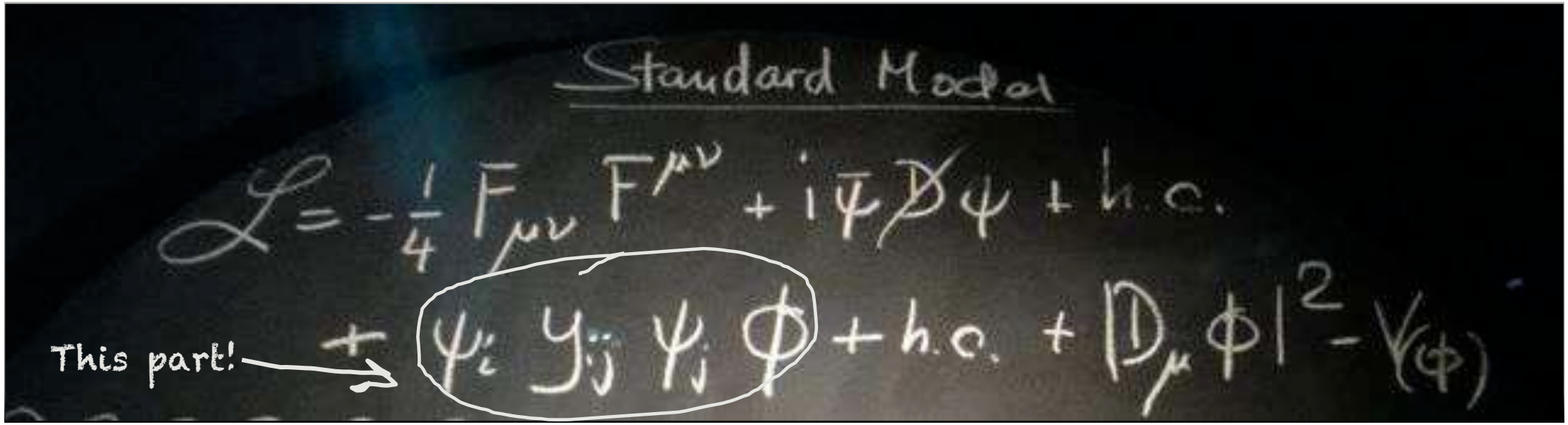

The Standard Model of Particle Physics

Matter Particles
Spin=1/2

- 3 families
- Quarks up/down, and electrons ➔ building bricks of ordinary matter
- Muon (μ) and Tau (τ) are unstable particles

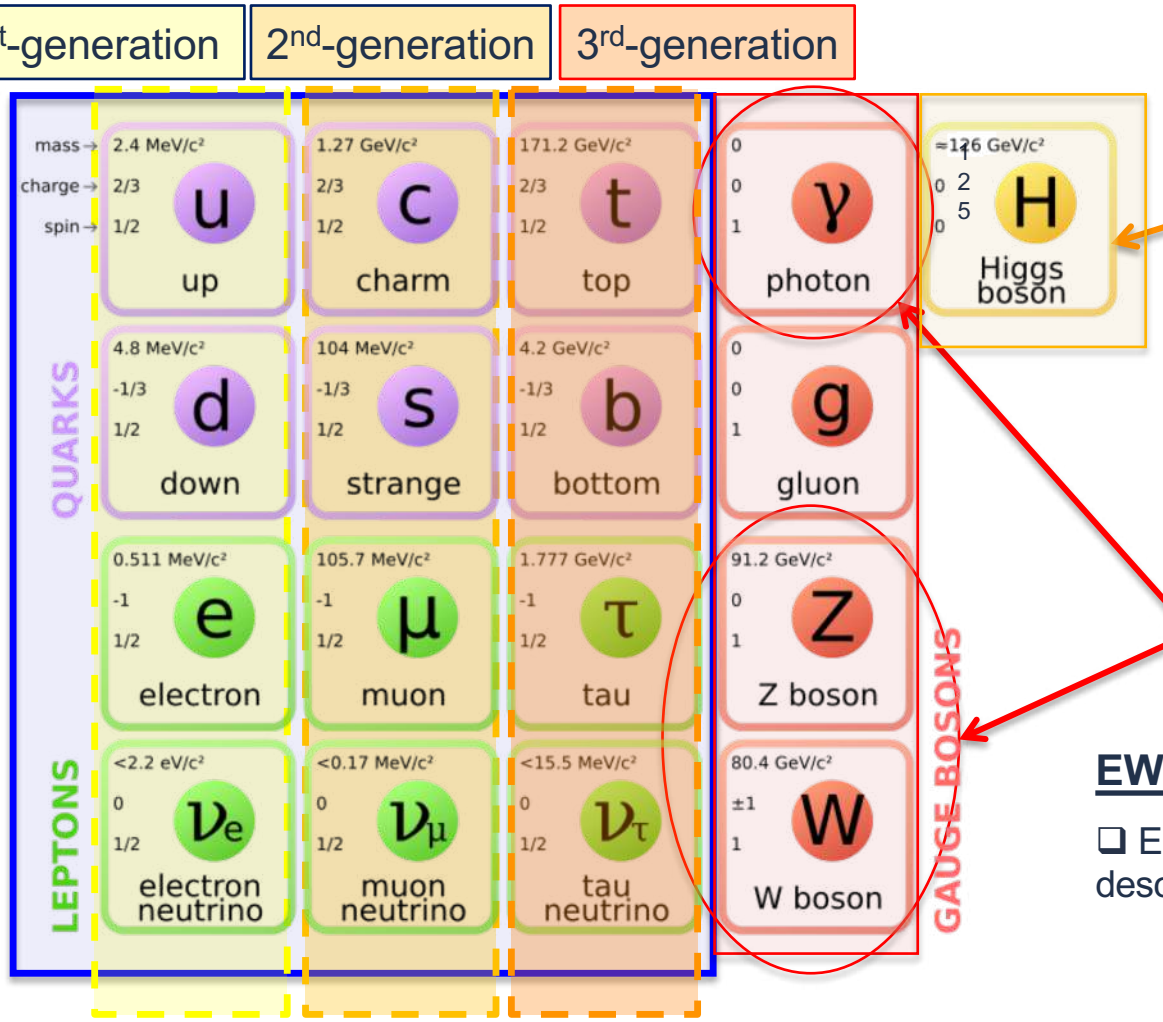

Higgs boson: mass generation

Interactions

Gauge bosons Spin=1

Focus on charm-quark

- 1974 by B. Richter, S. Ting
- 2nd generation quark
- m_c=1.3 GeV/c^2
- Transition rate 10^{-13} s

EWK unification

- EM and Weak interaction are described as a unique force

The Higgs mechanism in the Standard Model

- No explicit mass terms could be added in the SM lagrangian
  - Adding by ”hand” a mass term ($\sim m\psi\bar{\psi}$) would spoil the renormalizability of the theory
- Particles can gain mass through the Electroweak Symmetry Breaking Mechanism
- Introducing the Higgs potential: $V(\Phi) = -\mu^2\Phi^\dagger\Phi + \lambda\left(\Phi^\dagger\Phi\right)^2$
  - Invariant under local transformation $U(1)_Y \otimes SU(2)_L$
  - It must preserve Lorentz-invariance
  - It breaks $U(1)_Y \otimes SU(2)_L \rightarrow U(1)_{E.M.}$

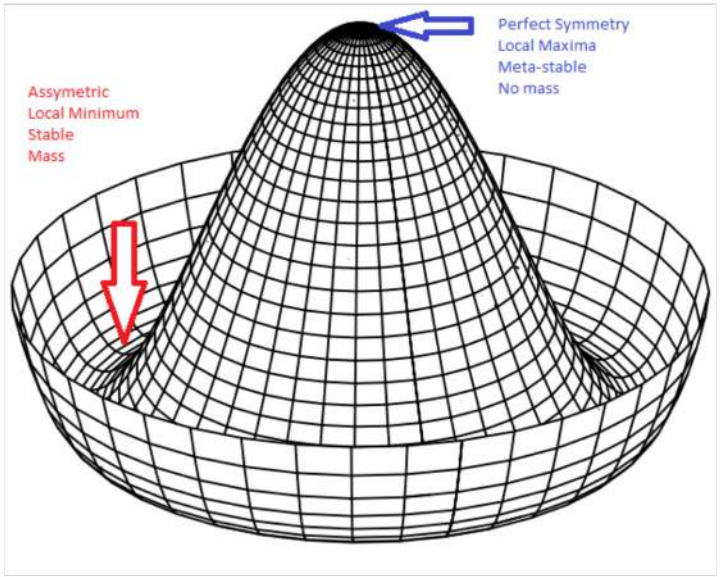

$$\Phi = \begin{pmatrix} \Phi^+ \\ \Phi^0 \end{pmatrix}_L \xrightarrow[\text{Small oscillations around the ground state}]{\text{Choice of a ground state}} \Phi = \begin{pmatrix} 0 \\ v + h(x) \end{pmatrix}$$

$$\Phi_0 = \begin{pmatrix} 0 \\ v \end{pmatrix} \rightarrow \text{Vacuum expectation value} \neq 0$$

Fermion masses in the Standard Model

- When the symmetry is spontaneously broken:
  - The **mass** terms for the **vector bosons** naturally appear: $m_W = \frac{vg}{2}$ and $m_Z = \frac{v\sqrt{g^2+g'^2}}{2}$
  - A **new massive particle emerges**: the Higgs boson, with a mass $m_H = \sqrt{2\lambda}v$
- … and what about the fermions masses? ➔ Introduction of Yukawa couplings

$$L_Y = y_l \bar{\chi}_L \phi l_R + y_u \bar{q}_L \tilde{\phi} u_R + y_d \bar{q}_L \phi d_R + \text{h.c.}$$

$$\phi = \begin{pmatrix} 0 \\ v+h \end{pmatrix} \rightarrow \frac{1}{\sqrt{2}} \begin{pmatrix} 0 \\ v+h \end{pmatrix}$$

$$L_Y = \frac{vy_l}{\sqrt{2}}\left(\bar{l}_L l_R + \bar{l}_R l_L\right) + \frac{vy_u}{\sqrt{2}}\left(\bar{u}_L u_R + \bar{u}_R u_L\right) + \frac{vy_l}{\sqrt{2}}\left(\bar{d}_L d_R + \bar{d}_R d_L\right)$$

$$y_i = \frac{m_i}{v}\sqrt{2}$$

Gauge invariant mass term

Yukawa coupling bring new non-gauge interactions!

The Higgs boson at the LHC

- Main Higgs boson production mechanisms at the LHC

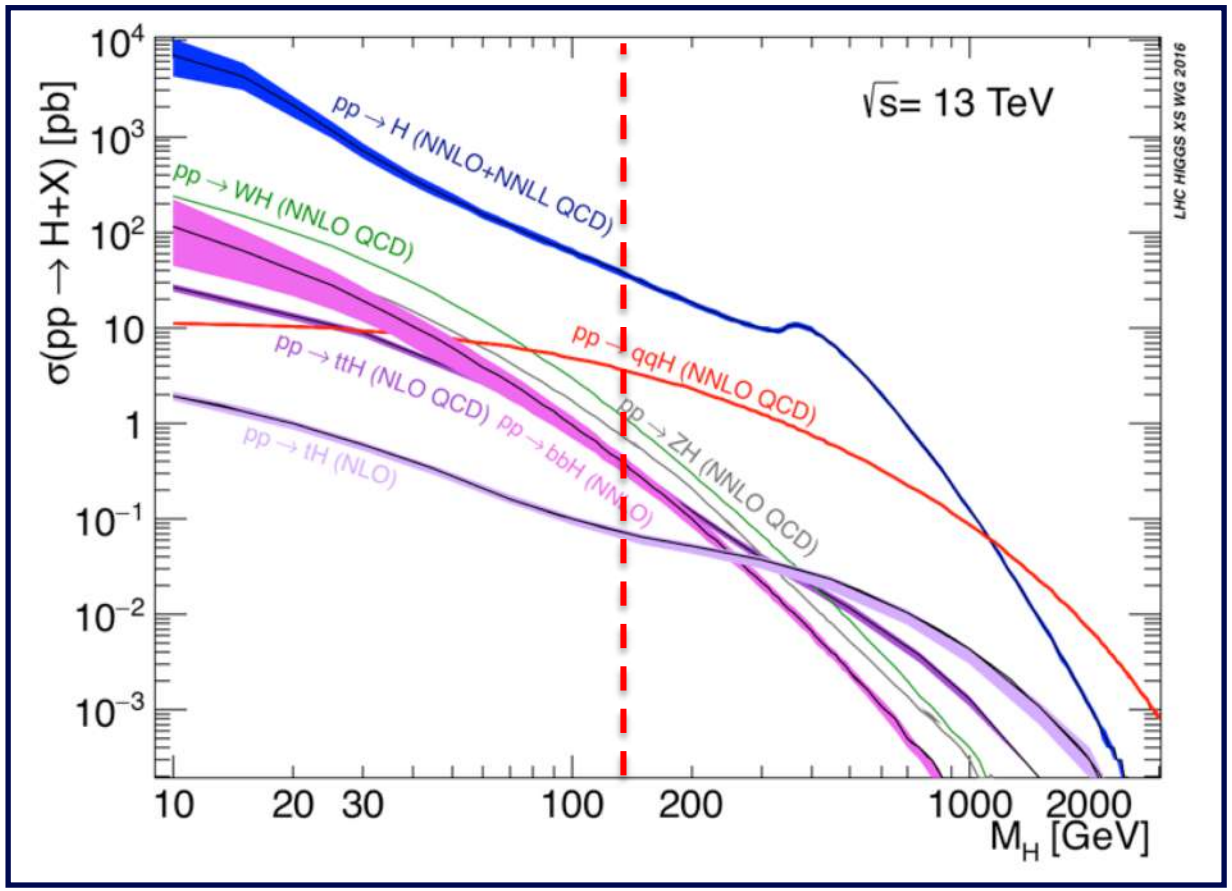

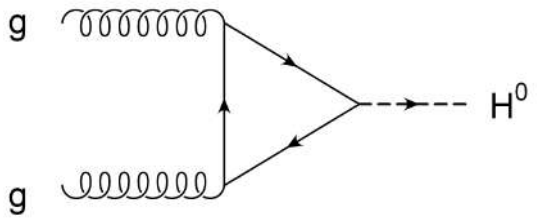

GGF: ~87%

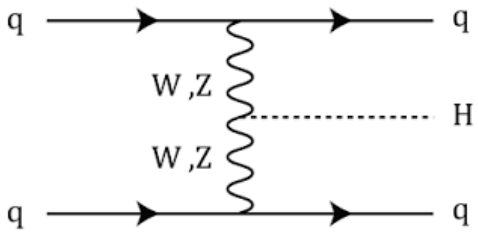

VBF: ~7%

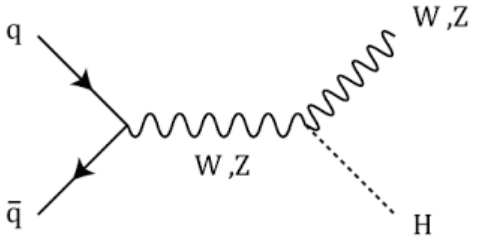

WH: ~3%
ZH: ~2%
ttH: ~1%

Discovery of the Higgs boson

- Discovery of the Higgs boson in 2012: A new chapter of particle physics

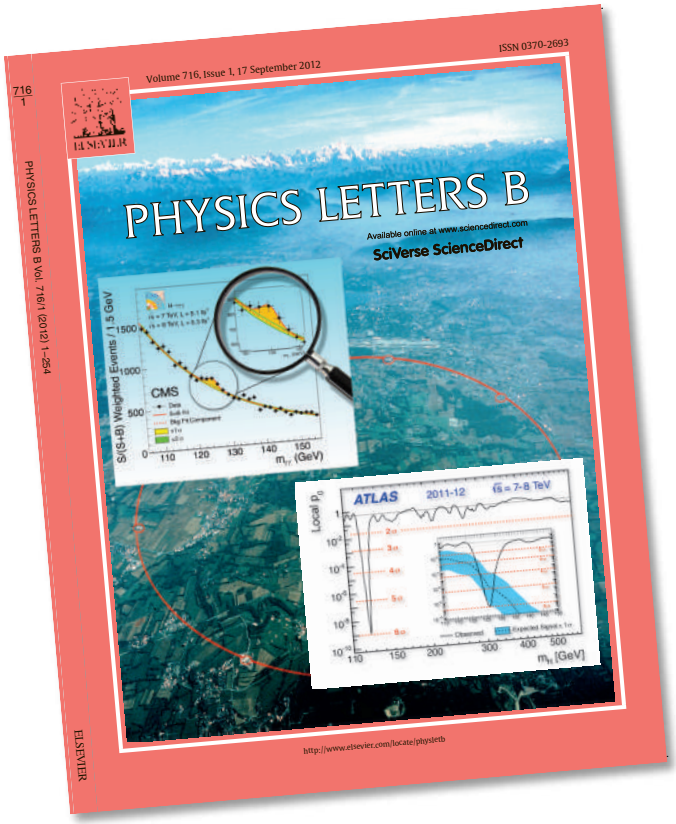

Understanding the Higgs boson

- Tremendous progress in our understanding of the Higgs boson in the past ten years
- Precision measurements of Higgs boson properties
- All couplings to 3rd generation fermions established

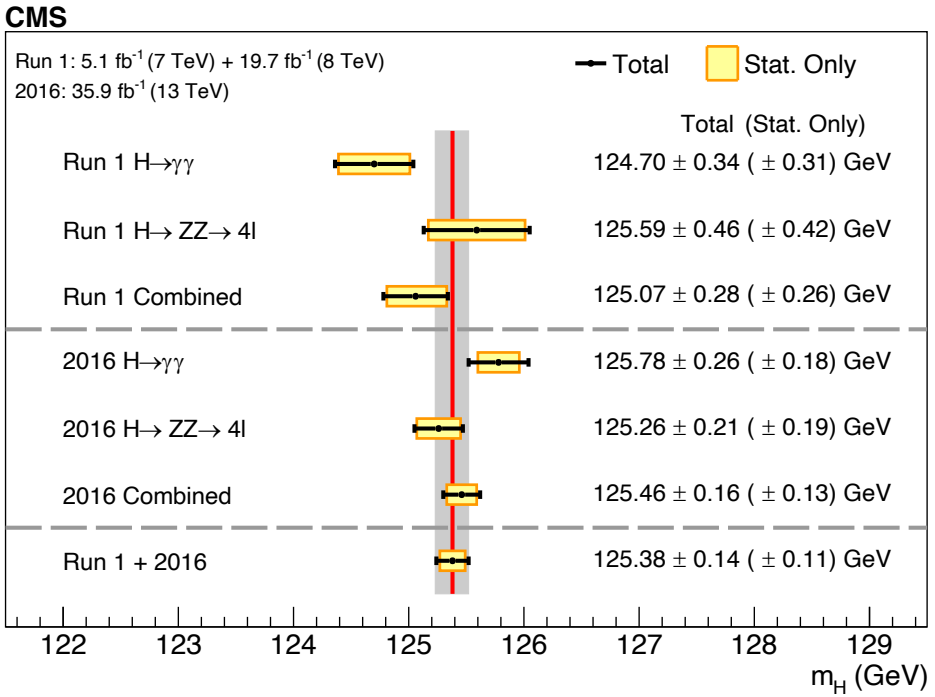

- Probing Higgs coupling to 2nd generation quarks
- BSM effects enhanced given small value of SM k_c

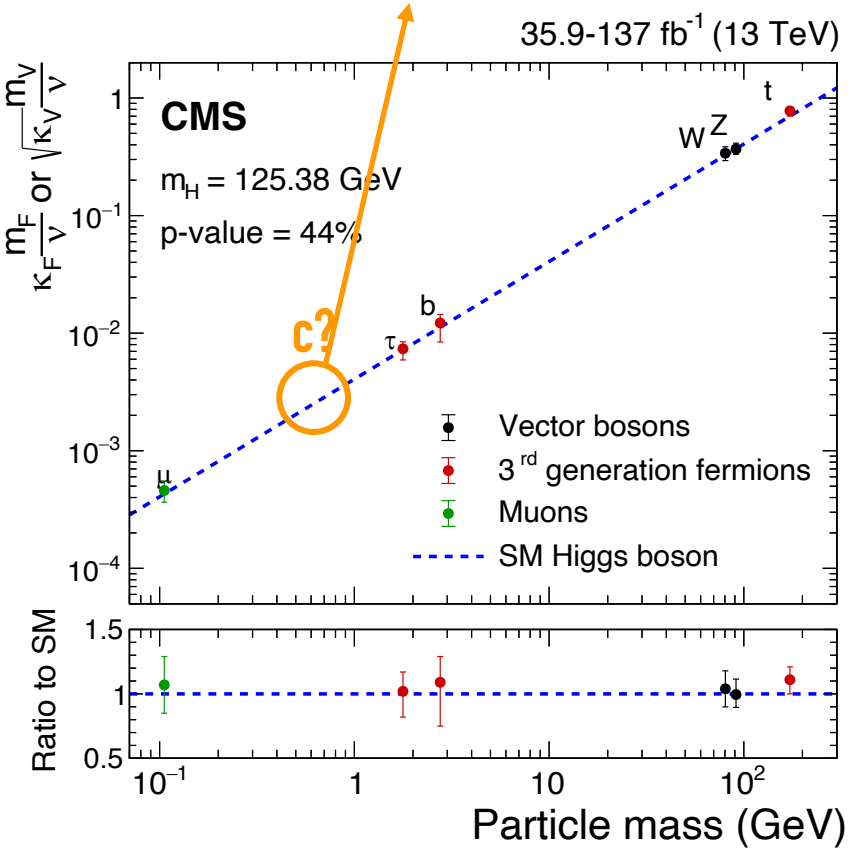

Probing the Higgs-charm coupling

- Several methods explored by CMS to probe the Higgs-charm Yukawa coupling (y_c)

Indirect constraint from Higgs kinematics

Phys. Rev. Lett. 118, 121801

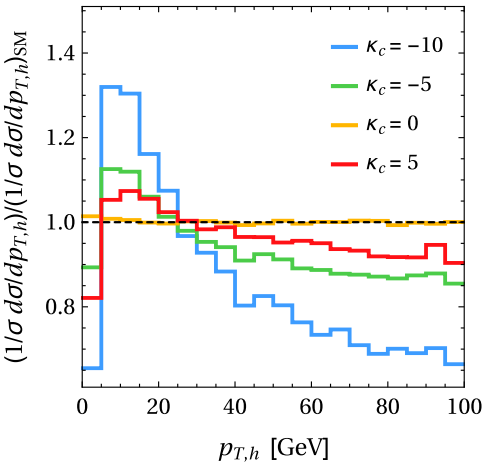

Variation of $p_T(H)$ shape as a function $\kappa_c = y_c/y_c^{SM}$

Phys. Lett. B 792 (2019) 369

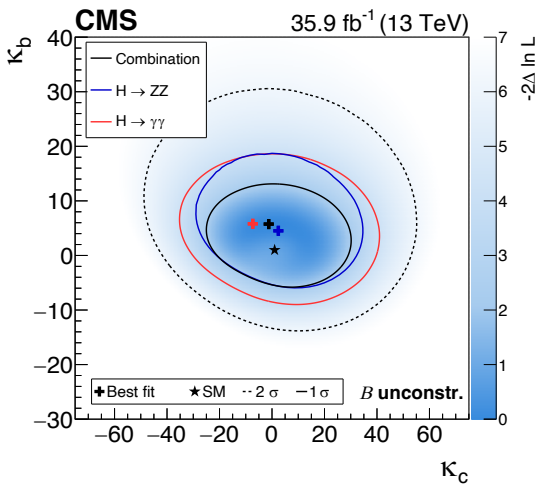

$-33 < \kappa_c < 38$ (obs.)

$-31 < \kappa_c < 36$ (exp.)

Search for exclusive H → J/Ψγ decays

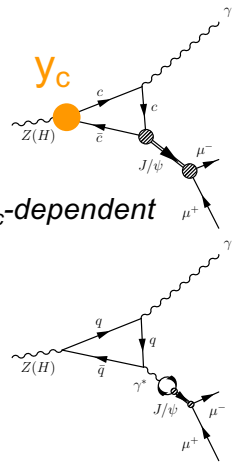

y_c-dependent

y_c-independent (dominant contribution)

[Phys.Rev.D 90 (2014) 11, 113010](#)
[JHEP 08 (2015) 012](#)
[Phys.Rev.D 95 (2017) 5, 054018](#)
[Phys.Rev.D 100 (2019) 5, 054038](#)

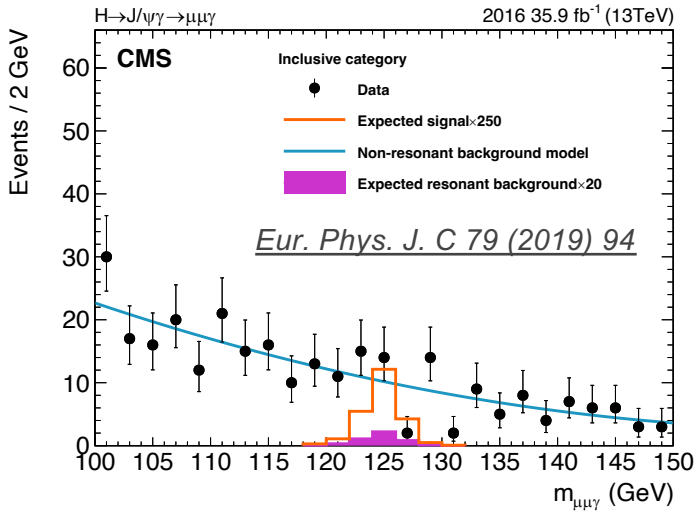

Eur. Phys. J. C 79 (2019) 94

$\mathcal{B}(H \to J/\Psi\gamma) < 220x$ SM(obs.)

$\mathcal{B}(H \to J/\Psi\gamma) < 170x$ SM(exp.)

Roughly translates to $\kappa_c < O(100)$

Corresponding ATLAS analyses: [ATLAS-CONF-2022-002](#); [Phys. Lett. B 786 (2018) 134](#).

Direct search for H → cc

- Search for H → cc decays: **directly sensitive to y_c, but very challenging**
  - Quite small branching ratio (x20 smaller than H → bb)
  - QCD (reducible) and V+jets (irreducible) background
  - Relatively poor invariant mass resolution

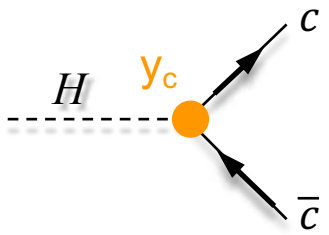

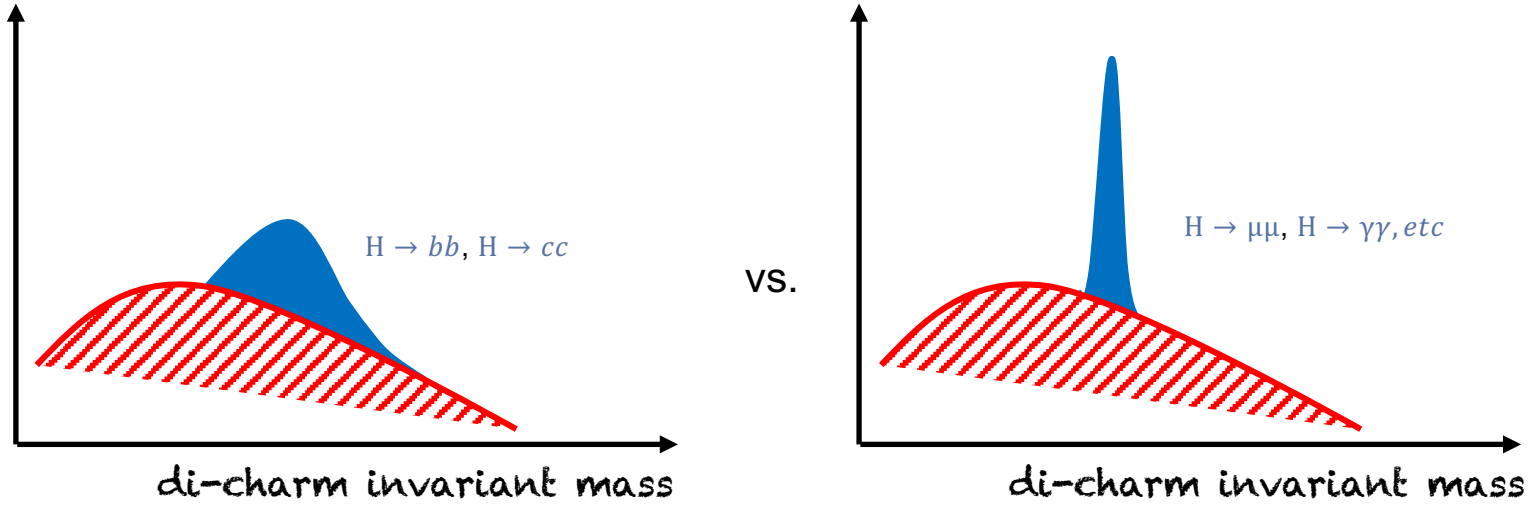

➔ **Charm quark identification + improvement of mass resolution play key roles**

Direct search for H → cc: Targeting VH production

- Main backgrounds
  - V + jets, single and pair production of top quarks, dibosons, VH(H → bb)

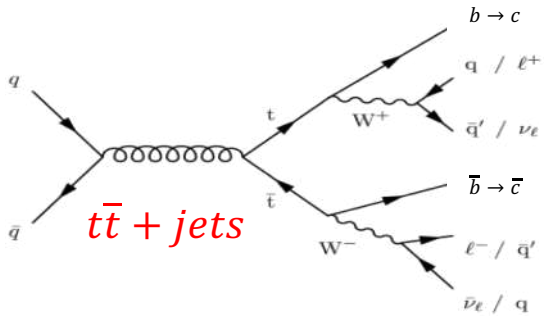

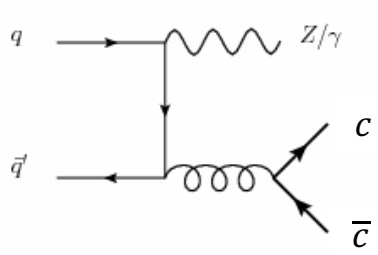

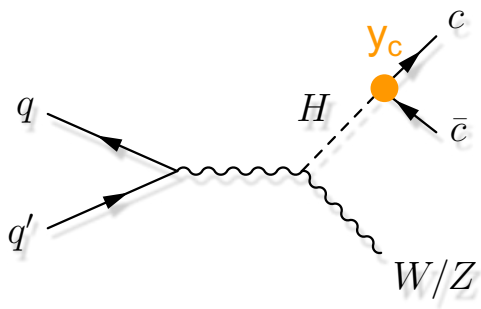

- Exploit associated VH production (V = W, Z)
  - Leptonic decays of V ➔ handle to trigger events
  - Boost of V ➔ Reduce backgrounds
  - Three channels: Z → νν (0L), W → ℓν (1L), Z → ℓℓ (2L) [ℓ = e, μ]
- Previous result (36 fb^{-1}): [JHEP 03 (2020) 131]
- **Today: result with the full Run 2 data set (138 fb^{-1})**

JHEP 03 (2020) 131

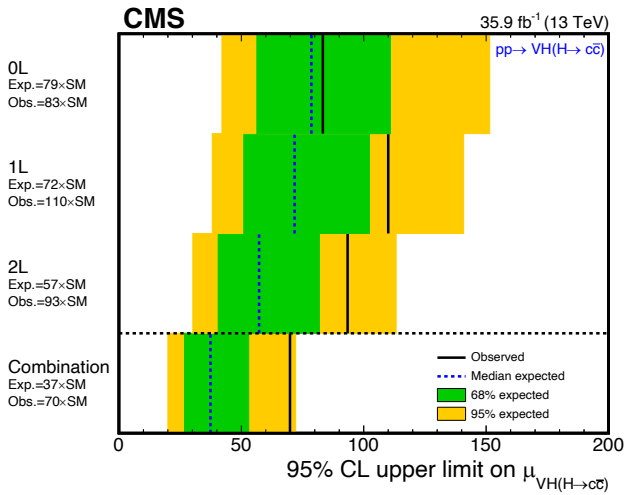

Corresponding ATLAS analysis: arXiv:2201.11428. See also recent LHC seminar by A. Chisholm.

Analysis overview

- $\Delta R(c,\bar{c}) \sim 2m(H)/p_T(H)$ ➔ Two complementary approaches for Higgs boson candidate reconstruction

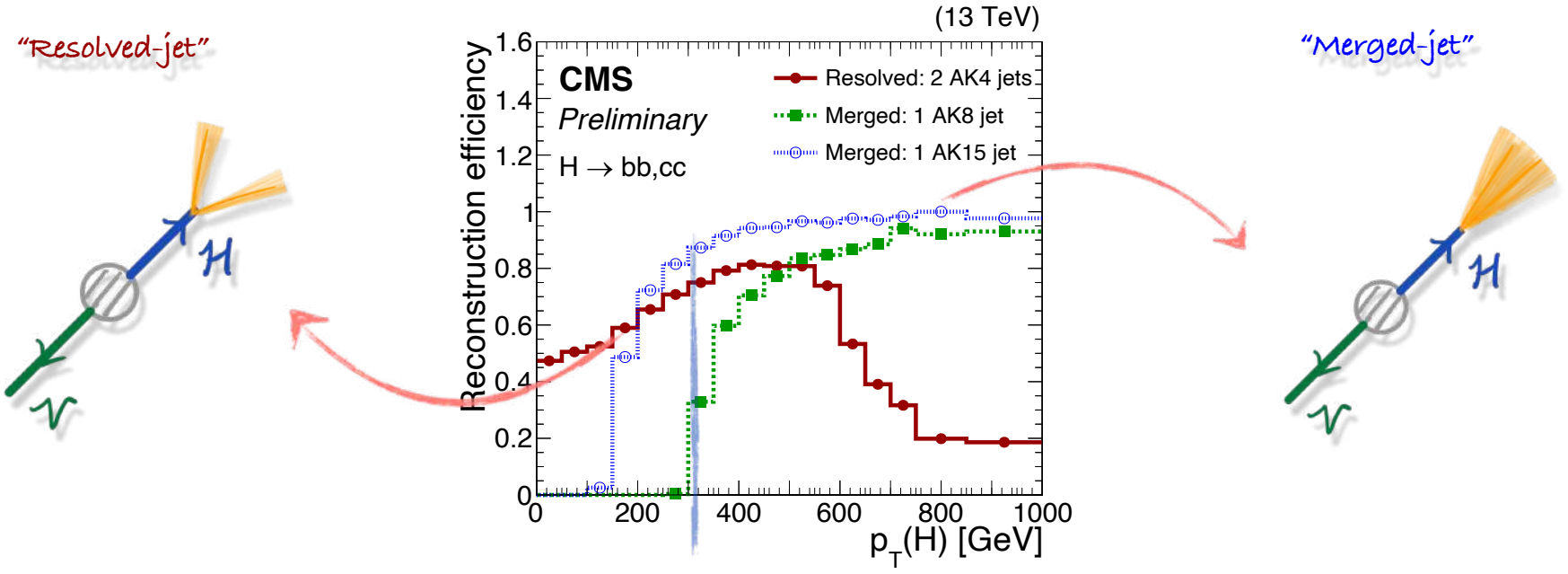

Resolved-jet topology

- reconstructs H → cc decay with two small-R jets (R=0.4, "**AK4**")
- probes the bulk (>95%) of the signal phase space

Merged-jet topology

- reconstructs H → cc decay with one large-R jets (R=1.5, "**AK15**")
- small signal acceptance (<5%) but higher purity
- better exploits the correlation between the two charm quarks

➔ The two topologies are made orthogonal via presence of AK15 jet with p_T > 300 GeV

CMS detector in a nutshell

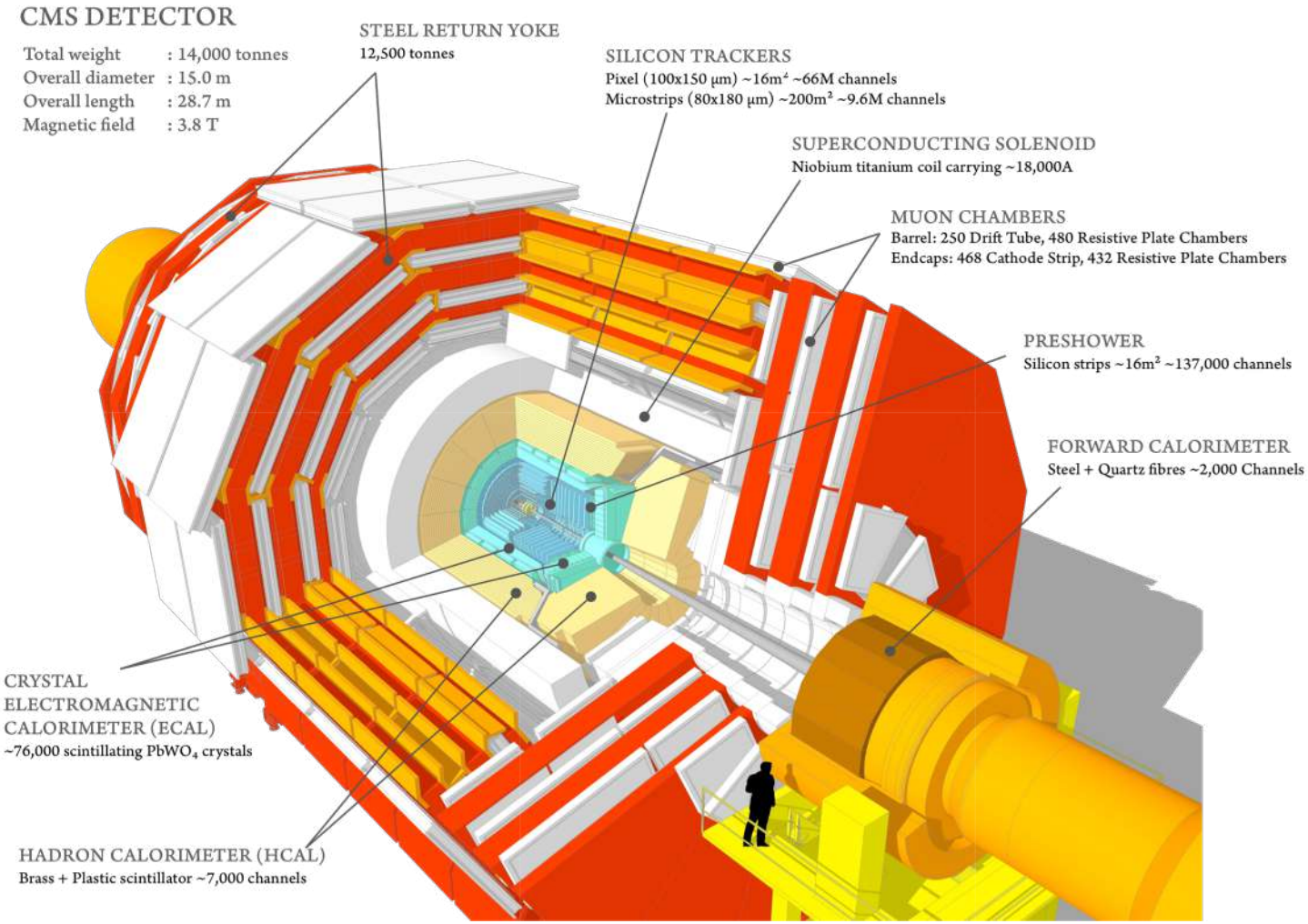

- A high quality central tracking system to give accurate momentum measurements
- A high resolution electromagnetic calorimeter to detect and measure electrons and photons
- A “hermetic” hadron calorimeter, designed to entirely surround the collision and prevent particles from escaping.
- A high performance system to detect and measure muons

Particle-Flow reconstruction

- Combines the information from the different CMS sub-detectors to identify all the stable particles in the event
  - Powerful approach for jet reconstruction and flavor tagging
  - Excellent energy and angular resolution
  - Each particle (PF candidate) contains a rich set of information from multiple sub-detectors → inputs to deep learning

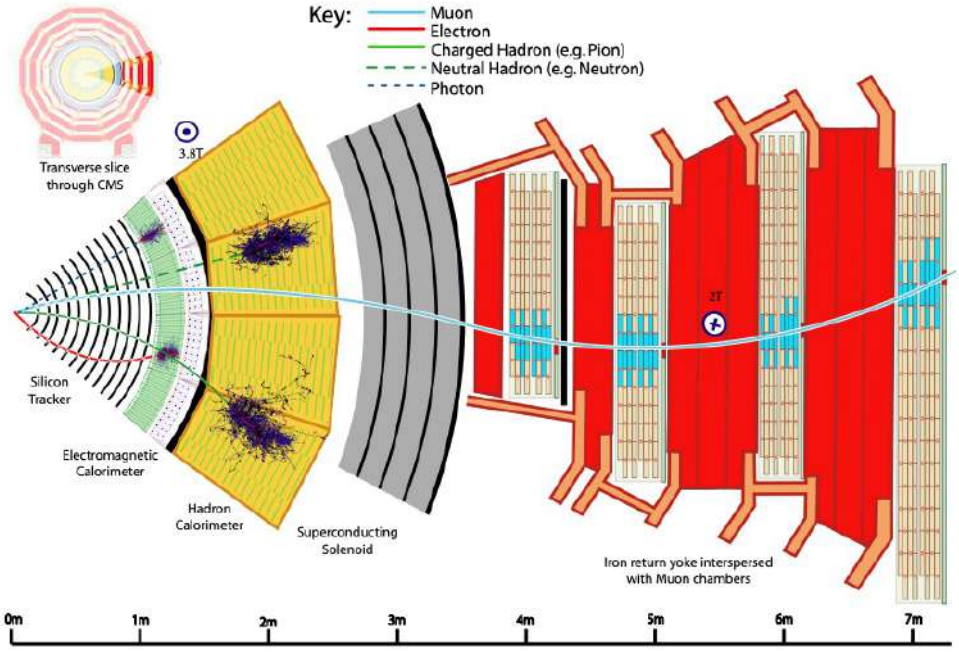

JINST 12 (2017) P10003

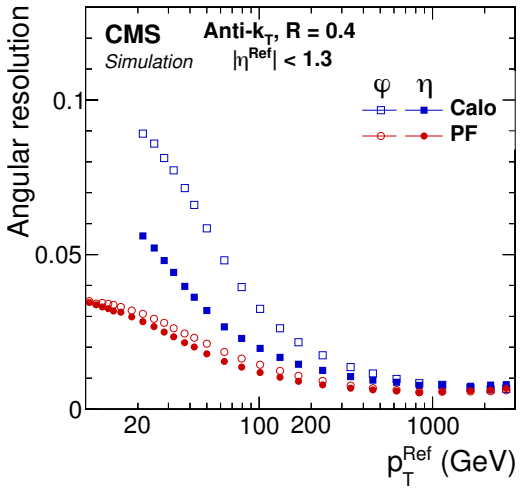

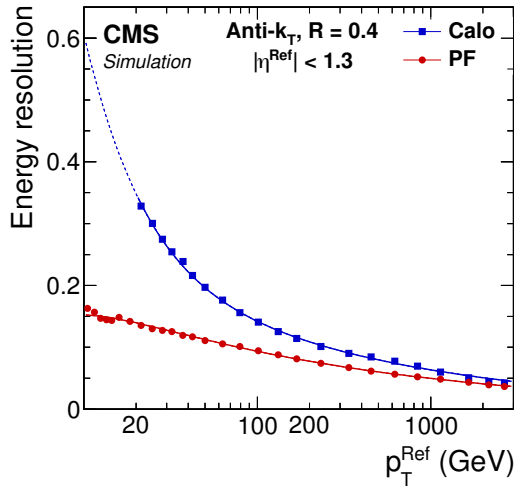

How to identify a charm jet?

- Bottom and charm initiated jets have quite peculiar characteristics
- During hadronization b- and c- quarks forms B and D mesons
- b- and c- quark can change flavor with the emission of a W
  - The W can decay leptonically → soft lepton inside the jet cone + MET (neutrino)
  - One or more secondary vertexes inside the cone

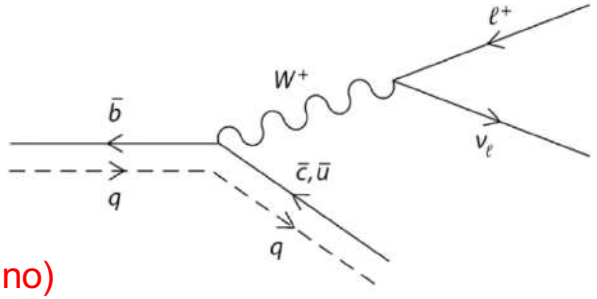

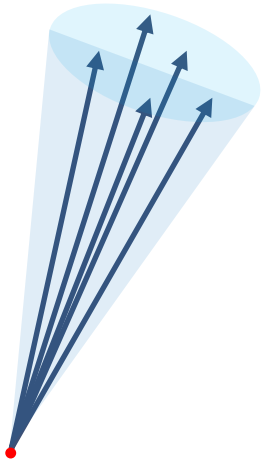

light-jet

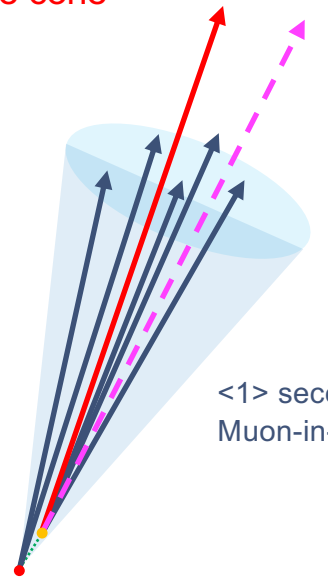

<1> secondary vertex
Muon-in-jet: ~8% of c-jets

c-jet

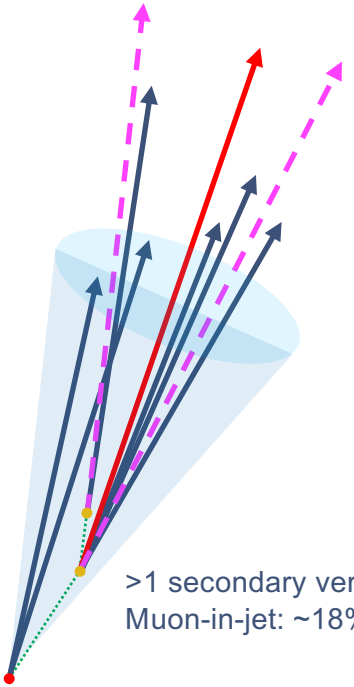

>1 secondary vertex
Muon-in-jet: ~18% of b-jets

b-jet

Merged-jet topology

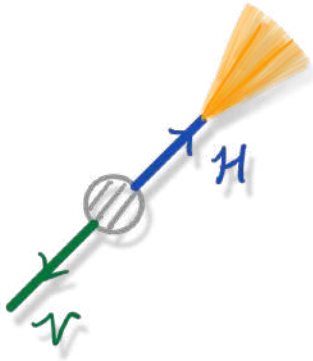

Overview of the merged-jet topology

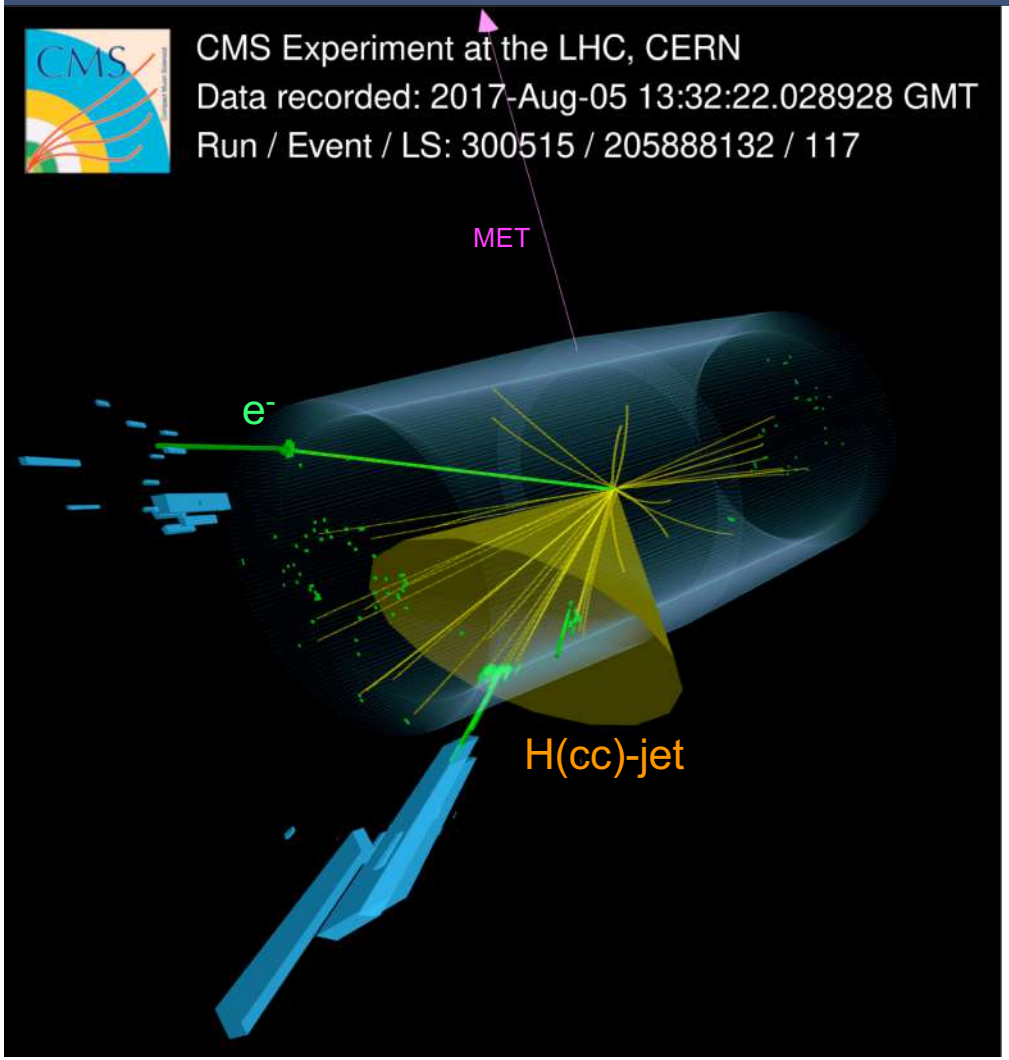

- Higgs candidate reconstruction
  - Select one AK15-jets with the highest p_T as H → cc jet
  - Identification of H → cc using ParticleNet tagger (dedicated calibration+mass sculpting mitigation)
  - Dedicated cc-jet mass regression for improved cc-jet mass scale and resolution
- Analysis strategy (three channels: 0L, 1L, 2L)
  - Control regions for background normalizations
  - Kinematic-BDT + cc-tagger score for categorization
  - Fit to soft-drop mass

H → cc identification

- Merged-jet topology: Higgs boson candidate reconstructed via a single large-R jet (p_T > 300 GeV)
- **ParticleNet** tagger used to identify H → cc decay ➔ Large improvement vs previous techniques
- Multi-class DNN boosted jet classifier ➔Trained targeting hadronic decays of a spin-0 particle X (X → bb, cc)

JHEP 03 (2020) 131 (2016 analysis)

DeepAK8 (DeepAK15) [JINST 15 (2020) P06005]

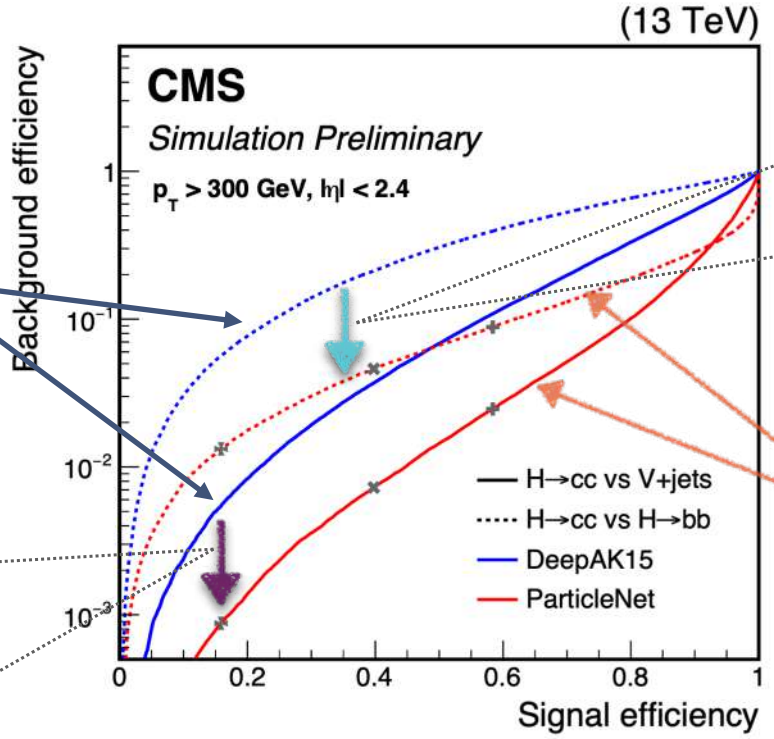

~5x better H→bb rejection

~5x better V+jet rejection

CMS-PAS-HIG-21-008 (Run 2 analysis)

ParticleNet [CMS-DP-2020-002]

>2x improvement in the final sensitivity

ParticleNet architecture

- New jet representation: “particle cloud”
  - treating a jet as an unordered set of particles, distributed in the η — φ space

- ParticleNet [Phys.Rev.D 101 (2020) 5, 056019]
  - graph neural network architecture adapted from DGCNN [arXiv:1801.07829]
  - Mass-decorrelation training to mitigate mass-sculpting (more in back-up)

Image from arXiv:2202.03772

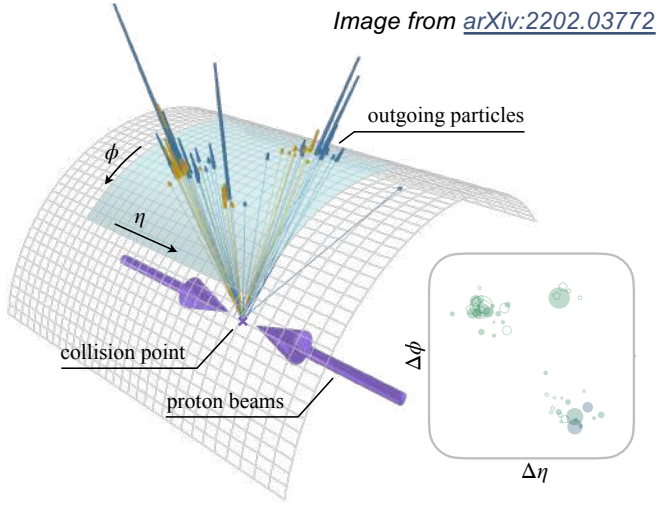

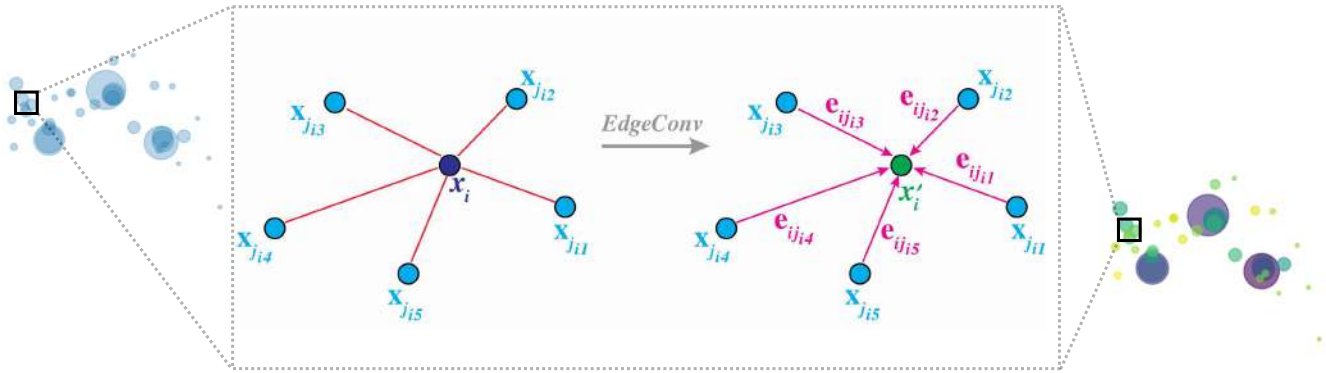

Performance on top quark tagging benchmark [SciPost Phys. 7, 014 (2019)]

	$1/\varepsilon_b$ at $\varepsilon_s = 30\%$
ResNeXt-50	1147 ± 58
P-CNN	759 ± 24
PFN	888 ± 17
ParticleNet-Lite	1262 ± 49
ParticleNet	$\mathbf{1615 \pm 93}$

Mass decorrelation

Plain training: no mass decorrelation

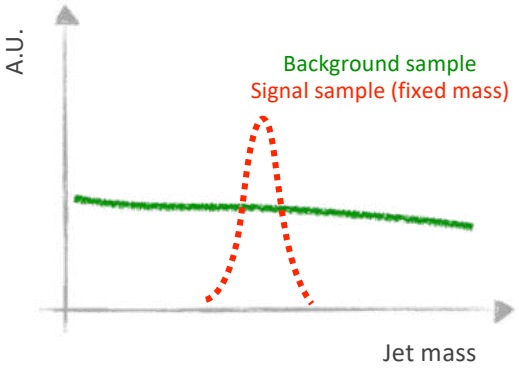

Background jet mass

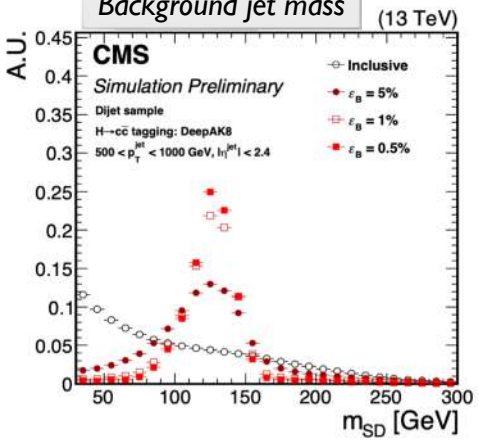

CMS-DP-2020-002

- "Mass sculpting": background jet mass shape becomes similar to signal after tagger selection

Mass decorrelation

Plain training: no mass decorrelation

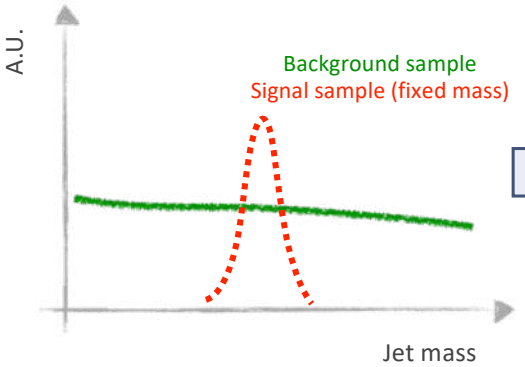

Mass-decorrelated training

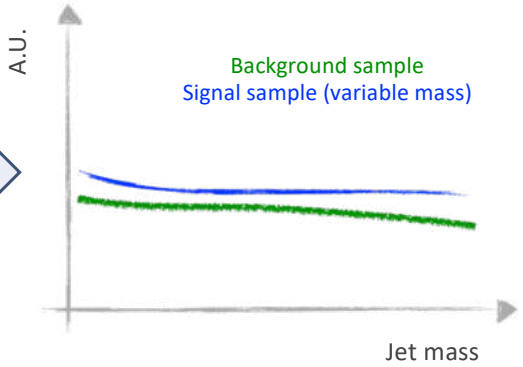

Background jet mass

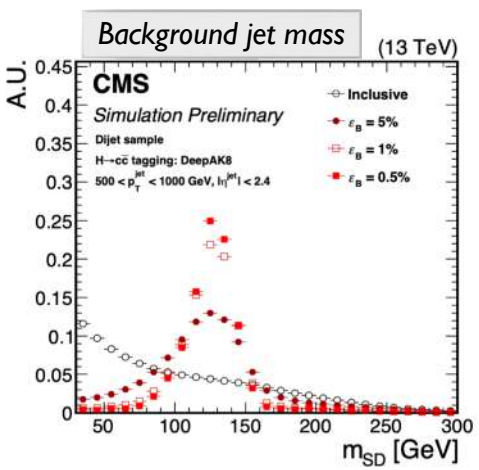

Background jet mass

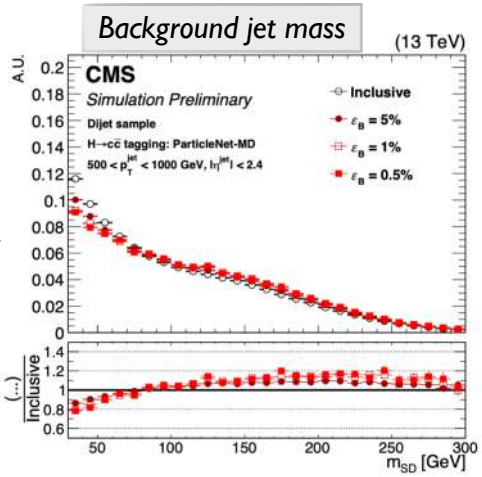

CMS-DP-2020-002

- "Mass sculpting": background jet mass shape becomes similar to signal after tagger selection
- New approach to prevent mass sculpting
  - using a special signal sample for training with a **flat mass spectrum** m(X) ∈ [15, 250] GeV
- Signal and background have the same (~flat) mass spectrum ➔ no sculpting in the training
- Performance loss due to mass decorrelation greatly reduced compared to the previous approach

Calibration of the cc-tagger

- Need to measure ParticleNet cc-tagging efficiency in data
  - No pure sample of H → cc jets (or even Z → cc) in data
  - Using g → cc in QCD multi-jet events as a proxy

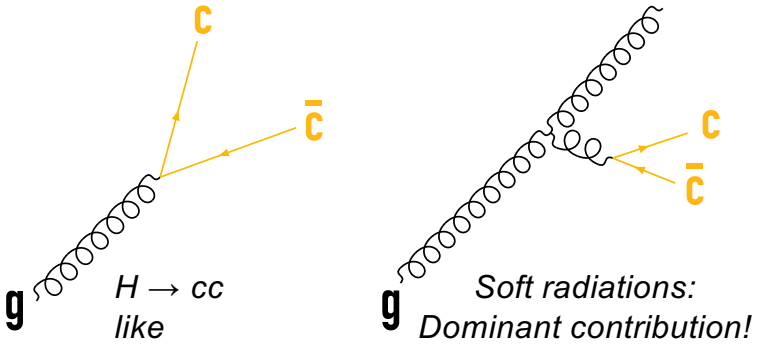

- Difficulty: select a phase-space in g → cc that resembles H → cc
  - Solution: BDT developed to distinguish hard 2-prong splittings from soft cc

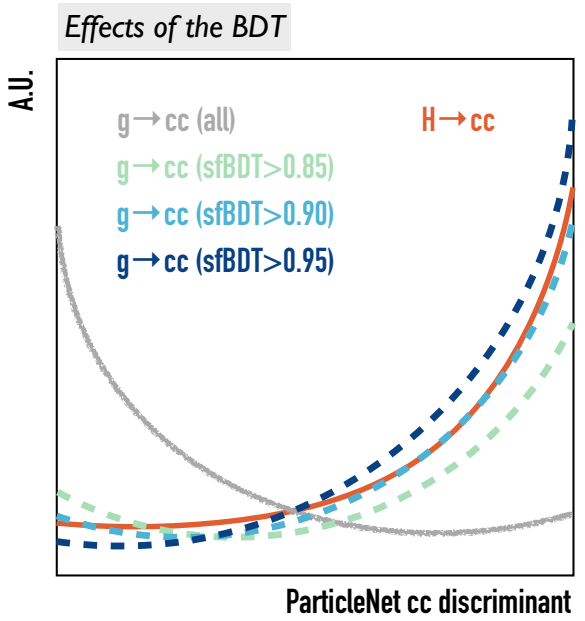

- Fit to the secondary vertex mass in the "passing" and "failing" regions simultaneously to extract the scale factors (typically 0.9-1.3)
  - three templates: cc (+ single c), bb (+ single b), light flavor jets
  - corresponding uncertainties are 20-30%

Large-R jet mass regression

- Jet mass: one of the most powerful observable to distinguish signal and backgrounds
- New ParticleNet-based regression algorithm to improve the large-R jet mass reconstruction

CMS DP-2021/017

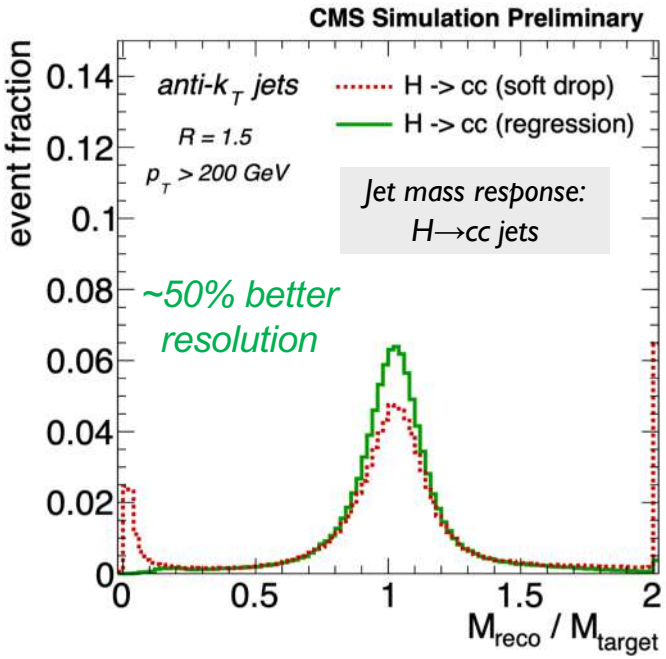

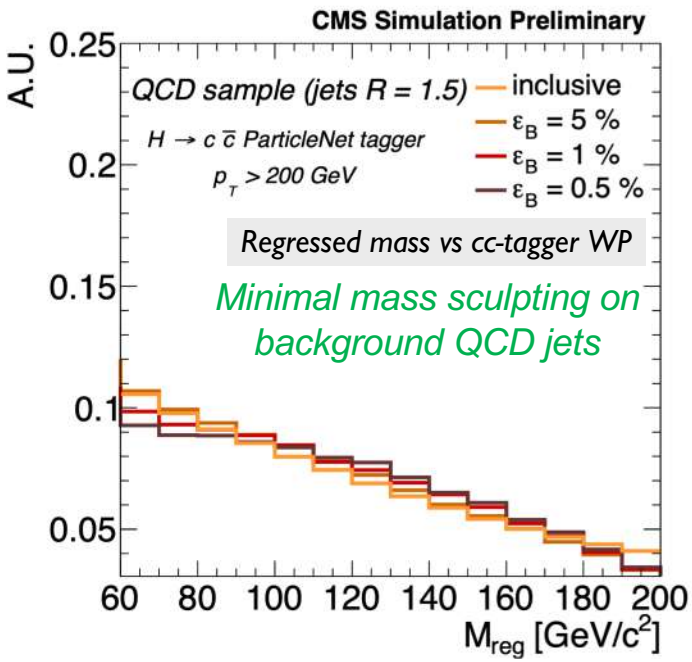

20 – 25% improvement in the final sensitivity

Analysis strategy – merged-jet topology

- Factorized approach for analysis design
  - event-level kinematic BDT developed in each channel to better suppress main backgrounds (V+jets, tt)
    - using only *event kinematics*, no intrinsic properties (e.g., mass/flavor) of the large-R jet
  - ParticleNet cc-tagger then used to define 3 cc-flavor enriched regions and reject light/bb-flavor jets
  - finally: fit to the ParticleNet-regressed large-R jet mass shape for signal extraction
- Kinematic BDT, ParticleNet cc-tagger and regressed jet mass largely independent of each other
  - Sand robust strategy for background estimation and signal extraction

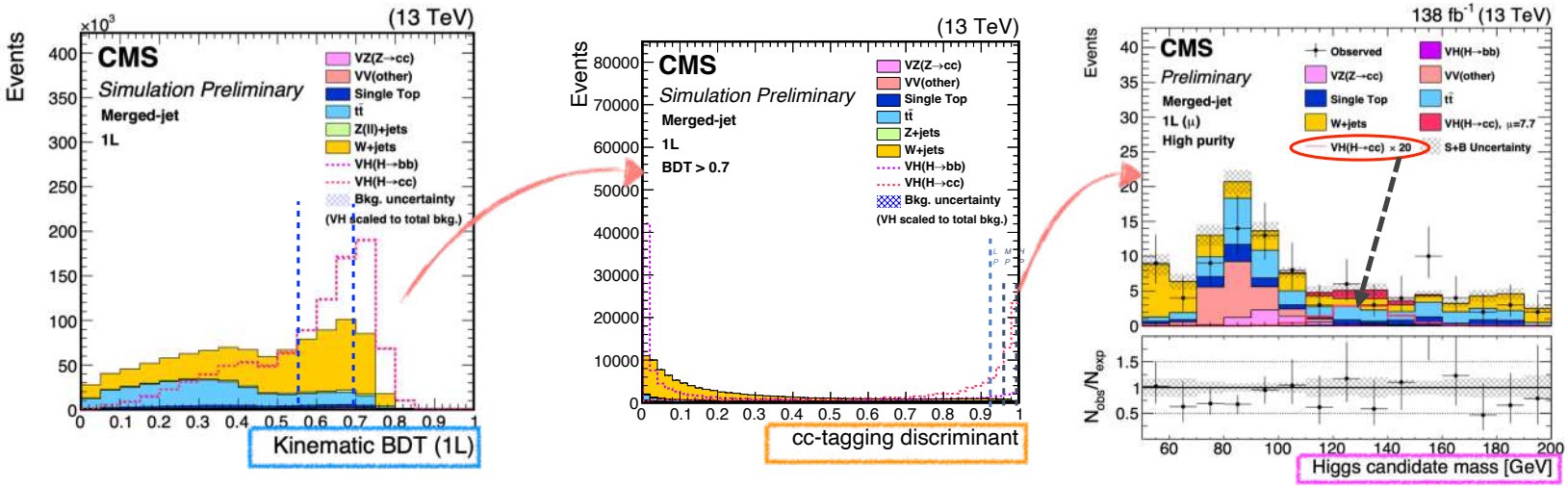

Background estimation

- Normalizations of main backgrounds estimated via dedicated data control regions (CRs)
  - **V+jets CR**: use the low kinematic BDT region
  - **tt CR** (0L & 1L): invert the cut on the number of additional small-R jets (i.e., $N_{aj} \geq 2$)
  - free-floating parameters scale the normalizations in CRs and signal regions (SRs) simultaneously

- CRs designed to have similar jet flavor composition as the SR
  - flavor-independent kinematic BDT + same cc-tagging requirement in CRs as in SR
  - allows to correct cc-tagging efficiency for backgrounds directly from data
  - cc-tagging SFs only needed for the signal VH(H → cc) process (and VZ(Z → cc))
    - conservative uncertainty (2x/0.5x) for the misidentification of H(Z) → bb as H(Z) → cc

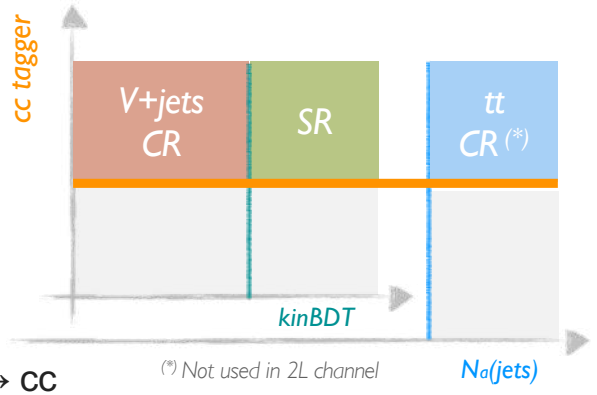

- Minor backgrounds (single top, dibosons, VH(H → bb)) estimated from simulation
  - dibosons: applying differential NNLO QCD + NLO EW corrections as a function of $p_T(V)$ [JHEP 2002 (2020) 087]

Resolved-jet topology

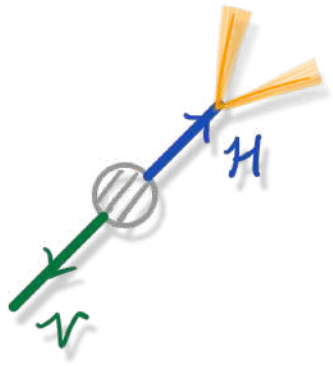

Overview of the resolved-jet topology

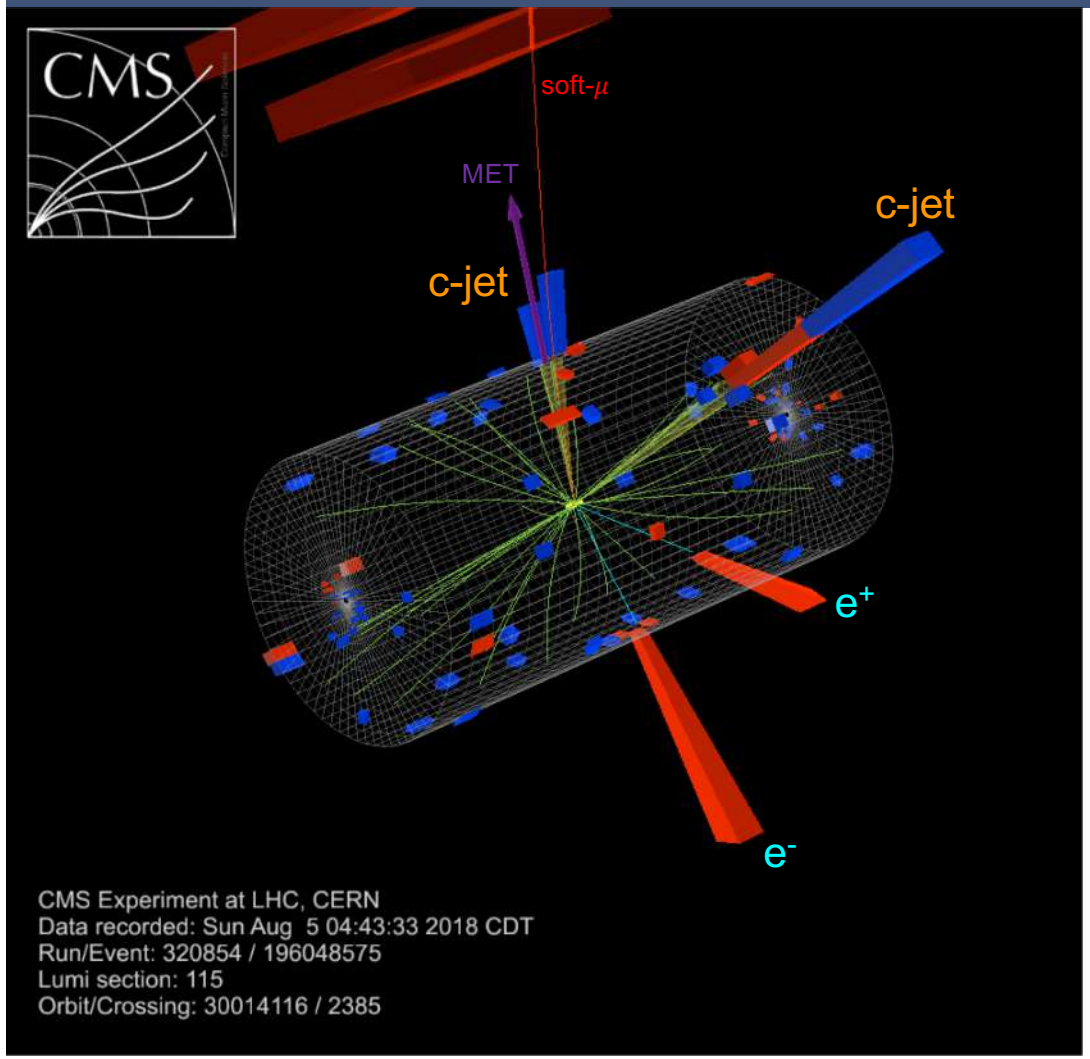

- Higgs candidate reconstruction
  - Select two AK4-jets with the highest c-tagger discriminant score as Higgs jets
  - Dedicated c-jet energy regression for improved c-jet energy scale and resolution + Recover FSR-jets
  - Kinematic-fit (2L channels)
- Analysis strategy (three channels: 0L, 1L, 2L)
  - Control regions for background normalizations
  - BDT for final signal extraction

Charm-tagging in the resolved-jet topology

DeepJet algorithm as charm tagger

- C-jets have “intermediate” properties to b- and light-jets
  - Separate **c-jets** simultaneously from **light-jets** and **bottom jets**
- From DeepJet output score it is possible to build two c-jet taggers
  - CvsL: it is optimized to differentiate charm-jets form light- or gluon-jets
  - CvsB: it is optimized to differentiate charm-jets from bottom-jets

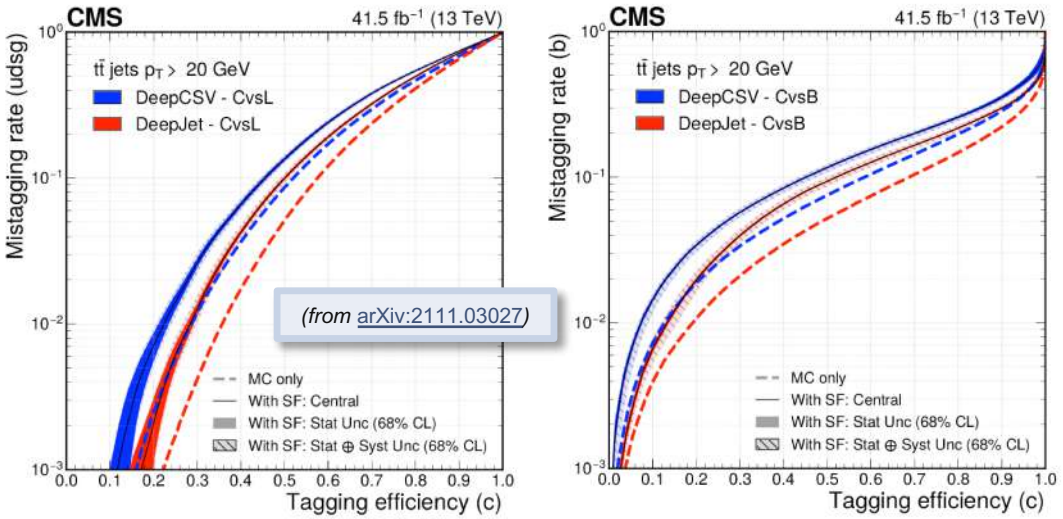

(from arXiv:2111.03027)

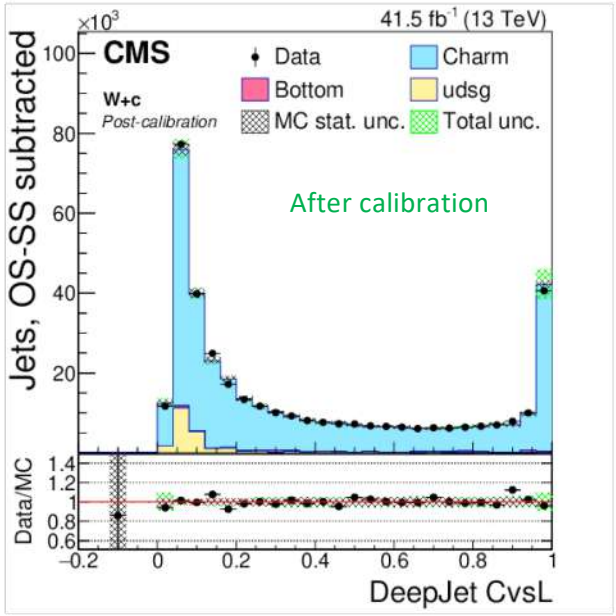

- Calibration in data with a novel technique!
- 2022 *JINST* **17** P03014 (**published by *JINST***)

- Improvement vs DeepCSV (used in 2016 analysis)
  - Increase leading-jet c-tagging efficiency by ~30% for fixed b-jet and light-jet mis-tagging rate

A new method to calibrate charm-taggers

- Methodology
  - Iterative approach exploiting 3 distinct CRs enriched in b-jets, c-jets, or light-flavour jets

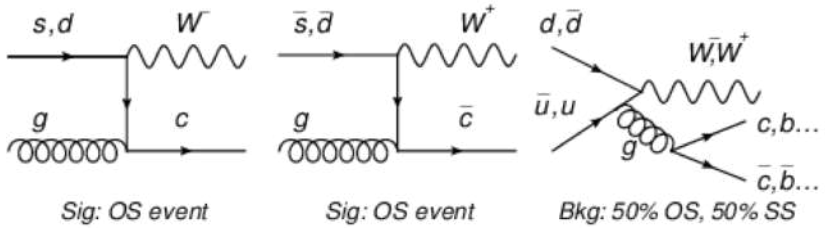

- Selecting an abundant and pure source of charm-jets
  - Target W production in association with charm quarks (W+c)
  - Major background has 50% chance to have SS or OS final states
    - performing an OS-SS subtraction reduces considerably the W+gluon process
  - To enrich in b-jets and light-jets: semi-(di-)leptonic $t\bar{t}$+jets and DY(Z→$\mu\mu/ee$)+jets

(from 2022 *JINST* **17** P03014)

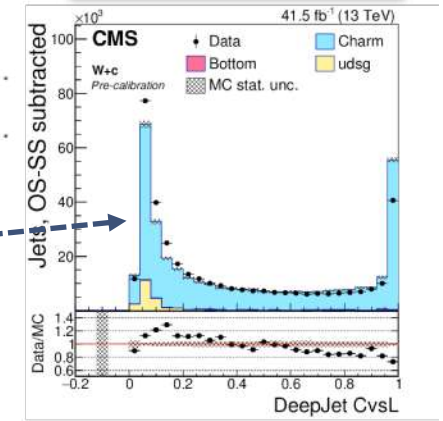

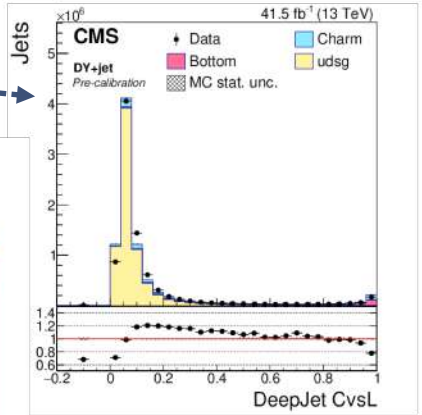

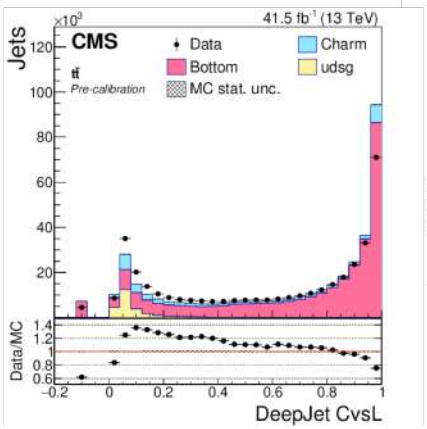

- First time that a calibration method to correct the 2D distribution of c-tagging discriminator shapes is presented

  ➔ 2022 *JINST* **17** P03014 (**published by *JINST***)

A new method to calibrate charm-taggers

Application of the reshaping scale-factors

*(from 2022 JINST **17** P03014)*

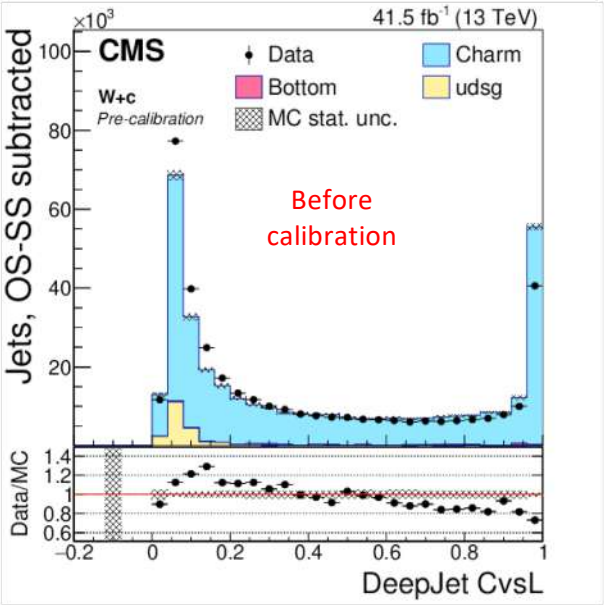

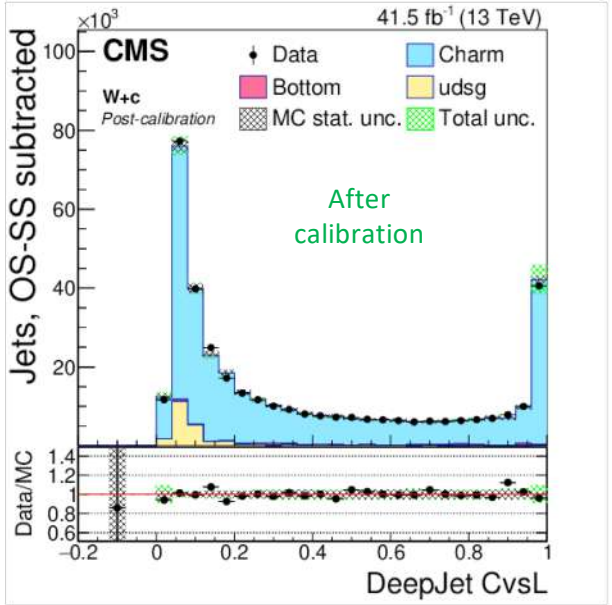

- Very good data/MC agreement after the calibration
  - Application through an event-by-event re-weighting:

$$w_i = \prod_{i=1}^{jets} sf_i(CvsL, CvsB)$$

Charm-tagging in the resolved-jet topology

- Definition of leading-jet working point
  - Studies of CvsB/CvsL jet score distributions in 2D plane
  - **CvsL>0.225, CvsB>0.4** ➔ c-jet ID efficiency of ~43%, b- and light-jet mis-tag. rate of ~15% and ~4%

c-jets mis-identified as light ones

c-jets

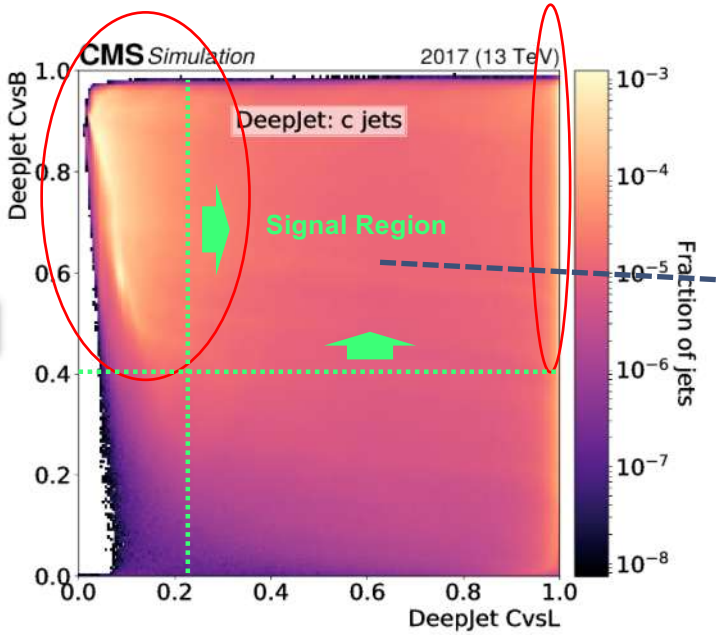

(from 2022 JINST 17 P03014)

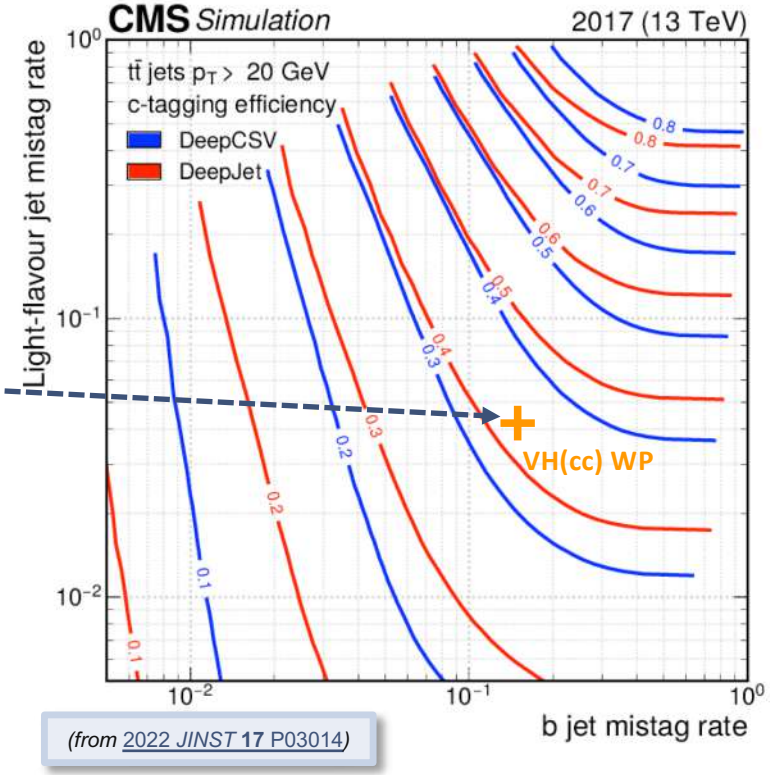

(from 2022 JINST 17 P03014)

A dedicated charm-jet energy regression

Goal: improve c-jet energy scale and resolution

- Inspired by b-jet energy regression [arXiv:1912.06046]
  - Jet energy measurements not always accurate:
    - neutrinos, hadrons outside jet radius, etc. Effect enhanced in c-jets and b-jets
  - Dedicated algorithm to determine c-jet energy scale and resolution
  - A DNN algorithm pioneered for the observation of the H→bb decay
- Regression performed using DNN architecture:
  - Trained using c-jets collected from W→cq decays in $t\bar{t}$+jets MC events
  - Target is represented by p_T(gen)/p_T(reco)
- Input features
  - Total of 43 input variables as input to the network
  - Jets: kinematics, energy fraction, leading+soft-lepton tracks, pile-up, secondary vertices
  - Jet energy shapes (e.g. energy fraction, etc), jet constituents, p_T(jet)/p_T(lepton)

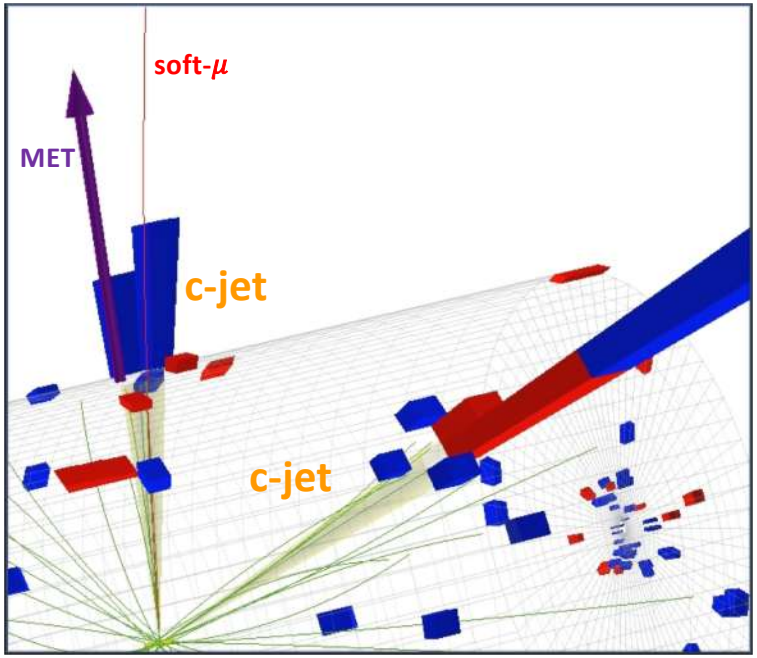

A dedicated charm-jet energy regression

- **~15% improvement in mass resolution**
  - Depending on the jet p_T
- Validated in VH(H→cc) control regions

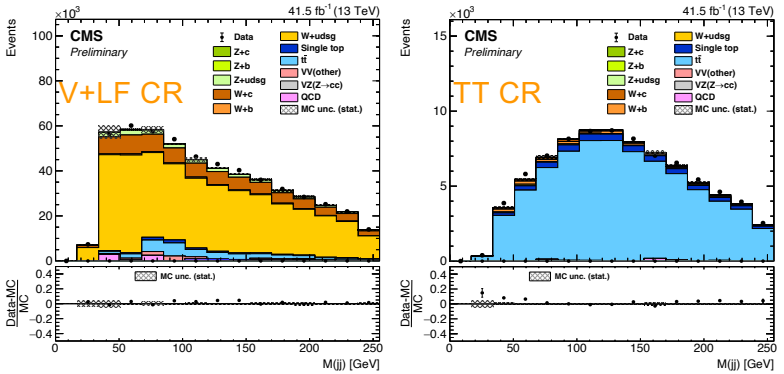

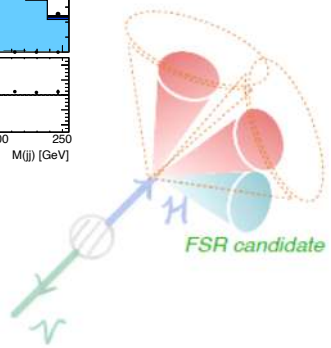

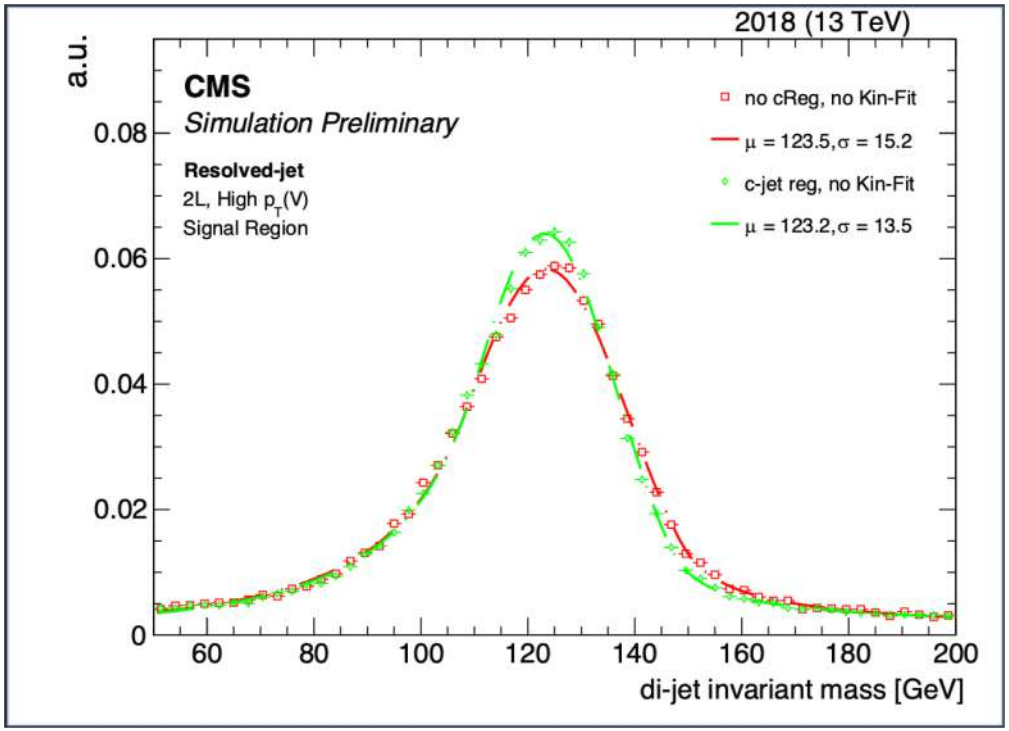

- FSR recovery
  - Further improve di-jet invarian
  - Jets with $p_T < 20$ GeV, $|\eta| < 3$, and within $\Delta R < 0.8$ of Higgs jets are included in Higgs 4-momentum

Kinematic-fit in the 2L channels

- **No intrinsic missing energy in Z($\ell\ell$)H(cc) process**

- Improve jet p_T measurement through a kinematic fit:
  - Constrain di-lepton system to the Z boson mass
  - Balance the $\ell\ell$+cc+jets system in the (p_x, p_y) plane
  - Allow MET to adjust within the experimental resolution

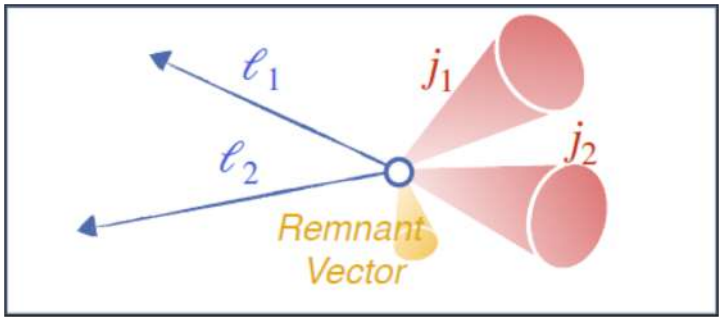

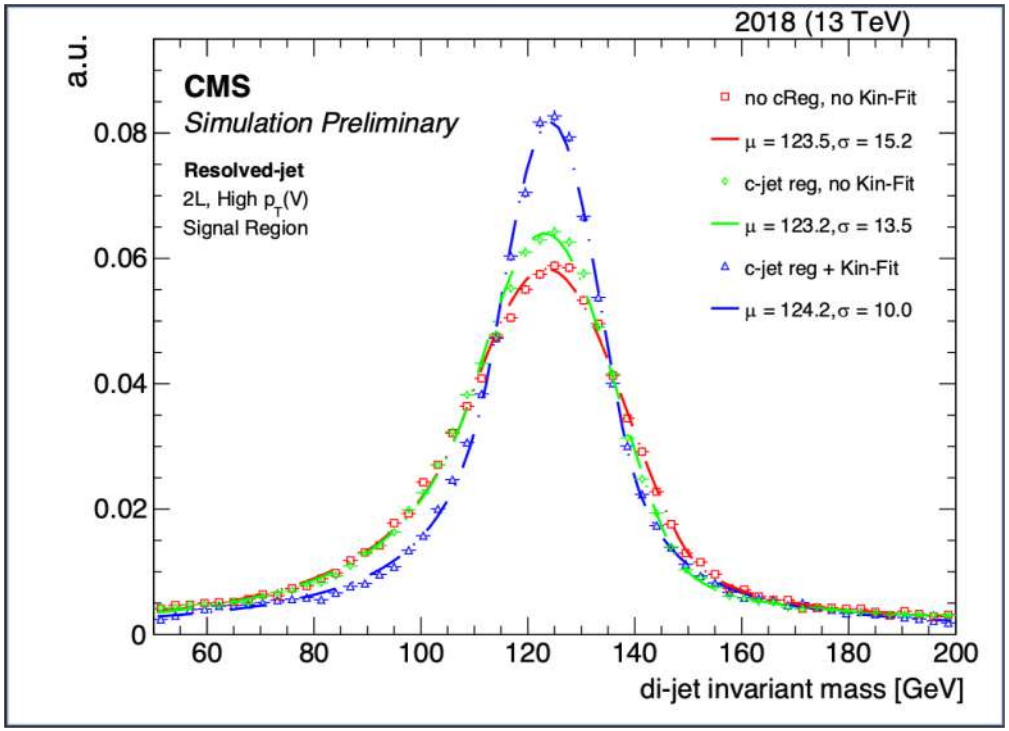

- Up to **~30% improvement in Higgs mass resolution**

Signal extraction – BDT training in SRs

- BDT trained to separate signal from background samples

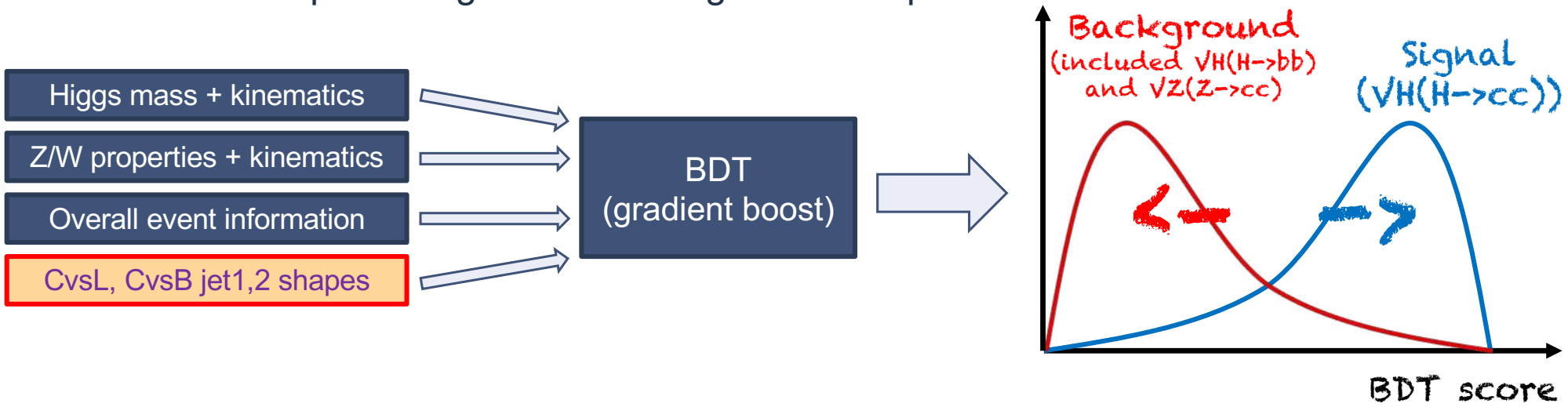

- Separate BDTs trained for each channel and data taking year
  - Separate BDTs trained for high- and low-p_T(V) 2L

- Reshaped BDT distributions used in SR for the final fit

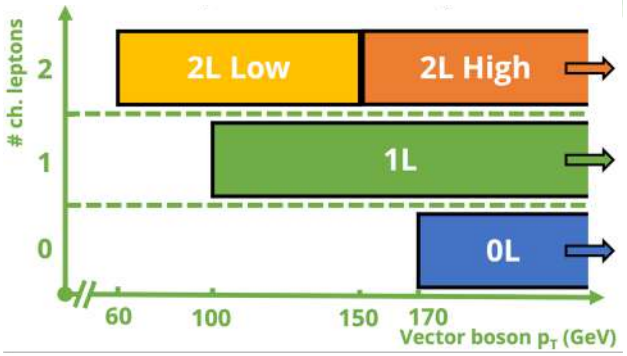

Analysis categories and background estimation

- Accurate modeling of jet flavor in V+Jet background is vital for proper signal extraction
  - Separate rate parameters for V+c, V+b, and V+light processes (no W+b) + $t\bar{t}$ +jets
  - Freely floating in each channel/year

- Selections optimized for the different decay of the vector boson considered

- Definition of 4 analysis categories
  - **0L**: $p_T(Z)>170$ GeV
  - **1L**: $p_T(W)>100$ GeV
  - **2L Low-p_T**: 60 GeV $<p_T(Z)<150$ GeV
  - **2L High-p_T**: $p_T(Z)>150$ GeV

- All the categories have TT, LF, HF and CC CRs (1L has not HF) + 1 SR

- Simultaneous fit to BDT in SR and tagger shapes in CRs

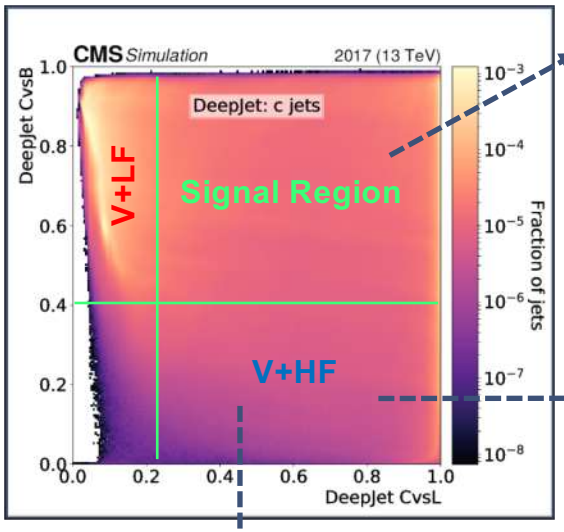

V+CC
Veto m(H)
region

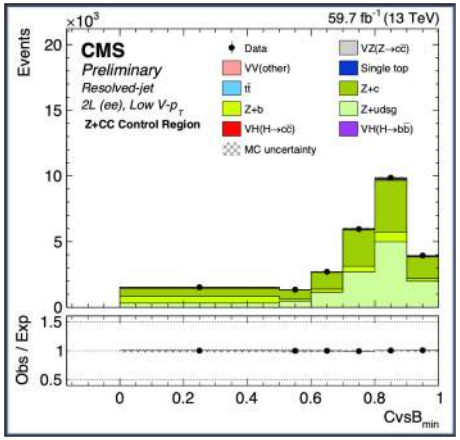

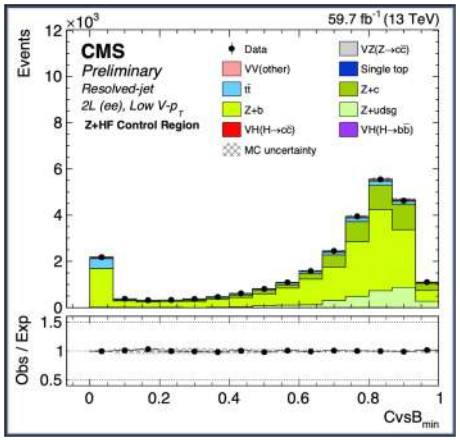

$t\bar{t}$
Invert Z mass (2L)
Require add jet (1L)*
Require add ℓ and jets (0L)

*1L: also require MET<170 GeV to keep orthogonal to 0L $t\bar{t}$ CR

Postfit plots – Signal regions

- Postfit distribution of the BDT discriminant obtained with the 2017 data (more in the back-up)
  - 7 Signal regions in each year: 2L(ee/$\mu\mu$) Low-p_T(V) and High-p_T(V), 1L(e/μ), and 0L

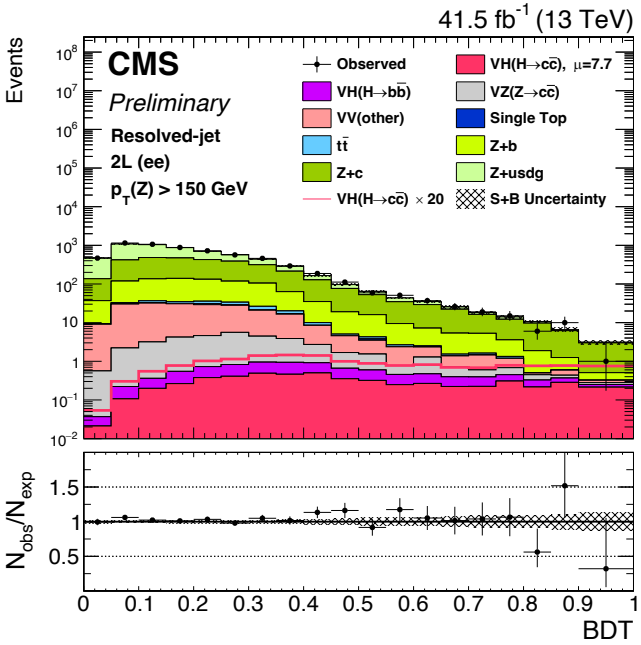

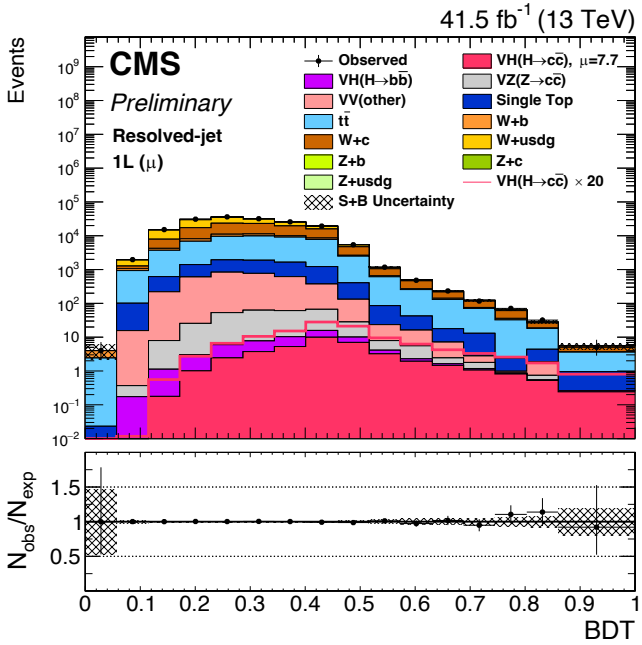

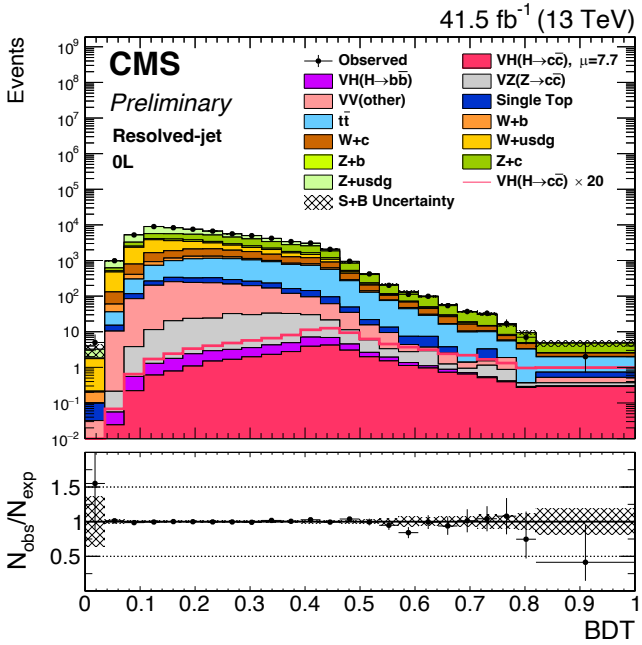

Results

Uncertainties

- All correlated between topologies, except:
  - Background normalization SFs for V+jets and $t\bar{t}$
  - c-tagging efficiencies
- Main uncertainties
  - Limited statistics of data
  - Statistical uncertainties of V+jets samples
  - Charm tagging efficiencies

Uncertainty source	$\Delta\mu / (\Delta\mu)_{\text{tot}}$
Statistical	**85%**
Background normalizations	37%
Experimental	**48%**
Sizes of the simulated samples	37%
Charm identification efficiencies	23%
Jet energy scale and resolution	15%
Simulation modeling	11%
Luminosity	6%
Lepton identification efficiencies	4%
Theory	**22%**
Backgrounds	17%
Signal	15%

VZ(Z→cc) results

- Analysis validated by looking for VZ(Z→cc) process
  - Same analysis procedure, but extracting VZ(Z→cc) signal
  - Resolved-jet: retrained BDTs with VZ(Z→cc) as signal
  - VH(H→cc) fixed to SM expectation

- Observed (expected) signal strength for VZ(Z→cc):

$$\mu_{VZ(Z\to cc)} = 1.01^{+0.23}_{-0.21}(1.00^{+0.22}_{-0.20})$$

with a significance of 5.7σ (5.9σ)

- **First observation of Z→cc at hadron collider!**

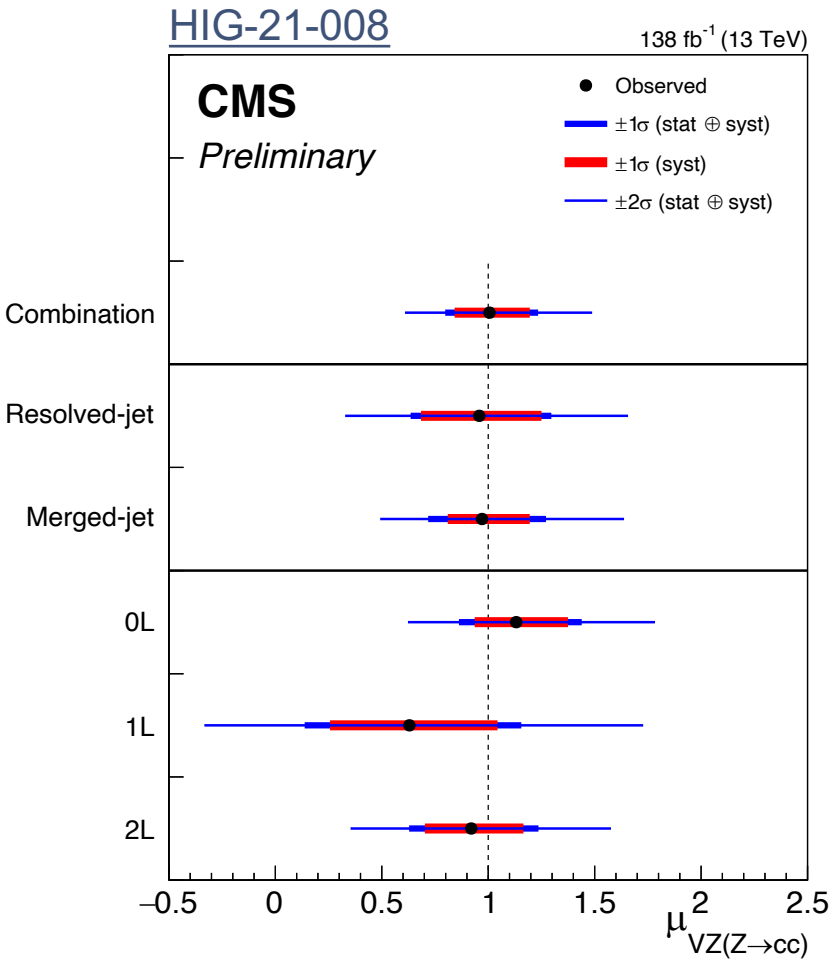

VZ(Z→cc) results

- Observing the excess: distribution of events ordered by $\log_{10}$(S/B)

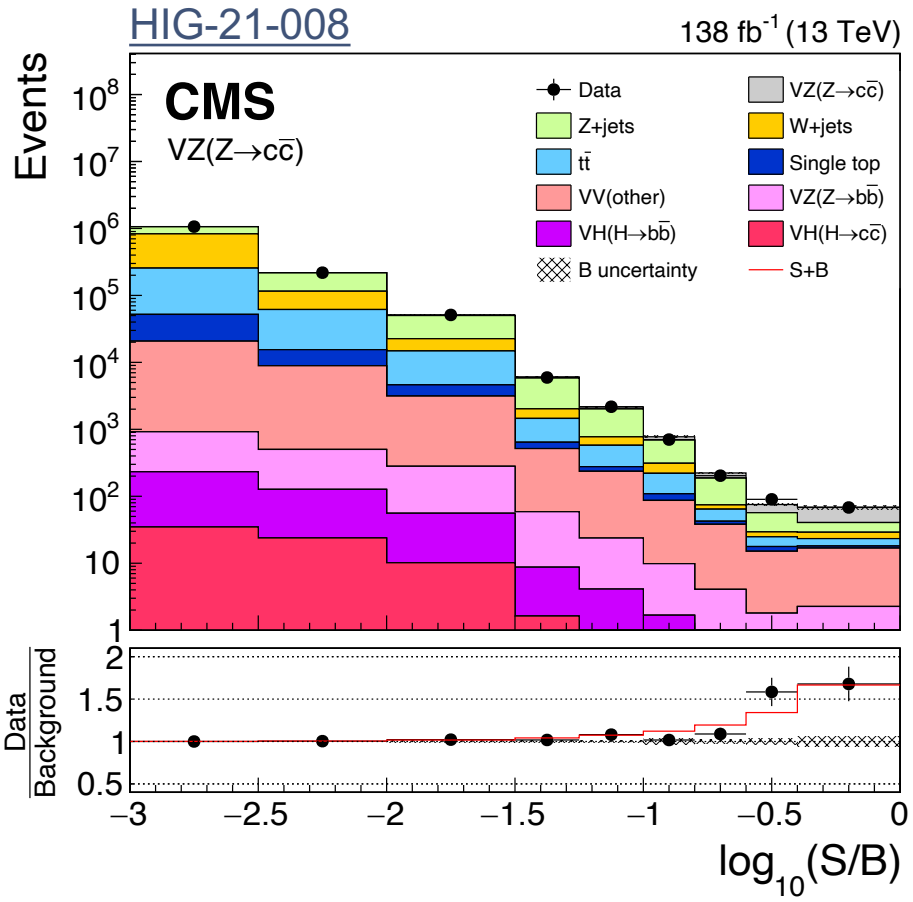

VH(H→cc) results

HIG-21-008

- Merged-jet topology: distribution of the Higgs boson candidate mass
- Resolved-jet topology and the combination: ordering the events by $\log_{10}(S/B)$

Merged-jet

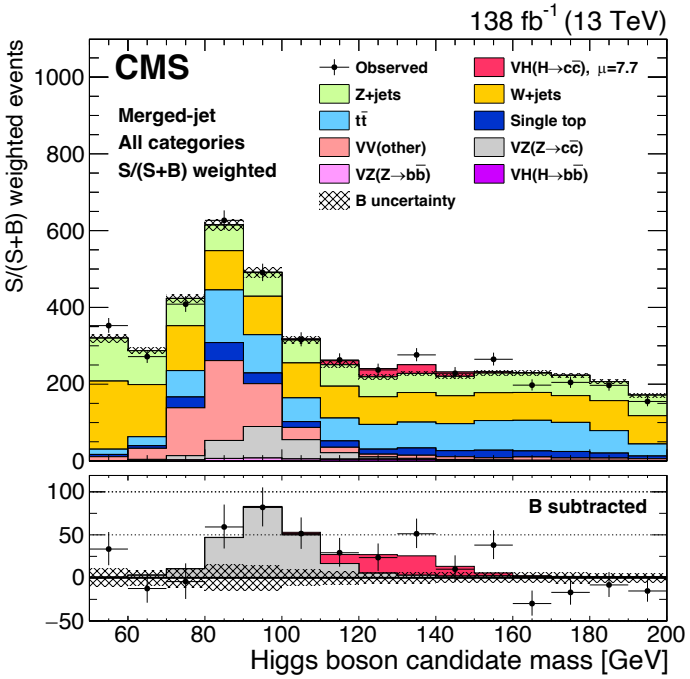

Resolved-jet

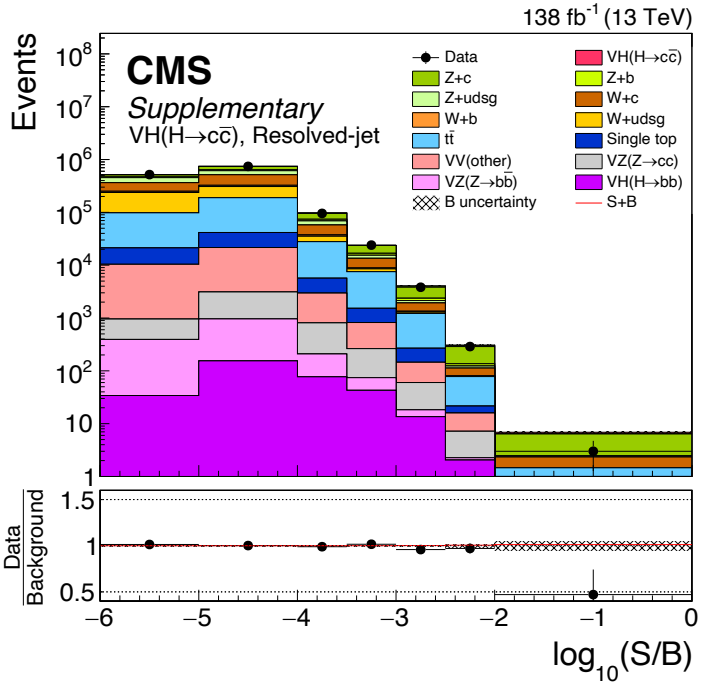

Merged + Resolved

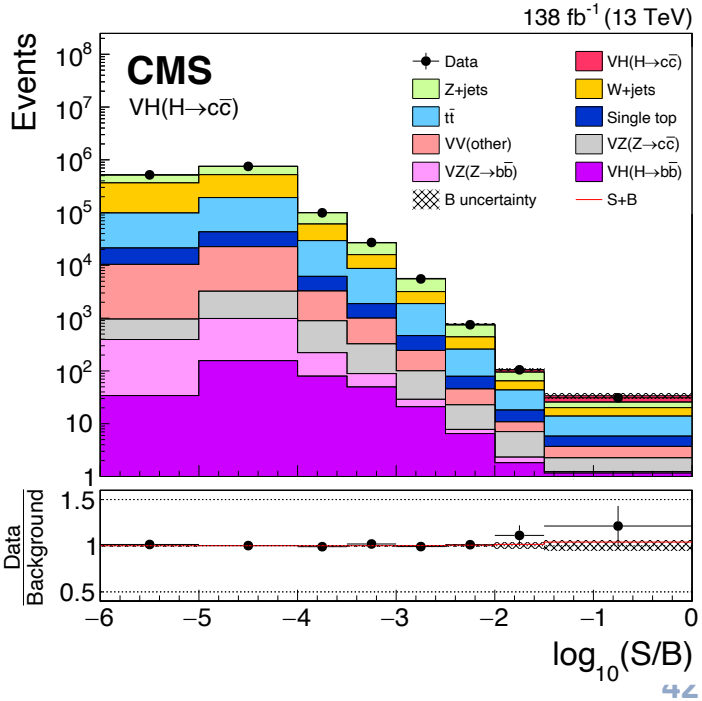

VH(H→cc) results

- Observed (expected) upper limit on VH(H→cc) signal strength at 95% CL: $\mu_{VH(H\to cc)} < 14\ (7.6^{+3.4}_{-2.3})$
  - **Strongest limits on VH(H→cc) process to date!**
  - ATLAS Full Run 2 result: $\mu_{VH(H\to cc)} < 26\ (31)$ [arXiv:2201.11428]

- Best fit signal strength: $\mu_{VH(H\to cc)} = 7.7^{+3.8}_{-3.5}$
  - Consistent with the SM prediction within 2σ

- Obs. (Exp.) upper limits from each topology:
  - **Resolved-jet** topology: **14(19) × SM**
  - **Merged-jet** topology: **17(8.8) × SM**

HIG-21-008

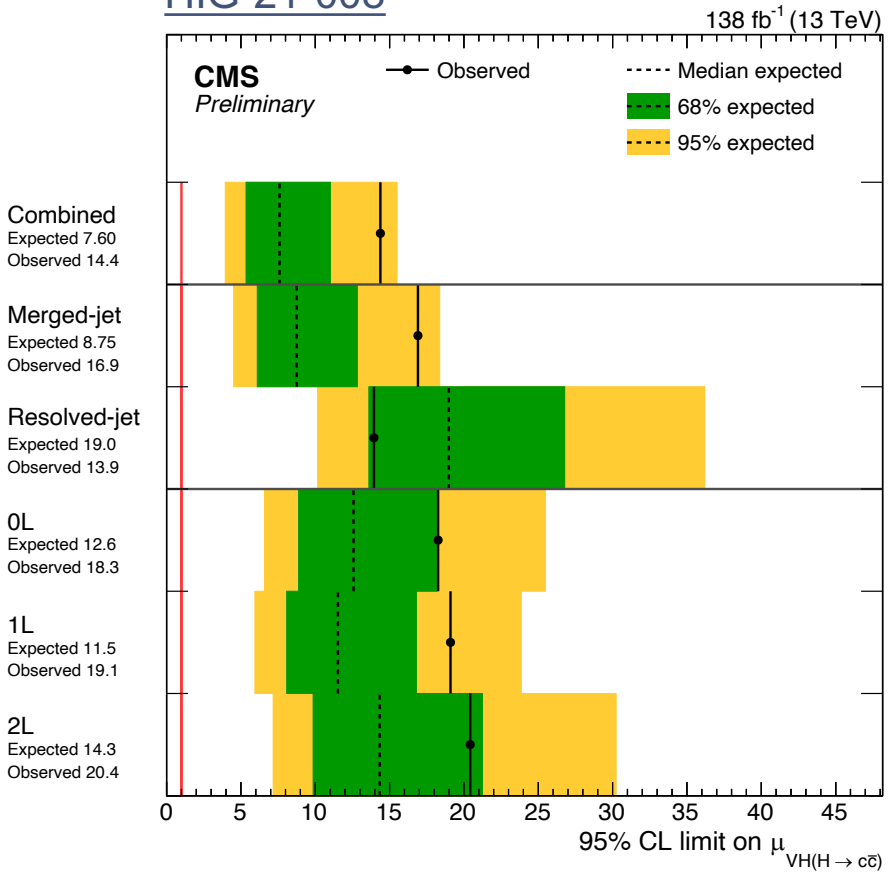

VH(H→cc) results

Results used to place new constraints on κ_c

- Only considering effects on $\mathcal{B}(\mathrm{H} \to \mathrm{cc})$ and fixing all other couplings to their SM values

$$\mu_{VH(H\to cc)} = \frac{\kappa_c^2}{1+\mathcal{B}_{SM}(H\to cc)\times(\kappa_c^2-1)}$$

- The 95% CL intervals obtained with likelihood scans
  - observed: $1.1 < |\kappa_c| < 5.5$
  - expected: $|\kappa_c| < 3.4$
- **Strongest constraints on $|\kappa_c|$ to date**
  - Competitive with indirect measurements of $|\boldsymbol{\kappa_c}|$: PRD 92 (2015) 033016 and arXiv:2202.00487
  - Comparable to the previous projection for HL-LHC [ATL-PHYS-PUB-2021-039]

HIG-21-008

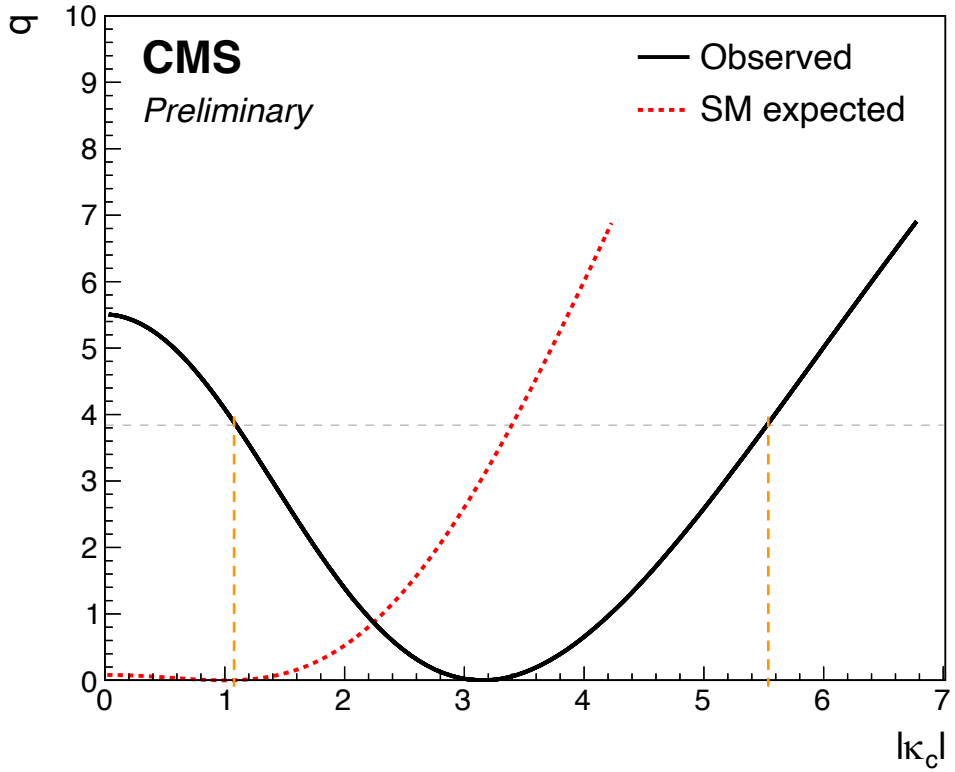

VH(H→cc) results

Results used to place new constraints on κ_c

- Only considering effects on $\mathcal{B}(\mathrm{H} \to \mathrm{cc})$ and fixing all other couplings to their SM values

$$\mu_{VH(H\to cc)} = \frac{\kappa_c^2}{1+\mathcal{B}_{SM}(H\to cc)\times(\kappa_c^2-1)}$$

- The 95% CL intervals obtained with likelihood scans
  - observed: $1.1 < |\kappa_c| < 5.5$
  - expected: $|\kappa_c| < 3.4$
- **Strongest constraints on $|\kappa_c|$ to date**
  - Competitive with indirect measurements of $|\boldsymbol{\kappa_c}|$: PRD 92 (2015) 033016 and arXiv:2202.00487
  - Comparable to the previous projection for HL-LHC [ATL-PHYS-PUB-2021-039]

HIG-21-008

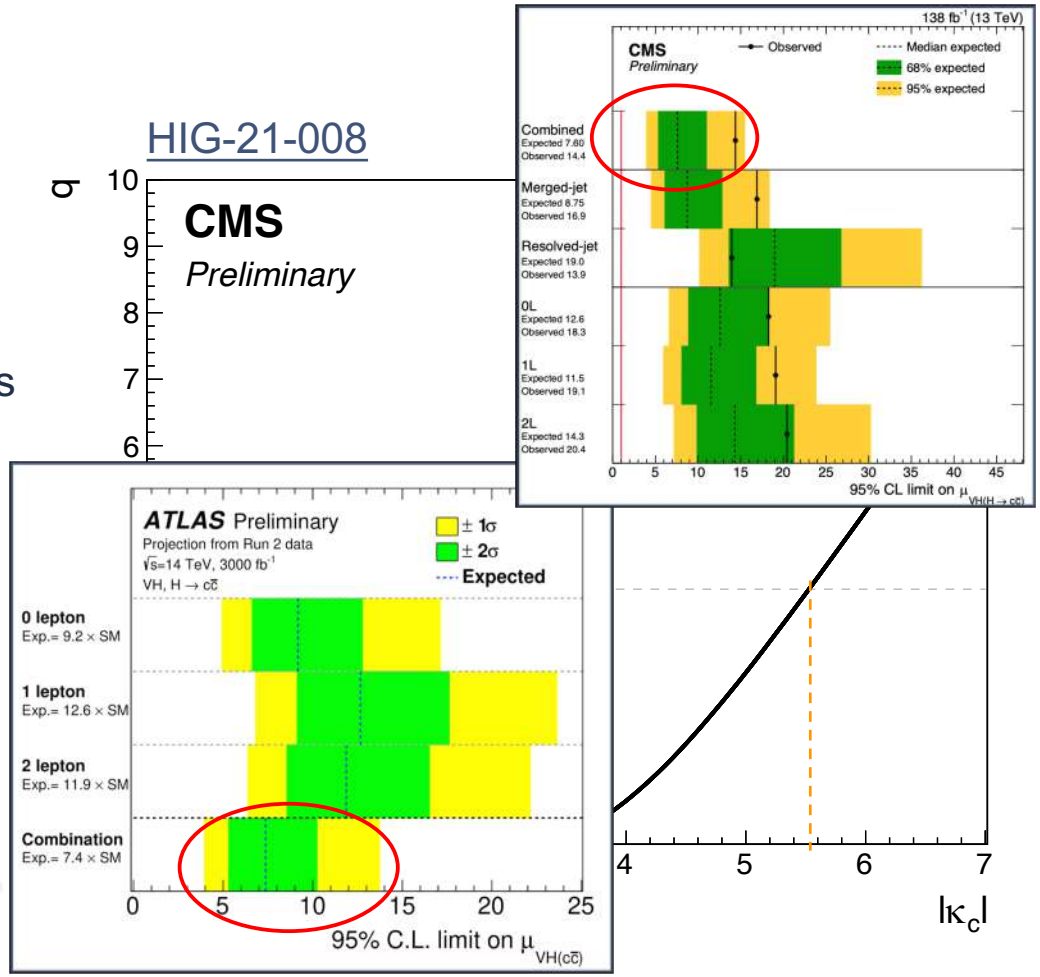

Conclusions

- New results of the CMS search for the VH(H→cc) process are presented
  - Benefit from the full Run 2 dataset
  - Substantial improvements in charm tagging performance
  - Major upgrades of analysis techniques, such as jet energy/mass regression, kinematic fits, etc.
- Analysis validated by measuring VZ(Z→cc) signal strength: $\mu_{VZ(Z \rightarrow cc)} = 1.01^{+0.23}_{-0.21}$
  - Significance of 5.7σ (5.9σ) ➔ First observation of Z→cc at a Hadron Collider!
- Upper limits on VH(H→cc): $\mu_{VH(H \rightarrow cc)} < 14$ (7.6 exp.)
  - Almost 5x increase in expected sensitivity compared to analysis using 2016 data
  - Constraints on Higgs-charm coupling: $1.1 < |\kappa_c| < 5.5$ ($|\kappa_c| < 3.4$ exp.) — Most stringent to date!

Prospects

Projection at HL-LHC: merged-jet with 3000 fb^{-1} data

- Modifications to the Run 2 analysis to allow for a simultaneous constraint on H → bb and H → cc
  - **addition of 3 categories enriched in H → bb decays**, very small (1-2%) overlap of bb and cc categories
  - **large-R jet p_T threshold lowered from 300 GeV to 200 GeV** – increasing signal acceptance
- Simultaneous extraction of the H → bb and H → cc signal strengths
  - $\mu_{VH(H \to bb)} = 1.00 \pm 0.03\ (stat.) \pm 0.04\ (syst.) = 1.00 \pm 0.05\ (total)$
  - $\mu_{VH(H \to cc)} = 1.0 \pm 0.6\ (stat.) \pm 0.5\ (syst.) = 1.0 \pm 0.8\ (total)$

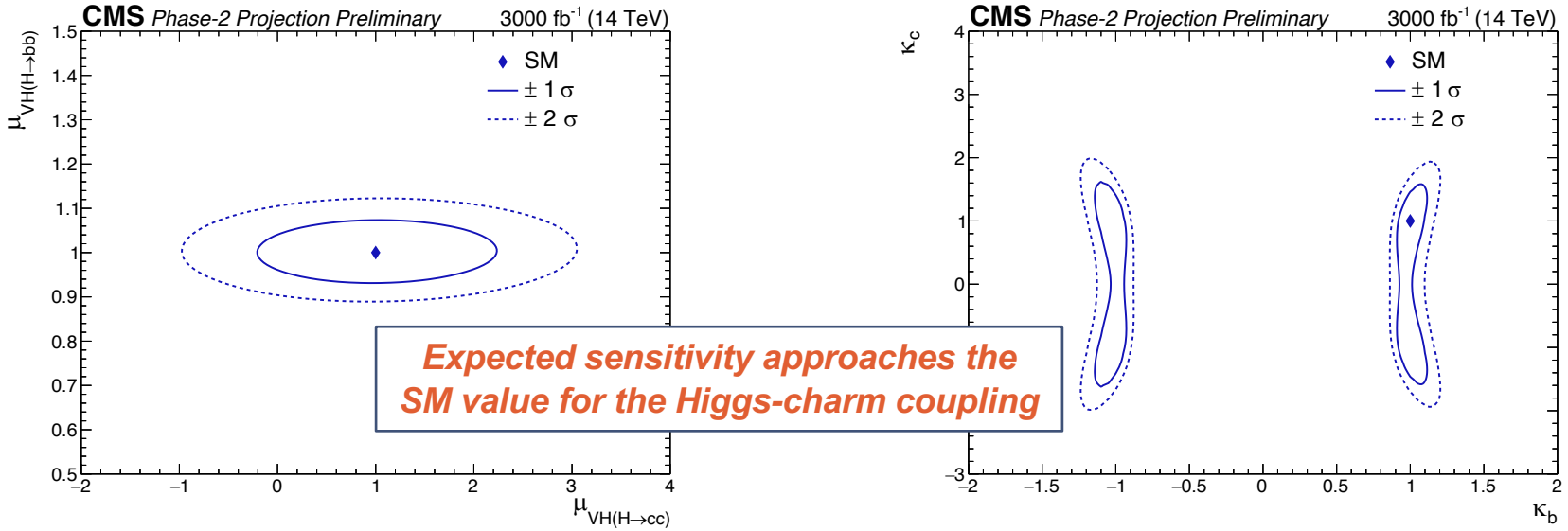

A charming journey

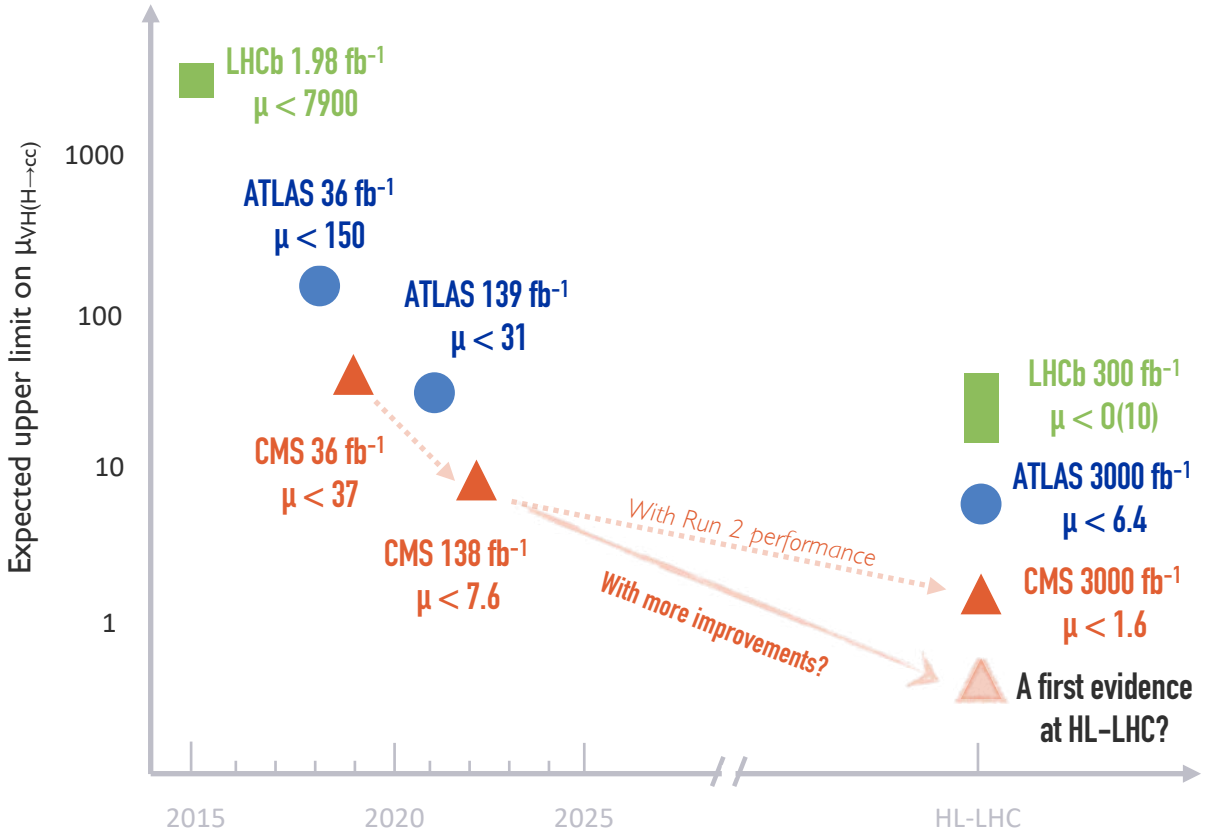

From $\mathcal{O}(1000)$ to $\mathcal{O}(100)$ to $\mathcal{O}(10)$ in ~5 years.
A combined effort and creativity from instrumentation, physics objects and analysis techniques!

Could we hope for an evidence at HL-LHC?

- More channels: ttH(cc), VBF H(cc), indirect constraints.
- Improvements in analysis techniques and instrumentation
- Reduction of systematic uncertainties: c-tagging, event modeling, theoretical uncertainties, …

A charming journey ahead!

CMS is already on track:

- ggH(cc) under approval (HIG-21-012)
- Efforts on H+charm have started

Back-Up

H → cc searches at the LHC

- ATLAS:
  - [Phys. Rev. Lett. 120 (2018) 211802] (36 fb^{-1})
  - [arXiv:2201.11428] (139 fb^{-1})
  - [ATL-PHYS-PUB-2021-039] (HL-LHC projection, 3000 fb^{-1})

- CMS:
  - [JHEP 03 (2020) 131] (36 fb^{-1})
  - [CMS-PAS-HIG-21-008] (138 fb^{-1}; HL-LHC projection, 3000 fb^{-1})

- LHCb:
  - [LHCb-CONF-2016-006] (1.98 fb^{-1})
  - [LHCb-PUB-2018-009] (HL-LHC projection, 300 fb^{-1})

Phase-1 pixel detector upgrade

- New pixel detector installed during year-end stop 2016/2017

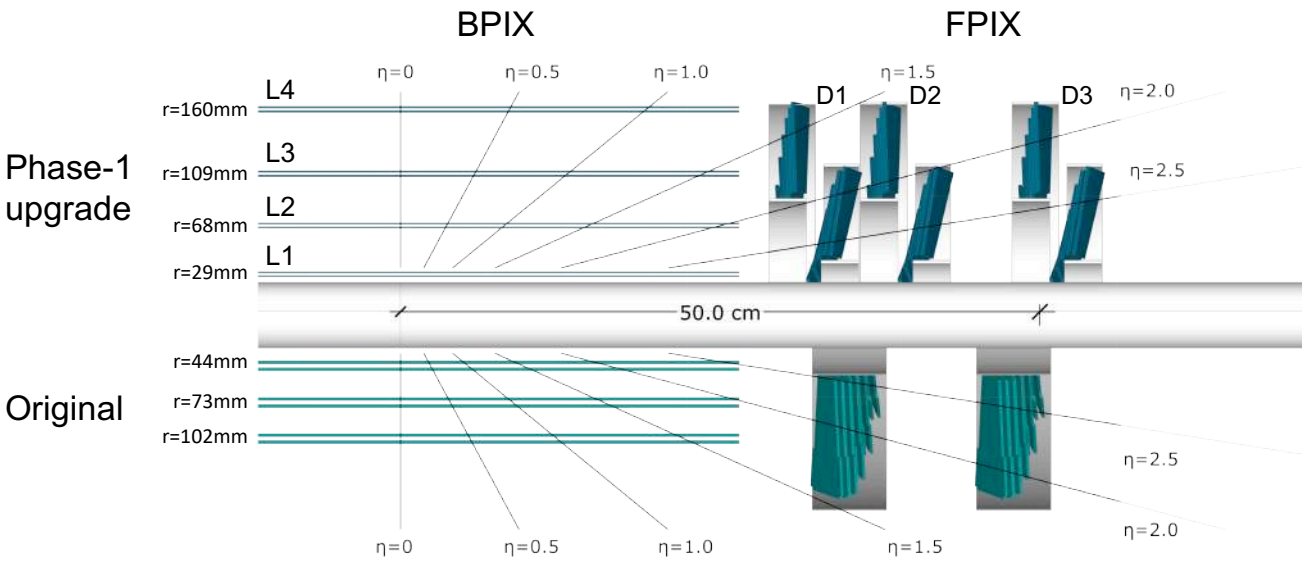

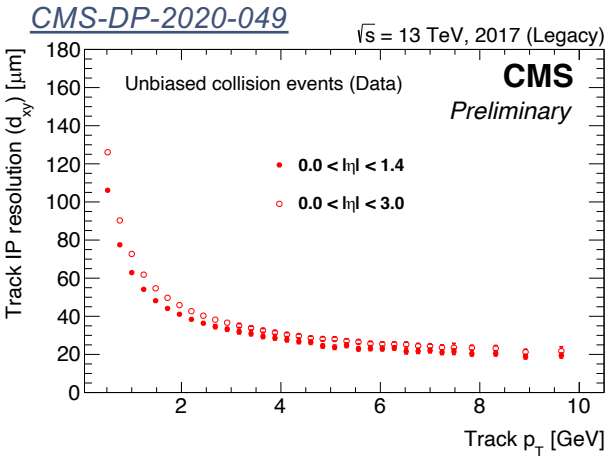

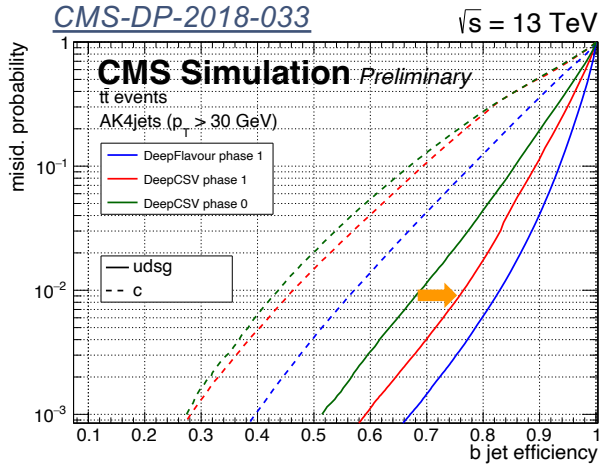

Improved tracking and flavour tagging performance in the 2017 — 2018 data set!

H → cc identification

- Merged-jet topology: Higgs boson candidate reconstructed via a single large-R jet (p_T > 300 GeV)
- A major improvement: **ParticleNet** tagger used to identify H → cc decay

JHEP 03 (2020) 131 (2016 analysis)

DeepAK8 (DeepAK15) [JINST 15 (2020) P06005]
- multi-class DNN boosted jet classifier
- directly uses jet constituents (particle-flow candidates / secondary vertices)
- 1D convolutional neural network
- mass decorrelation via adversarial training

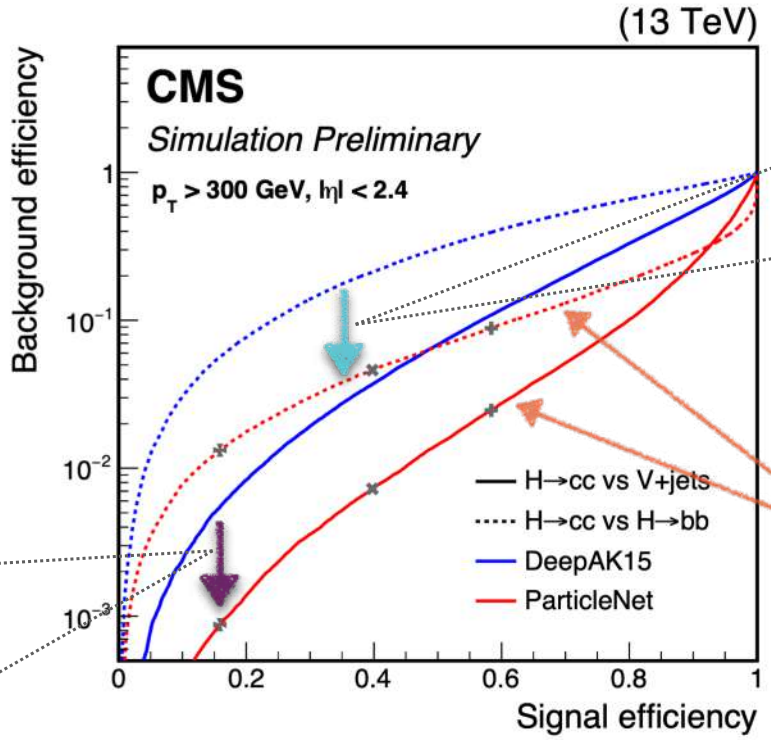

~5x better H→bb rejection

~5x better V+jet rejection

CMS-PAS-HIG-21-008 (Run 2 analysis)

ParticleNet [CMS-DP-2020-002]
- same spirit as DeepAK8, but substantially improved:
- **graph neural network architecture**
- **novel mass decorrelation technique**

>2x improvement in the final sensitivity

Mass decorrelation (II)

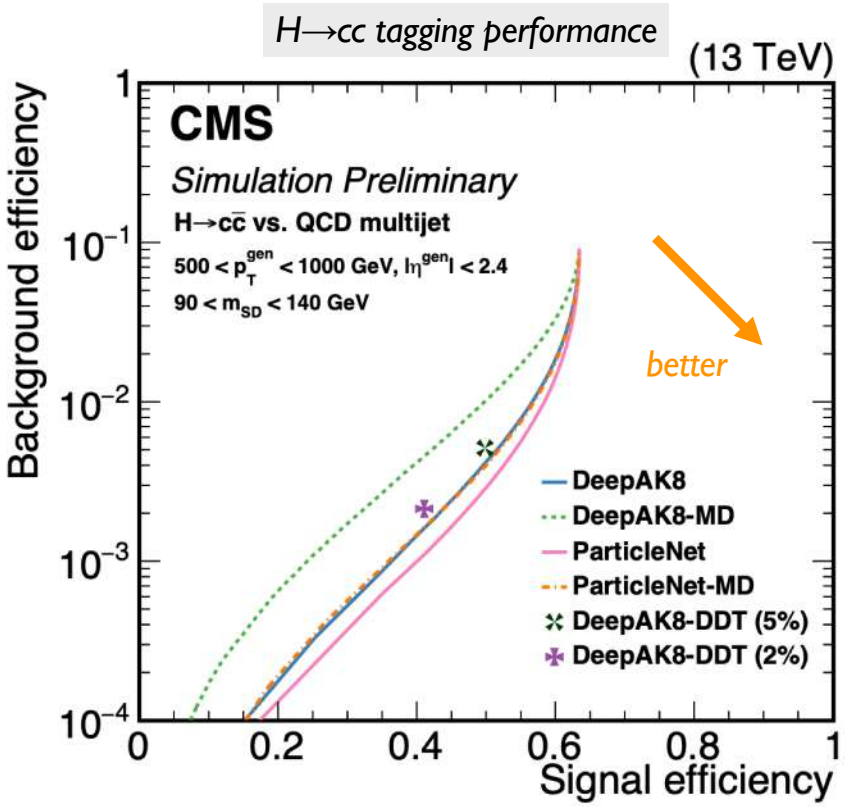

CMS-DP-2020-002

- "Mass sculpting": background jet mass shape becomes similar to signal after tagger selection
- New approach to prevent mass sculpting
  - using a special signal sample for training
    - hadronic decays of a spin-0 particle X
      - $X \to bb$, $X \to cc$, $X \to qq$
    - not a fixed mass, but a **flat mass spectrum**
      - $m(X) \in [15, 250]$ GeV
  - allows to easily reweight both signal and background to a ~flat 2D distribution in (p_T, mass) for the training
- Performance loss due to mass decorrelation greatly reduced compared to the previous approach (DeepAK8-MD, based on "adversarial training")

ParticleNet

ParticleNet input variables

TABLE I. Input variables used in the top tagging task (TOP) and the quark-gluon tagging task (QG) with and without PID information.

Variable	Definition	TOP	QG	QG-PID
$\Delta\eta$	Difference in pseudorapidity between the particle and the jet axis	×	×	×
$\Delta\phi$	Difference in azimuthal angle between the particle and the jet axis	×	×	×
$\log p_T$	Logarithm of the particle's p_T	×	×	×
$\log E$	Logarithm of the particle's energy	×	×	×
$\log \frac{p_T}{p_T(\text{jet})}$	Logarithm of the particle's p_T relative to the jet p_T	×	×	×
$\log \frac{E}{E(\text{jet})}$	Logarithm of the particle's energy relative to the jet energy	×	×	×
ΔR	Angular separation between the particle and the jet axis $\left(\sqrt{(\Delta\eta)^2+(\Delta\phi)^2}\right)$	×	×	×
q	Electric charge of the particle			×
`isElectron`	If the particle is an electron			×
`isMuon`	If the particle is a muon			×
`isChargedHadron`	If the particle is a charged hadron			×
`isNeutralHadron`	If the particle is a neutral hadron			×
`isPhoton`	If the particle is a photon			×

Baseline event selections

Merged-jet topology

Variable	0L	1L	2L
p_{T}^{ℓ}	—	(>25,>30)	>20
Lepton isolation	—	(<0.06, —)	(<0.25, —)
$N_{\mathrm{a}\ell}$	=0	=0	—
$M(\ell\ell)$	—	—	75–105
$N_{\text{small-}R}^{\mathrm{aj}}$	<2	<2	<3
$p_{\mathrm{T}}^{\mathrm{miss}}$	>200	>60	—
$p_{\mathrm{T}}(\mathrm{V})$	>200	>150	>150
$p_{\mathrm{T}}(\mathrm{H_{cand}})$	>300	>300	>300
$m\,(\mathrm{H_{cand}})$	50–200	50–200	50–200
$\Delta\phi(\mathrm{V},\mathrm{H_{cand}})$	>2.5	>2.5	>2.5
$\Delta\phi(\vec{p}_{\mathrm{T}}^{\mathrm{miss}},\mathrm{j})$	>0.5	—	—
$\Delta\phi(\vec{p}_{\mathrm{T}}^{\mathrm{miss}},\ell)$	—	<1.5	—
Kinematic BDT	>0.55	0.55–0.7, >0.7	>0.55
$\mathrm{c\bar{c}}$ discriminant			
High purity	>0.99	>0.99	>0.99
Medium purity	0.96–0.99	0.96–0.99	0.96–0.99
Low purity	0.90–0.96	0.90–0.96	0.90–0.96

Resolved-jet topology

Variable	0L	1L	2L low-$p_{\mathrm{T}}(\mathrm{V})$	2L high-$p_{\mathrm{T}}(\mathrm{V})$
p_{T}^{ℓ}	—	(>25,>30)	>20	>20
Lepton isolation	—	(<0.06, —)	(<0.25, —)	(<0.25, —)
$N_{\mathrm{a}\ell}$	=0	=0	—	—
$M(\ell\ell)$	—	—	75–105	75–105
$p_{\mathrm{T}}(\mathrm{j}_1)$	>60	>25	>20	>20
$p_{\mathrm{T}}(\mathrm{j}_2)$	>35	>25	>20	>20
$CvsL(\mathrm{j}_1)$	>0.225	>0.225	>0.225	>0.225
$CvsB(\mathrm{j}_2)$	>0.4	>0.4	>0.4	>0.4
$N_{\text{small-}R}^{\mathrm{aj}}$	—	<2	—	—
$p_{\mathrm{T}}^{\mathrm{miss}}$	> 170	—	—	—
$p_{\mathrm{T}}^{\mathrm{miss}}$ significance	—	>4	—	—
$p_{\mathrm{T}}(\mathrm{V})$	>170	>100	60–150	>150
$p_{\mathrm{T}}(\mathrm{H_{cand}})$	>120	>100	—	—
$m\,(\mathrm{H_{cand}})$	<250	<250	<250	<250
$\Delta\phi(\mathrm{V},\mathrm{H_{cand}})$	>2.0	>2.5	>2.5	>2.5
$\Delta\phi(\vec{p}_{\mathrm{T}}^{\mathrm{miss}},\mathrm{j})$	>0.5	—	—	—
$\Delta\phi(\vec{p}_{\mathrm{T}}^{\mathrm{miss}},\ell)$	—	<2.0	—	—

Uncertainties

- Breakdown of the uncertainties in each topology

Merged-jet topology

Table 3: The relative contributions to the total uncertainty on $\mu_{VH(H\to c\bar{c})}$ in the merged-jet analysis, with a best fit value $\mu_{VH(H\to c\bar{c})} = 8.7^{+4.6}_{-4.0}$.

Uncertainty source	$\Delta\mu / (\Delta\mu)_{tot}$
Statistical	**88%**
Background normalizations	39%
Experimental	**40%**
Sizes of the simulated samples	24%
Charm identification efficiencies	26%
Jet energy scale and resolution	15%
Simulation modeling	1%
Luminosity	5%
Lepton identification efficiencies	2%
Theory	**25%**
Backgrounds	21%
Signal	14%

Resolved-jet topology

Table 4: The relative contributions to the total uncertainty on $\mu_{VH(H\to c\bar{c})}$ in the resolved-jet analysis, with a best fit value $\mu_{VH(H\to c\bar{c})} = -9.5 \pm 9.6$.

Uncertainty source	$\Delta\mu / (\Delta\mu)_{tot}$
Statistical	**66%**
Background normalizations	28%
Experimental	**72%**
Sizes of the simulated samples	59%
Charm identification efficiencies	27%
Jet energy scale and resolution	17%
Simulation modeling	20%
Luminosity	13%
Lepton identification efficiencies	10%
Theory	**22%**
Backgrounds	21%
Signal	7%

Merged-jet topology: signal regions

2L(μμ), high cc-purity

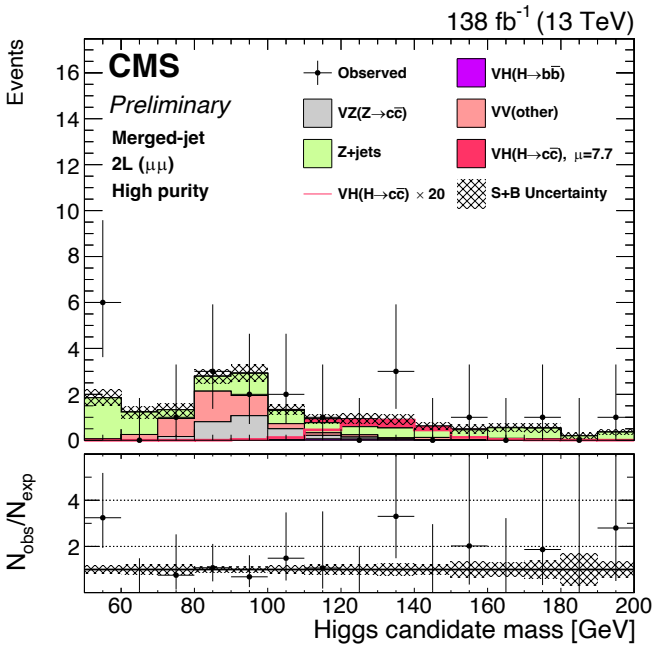

1L(e), high cc-purity

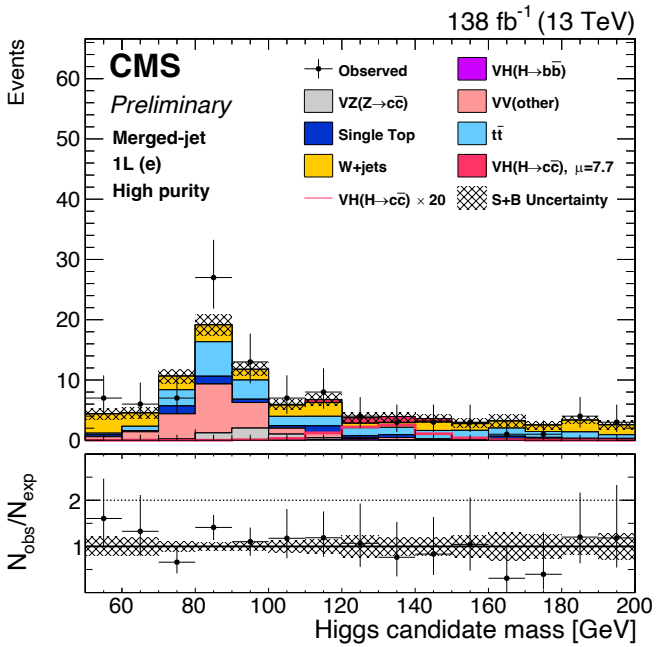

0L, high cc-purity

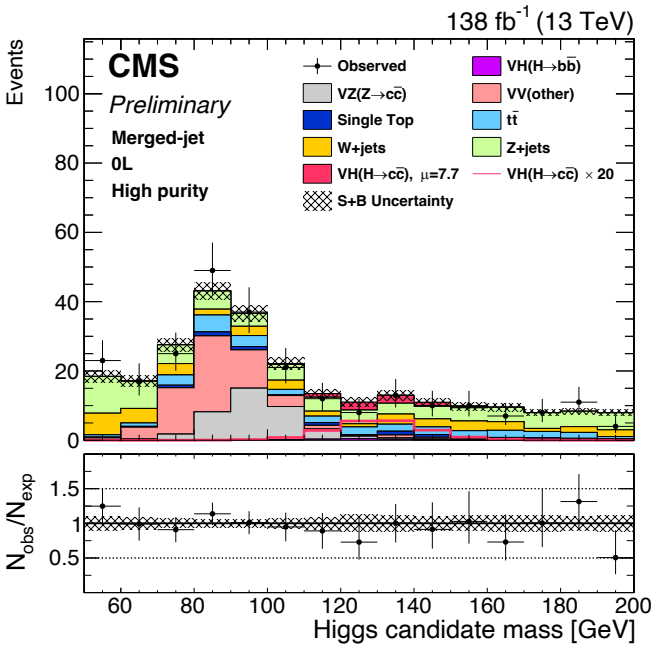

Merged-jet topology: control regions

2L(ee), V+jets CR, low cc-purity

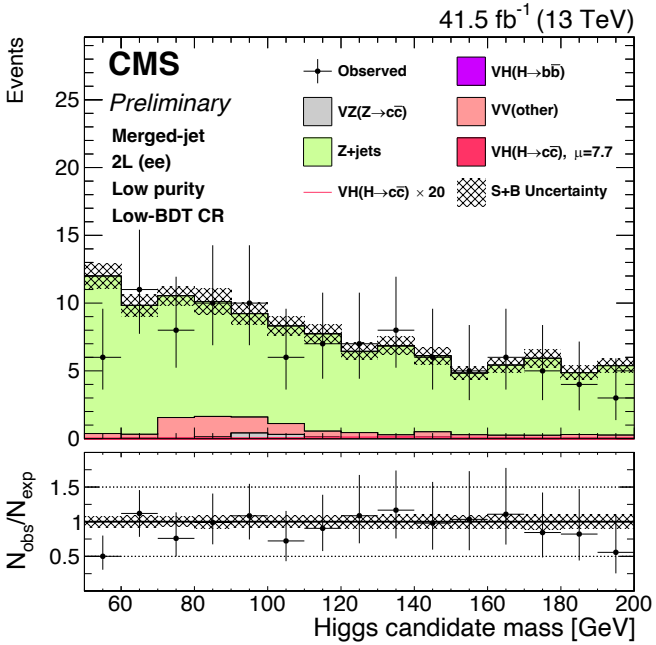

1L(μ), tt CR, high cc-purity

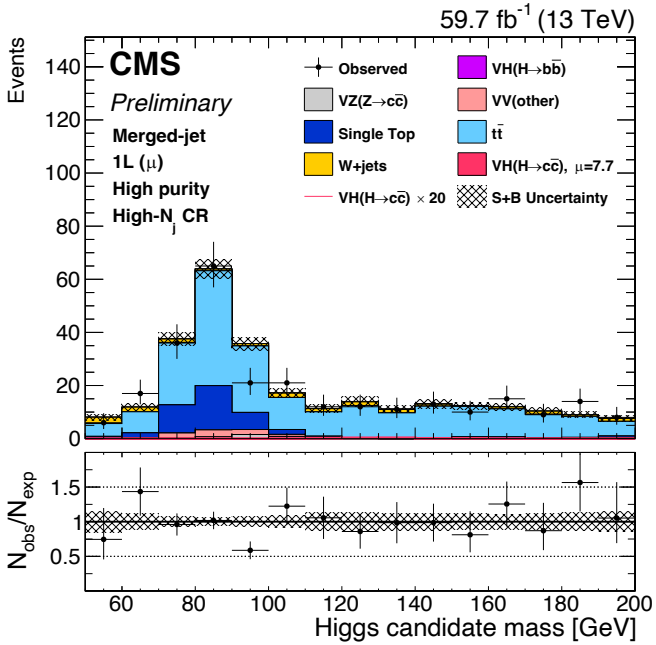

0L, V+jets CR, medium cc-purity

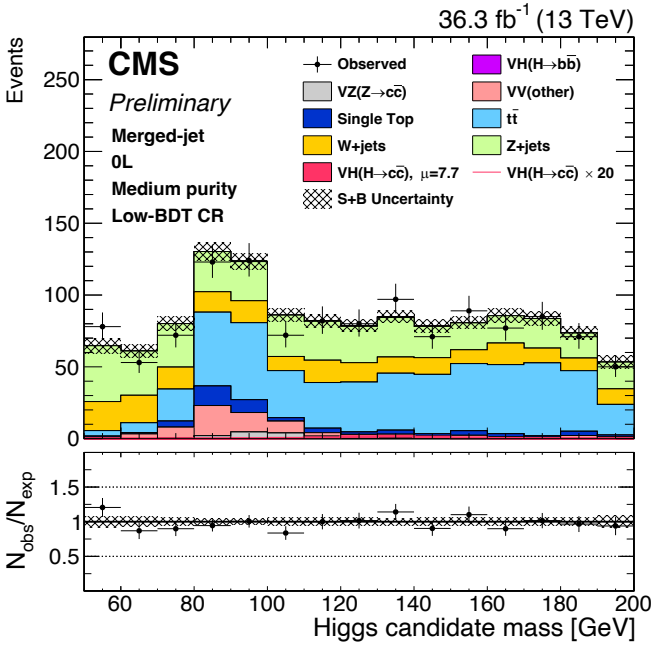

Comparison of mass decorrelation methods

DeepAK8-MD

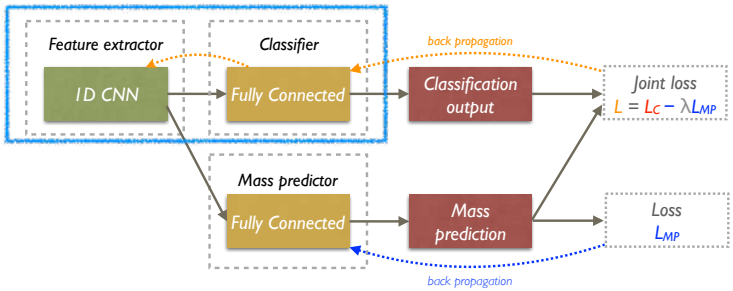

Background jet mass

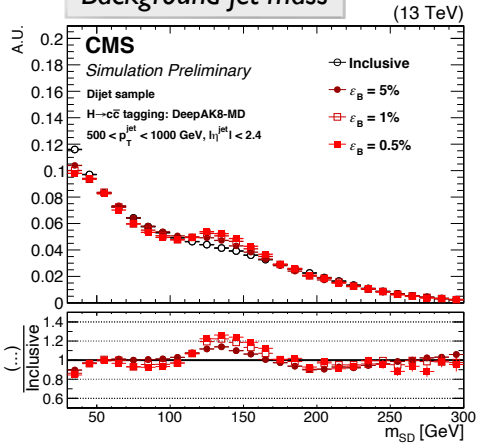

ParticleNet-MD

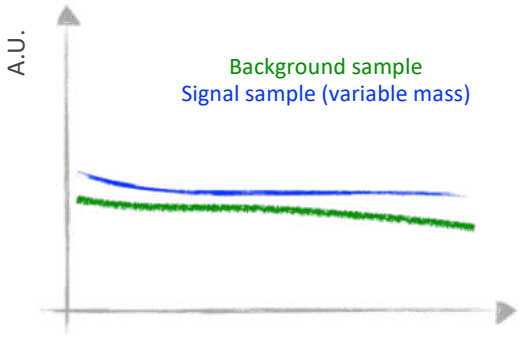

Background jet mass

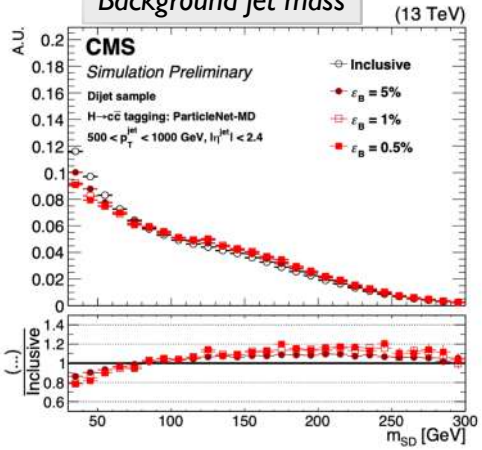

H→cc tagging performance

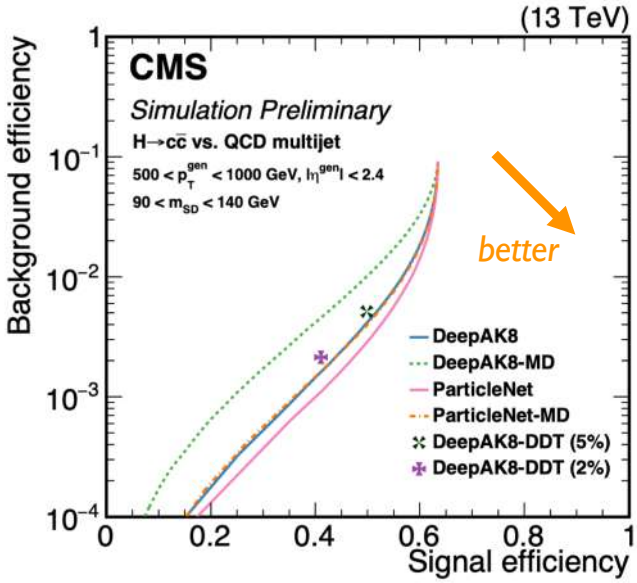

Large-R jet mass regression

Loss function: LogCosh

$$L(y, y^p) = \sum_{i=1}^{n} \log(\cosh(y_i^p - y_i))$$

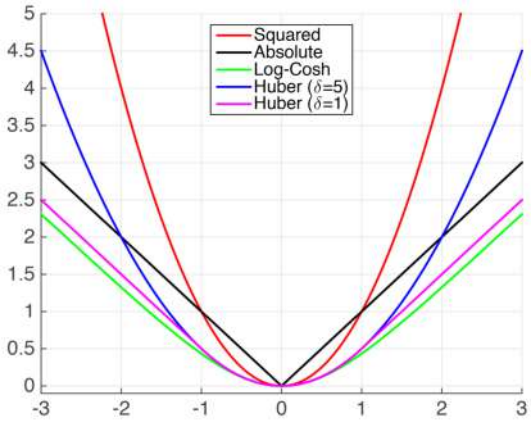

https://www.cs.cornell.edu/courses/cs4780/2015fa/web/lecturenotes/lecturenote10.html

Signal jet mass resolution

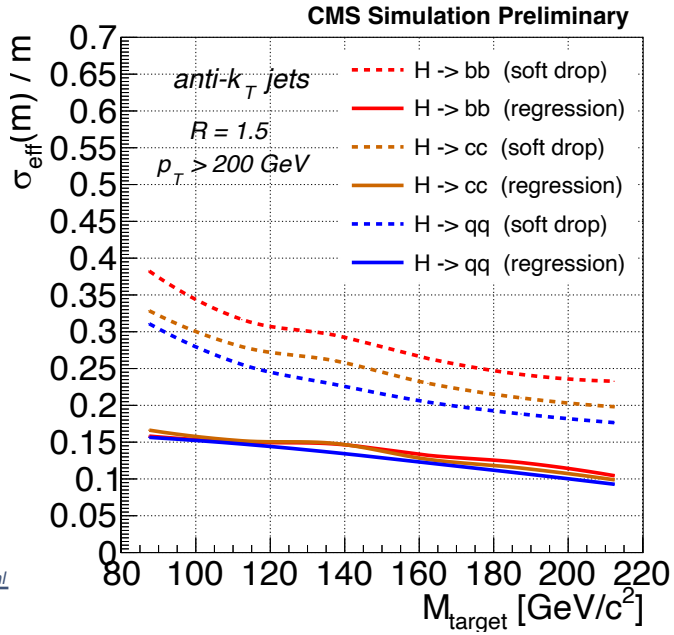

Background jet mass response

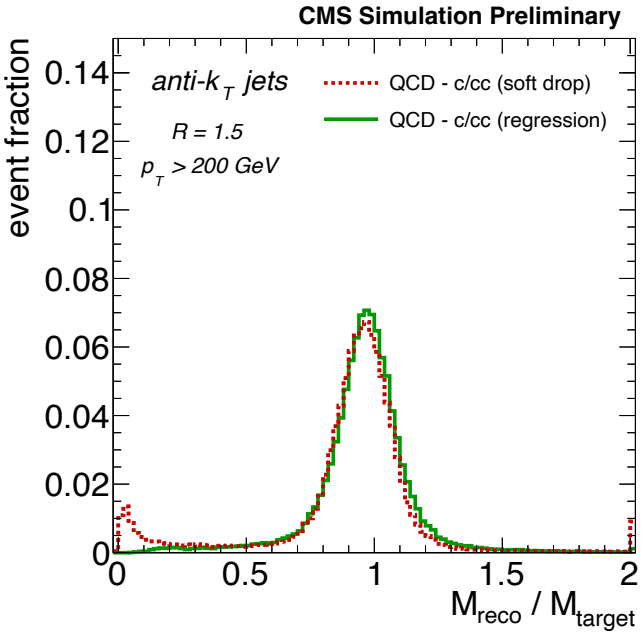

C-tagger ROC curves

2016

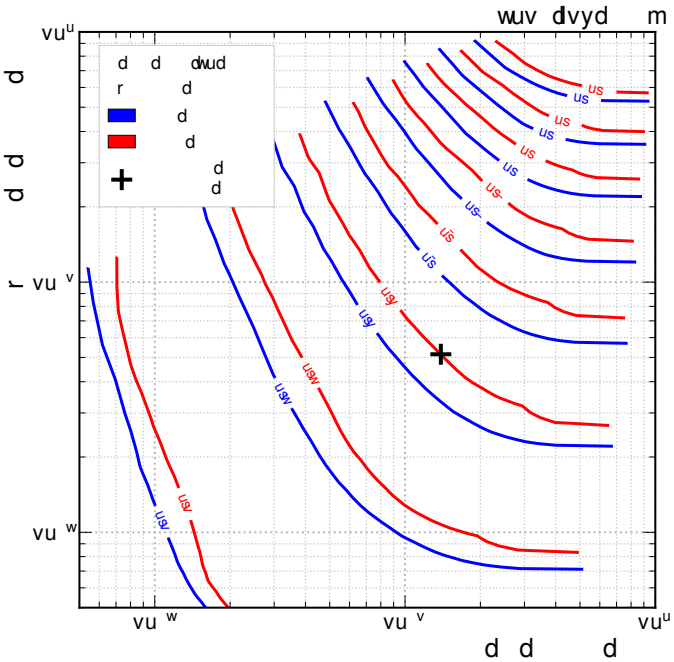

2017

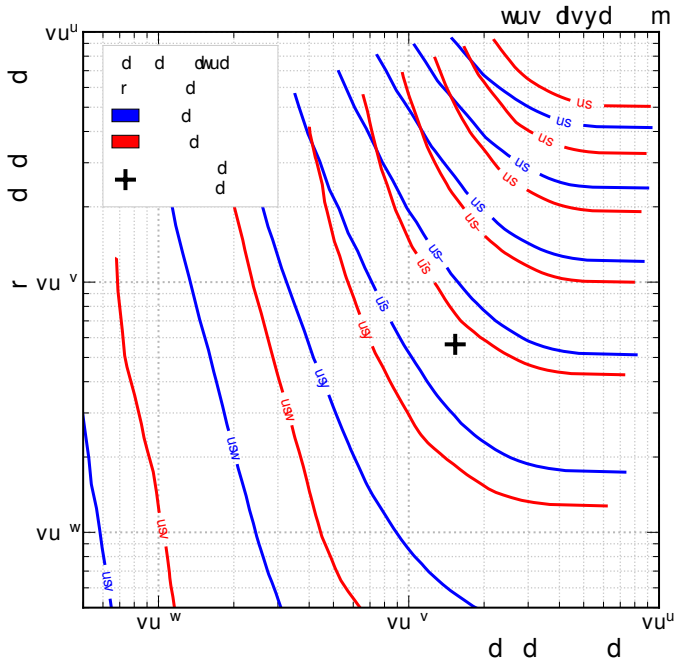

2018

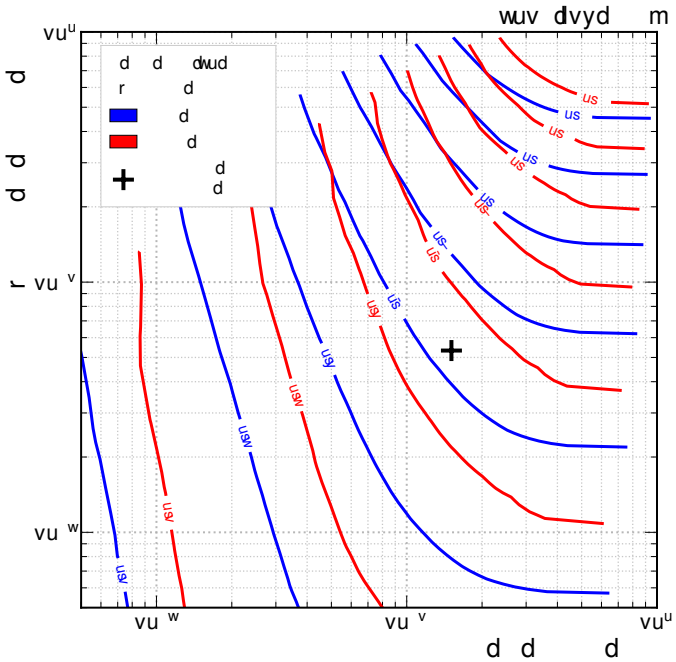

- CMS c-tagging WP: ~40% (c), ~16% (b), ~4% (light)
- ATLAS c-tagging WP [arXiv:2201.11428]: 27% (c), 8% (b), 1.6% (light)

C-jet energy regression and kinematic fit

- 2-lepton Low-$p_T(V)$ category – 60 GeV < $p_T(V)$ < 150 GeV

2016

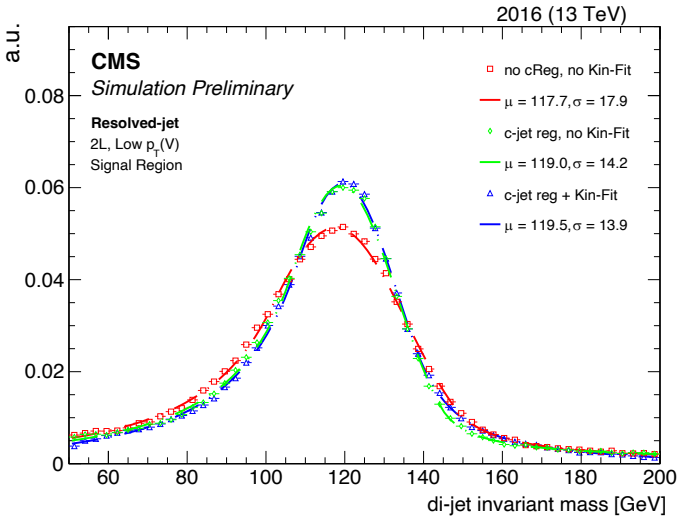

2017

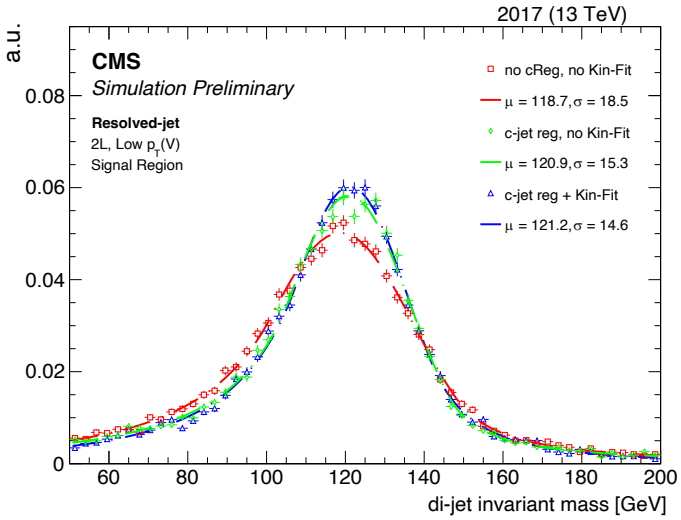

2018

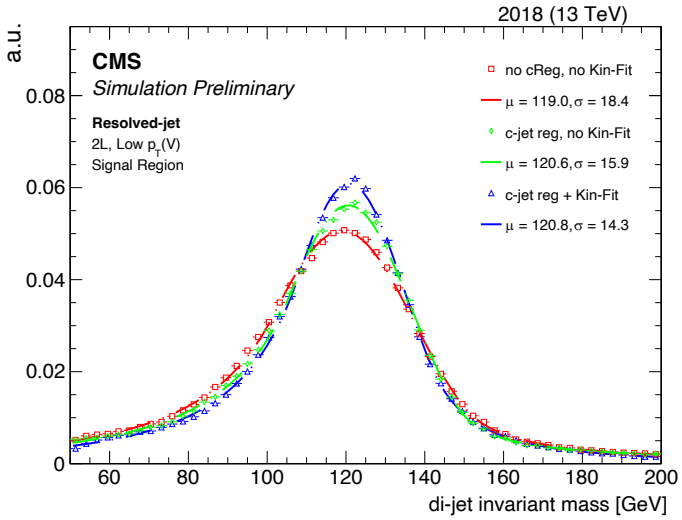

C-jet energy regression and kinematic fit

- 2-lepton High-$p_T(V)$ category – $p_T(V) > 150$ GeV

2016

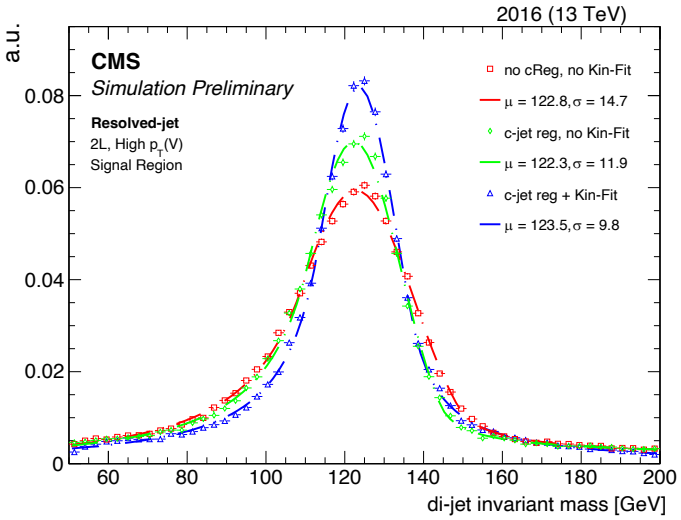

2017

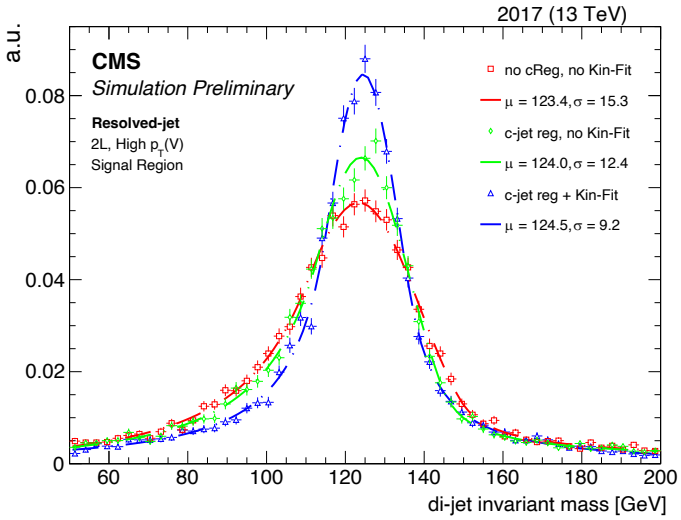

2018

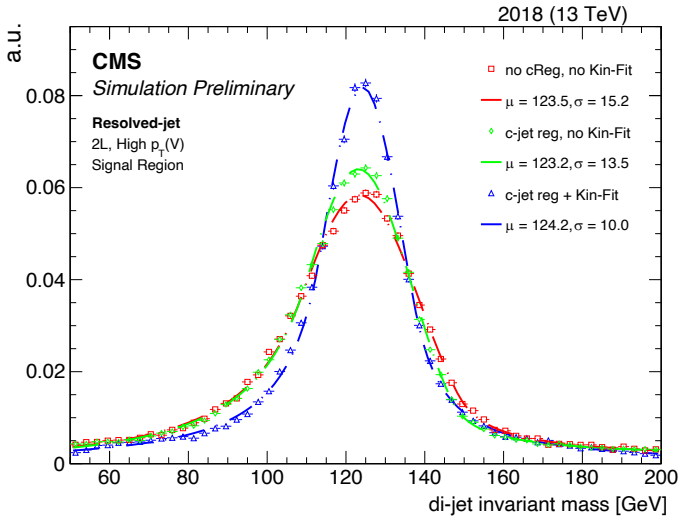

Charm-tagging in the “resolved-jet” topology

DeepJet algorithm – the cornerstone of the VH(cc) resolved-jet topology analysis

- Multiclassifier Deep Neural Network
  - Optimized for AK4-jets
  - Returns the probability for a given jet to be originated by a b-, c- or light-quark
- DNN architecture:
  - Separate 1D CNNs to process three low-level feature classes
    - For each class, concatenate multiple CNNs with decreasing dimensions
    - Compress the features to lower dimensional space
  - RNNs (LSTM type) applied after CNNs
    - Better handles the variable length sequence (PF candidates/SV)
  - Fully connected layer to connect all channels
- Input variables:
  - Properties of PF-candidates
  - Global jet features
  - Secondary vertices
- Output:
  - 6 raw scores

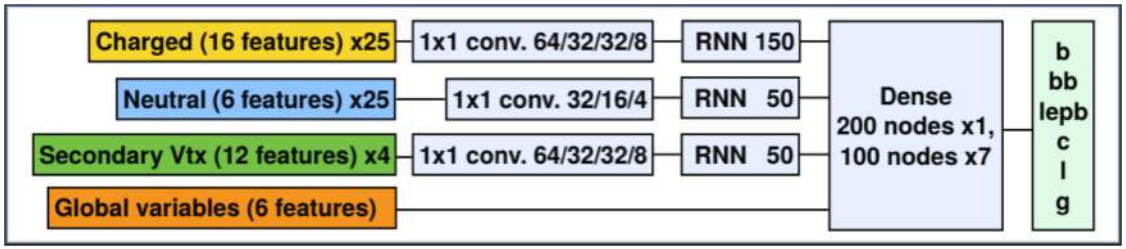

DeepJet architecture (from 2008.10519)

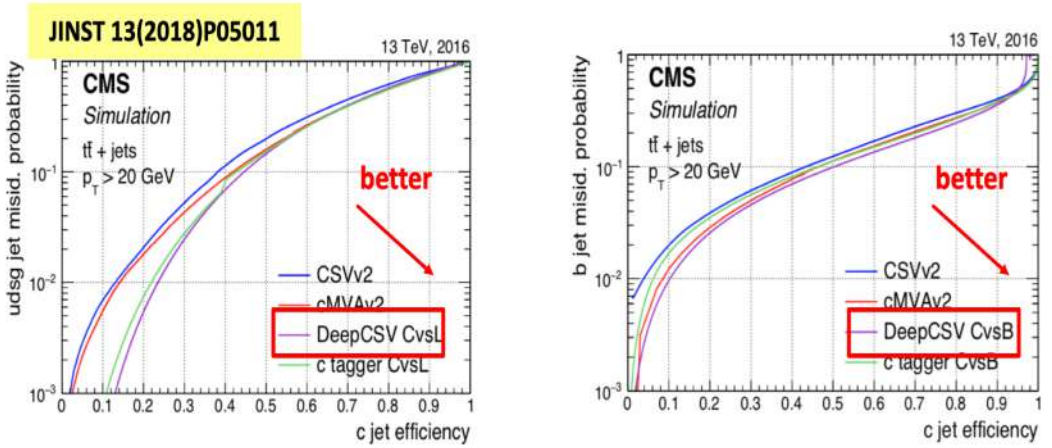

- DeepCSV: predecessor of DeepJet
- Used in the CMS VH(cc) analysis with 2016 data [*JHEP* **2020**,131]

A new method to calibrate charm-taggers

Extraction of reshaping data-to-simulation scale factors

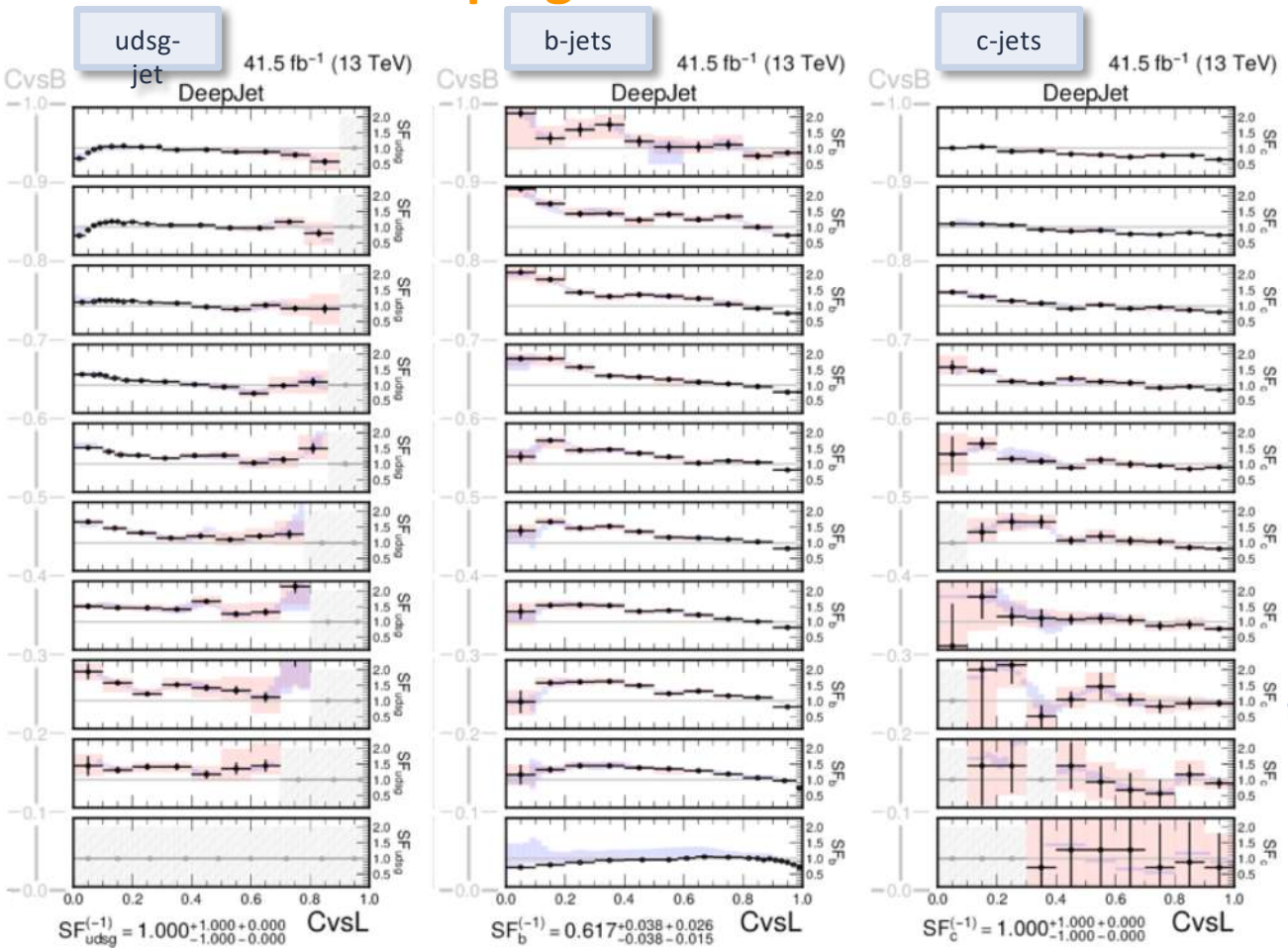

- SFs as a function of CvsL in bins of CvsB
  - Fixed bin width along CvsB and an adaptive binning scheme along CvsL (stat. depending)
  - Total uncertainties (red envelopes) relatively small in the region of interest of the analysis
  - Total uncertainties breakdown
    - Overall smaller than DeepCSV

(from arXiv:2111.03027)

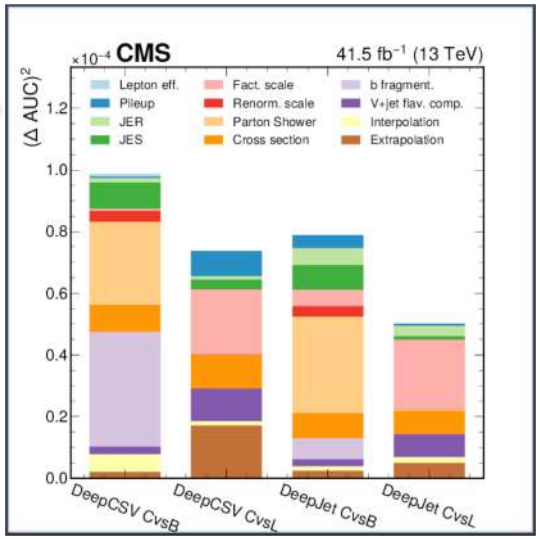

A new method to calibrate charm-taggers

Validate robustness of the SFs derivation

(from arXiv:2111.03027)

- Check possible bias due to the soft-μ-in-jet selection
  - SFs are derived without soft-μ selection
- Check possible bias between semileptonic or di-leptonic tt final states
  - SFs are derived also for the two separate processes independently
- Check possible bias due in the fit:
  - Inject *artificial* SFs to calculate the pulls between the fit result and the injected one

All the checks shown no bias in the SFs derivation

Only di-lep. tt

No soft-μ-in-jet

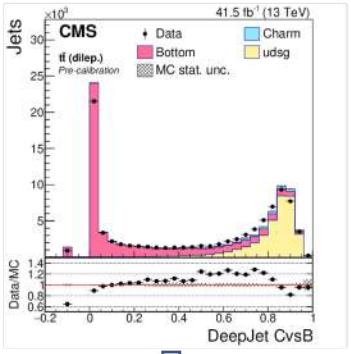

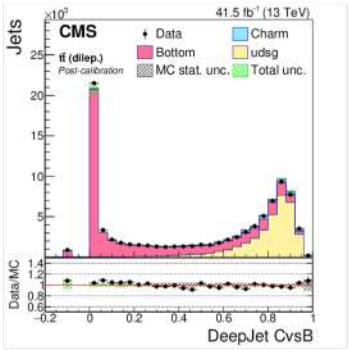

Only semi-lep. tt

No soft-μ-in-jet

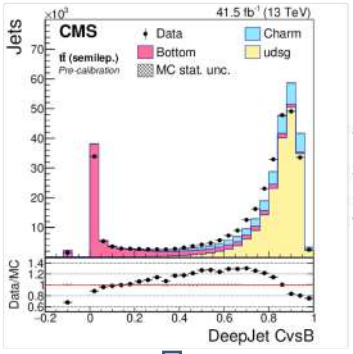

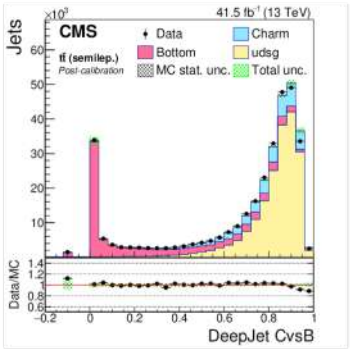

Bias test – pull distribution

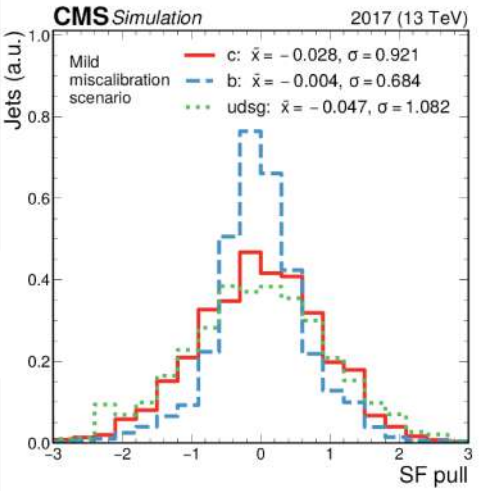

A dedicated charm-jet energy regression

Goal: improve c-jet energy scale and resolution

- Inspired by b-jet energy regression [arXiv:1912.06046]
  - Jet energy measurements not always accurate:
    - loss of neutrinos, hadrons outside jet radius. Effect enhanced in c-jets and b-jet.
  - Dedicated algorithm to determine c-jet energy scale and resolution
  - Algorithm pioneered for the observation of the H→bb decay mode

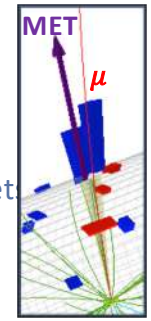

Charm-jet

- Regression performed using DNN architecture:
  - Feed-forward fully connected Deep NN (neurons with Leaky ReLu activation)
    - 6 hidden layers + batch normalization + dropout
  - Trained using c-jets collected from W → cq decays in $t\bar{t}$ MC events
  - Target is represented by p_T(gen)/p_T(reco)

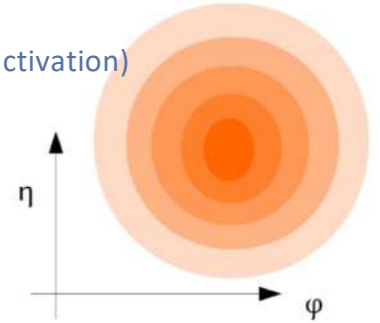

- Input features
  - Total of 43 input variables in input to the network
  - Jets: kinematics, energy fraction, leading+soft-lepton tracks, pile-up, secondary vertexes
  - Jet energy shapes (e.g. energy fraction, etc), jet constituents, p_T(jet)/p_T(lepton)

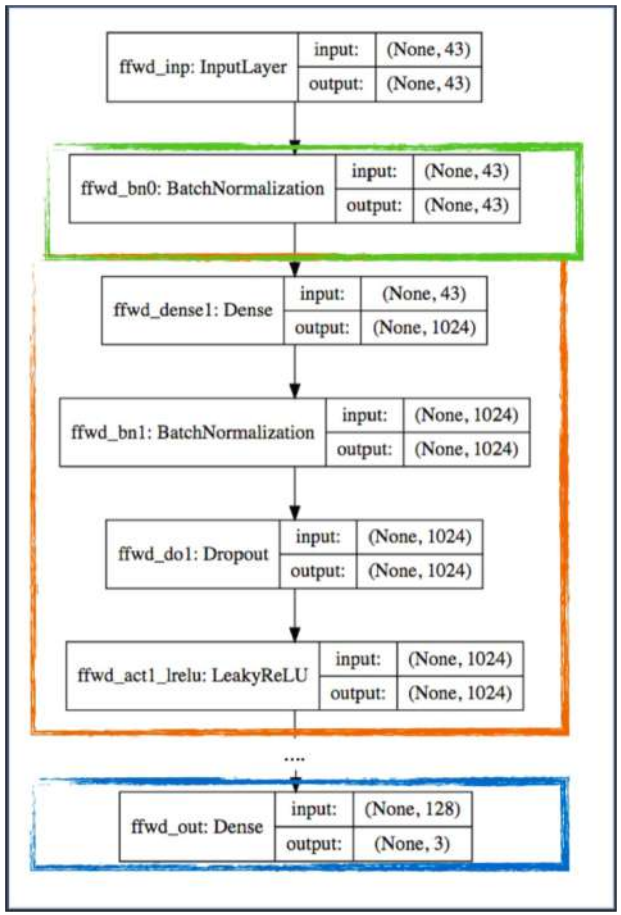

Signal extraction – BDT training in SRs

Variable	Description	0L	1L	2L
$m(H)$	H mass	✓	✓	✓
$p_T(H)$	H transverse momentum	—	✓	✓
$p_T(V)$	vector boson transverse momentum	—	✓	✓
$m_T(V)$	vector boson transverse mass	—	✓	—
p_T^{miss}	missing transverse momentum	✓	✓	—
$p_T(V)/p_T(H)$	ratio between vector boson and H transverse momenta	✓	✓	✓
$CvsL_{max}$	*CvsL* value of the leading *CvsL* jet	✓	✓	✓
$CvsB_{max}$	*CvsB* value of the leading *CvsL* jet	✓	✓	✓
$CvsL_{min}$	*CvsL* value of the subleading *CvsL* jet	✓	✓	✓
$CvsB_{min}$	*CvsB* value of the subleading *CvsL* jet	✓	✓	✓
p_{Tmax}	p_T of the leading *CvsL* jet	✓	✓	✓
p_{Tmin}	p_T of the subleading *CvsL* jet	✓	✓	✓
$\Delta\phi(V,H)$	azimuthal angle between vector boson and H	✓	✓	✓
$\Delta R(j_1,j_2)$	ΔR between leading and subleading *CvsL* jets	—	✓	✓
$\Delta\phi(j_1,j_2)$	azimuthal angle between leading and subleading *CvsL* jets	✓	✓	—
$\Delta\eta(j_1,j_2)$	difference in pseudorapidity between leading and subleading *CvsL* jets	✓	✓	✓
$\Delta\phi(\ell_1,\ell_2)$	azimuthal angle between leading and subleading p_T leptons	—	—	✓
$\Delta\eta(\ell_1,\ell_2)$	difference in pseudorapidity between leading and subleading p_T leptons	—	—	✓
$\Delta\phi(\ell_1,j_1)$	azimuthal angle between leading p_T lepton and leading *CvsL* jet	—	✓	—
$\Delta\phi(\ell_2,j_1)$	azimuthal angle between subleading p_T lepton and leading *CvsL* jet	—	—	✓
$\Delta\phi(\ell_2,j_2)$	azimuthal angle between subleading p_T lepton and subleading *CvsL* jet	—	—	✓
$\Delta\phi(\ell_1,p_T^{miss})$	azimuthal angle between leading p_T lepton and missing transverse momentum	—	✓	—
$\Delta\eta(\ell_1,t)$	difference in pseudorapidity between leading p_T lepton and b-tagged jet from top quark decay	—	✓	—
$\Delta\phi(\ell_1,t)$	azimuthal angle between leading p_T lepton and b-tagged jet from top quark decay	—	✓	—
$\Delta R(\ell_1,t)$	ΔR between leading p_T lepton and b-tagged jet from top quark decay	—	✓	—
$CvsL_t$	*CvsL* value of the b-tagged jet from top quark decay	—	✓	—
$CvsB_t$	*CvsB* value of the b-tagged jet from top quark decay	—	✓	—
$P(b+bb)_t$	*DeepJet prob(b+bb)* value of the b-tagged jet from top quark decay	—	✓	—
$m(t)$	Reconstructed top quark mass	—	✓	—
$N^{aj}_{small\text{-}R}$	Number of small-R additional jets after the FSR subtraction	—	✓	—
$\sigma_{cReg}(j_1)$	leading p_T jet resolution from c-jet energy regression	✓	✓	✓
$\sigma_{cReg}(j_2)$	subleading p_T jet resolution from c-jet energy regression	✓	✓	✓
$\Delta\eta(V,H)\|_{kinfit}$	difference in pseudorapidity between vector boson and H, after kinematic-fit	—	—	✓
$\Delta\phi(V,H)\|_{kinfit}$	azimuthal angle between vector boson and H, after kinematic-fit	—	—	✓
$m(H)\|_{kinfit}$	H mass after kinematic-fit	—	—	✓
$p_T(H)\|_{kinfit}$	H transverse momentum after kinematic-fit	—	—	✓
$p_{Tmax}\|_{kinfit}$	p_T of the leading *CvsL* jet after kinematic-fit	—	—	✓
$p_{Tmin}\|_{kinfit}$	p_T of the subleading *CvsL* jet after kinematic-fit	—	—	✓
$p_T(V)/p_T(H)\|_{kinfit}$	ratio between vector boson and H transverse momenta after kinematic-fit	—	—	✓
$\sigma(H)\|_{kinfit}$	H invariant mass resolution from kinematic fit	—	—	✓

Higgs and vector boson properties

c-tagging score

event kinematics

Kinfit Variables (2L only)

- BDT trained to separate signal from background samples
  - Use combination of kinematic observables and particle flavor variables (tagger informations)
- Separate BDTs trained for each channel and data taking year
  - Separate BDTs trained for high- and low-$p_T(V)$ 2L
  - Variables used dependent on channel
- Reshaped BDT distribution used in SR during final fit

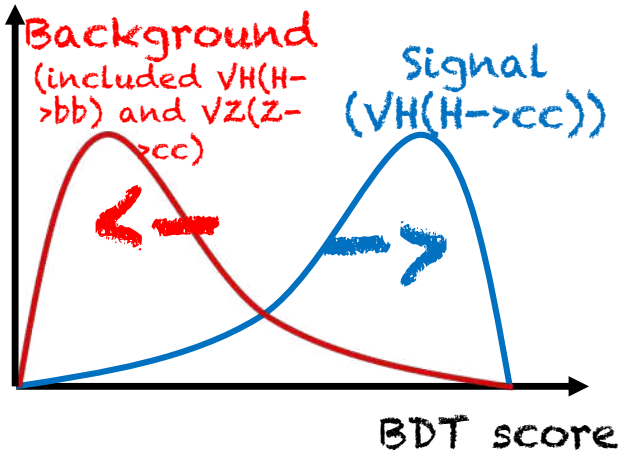

Background estimation – Resolved-jet

- Accurate modeling of jet flavor in V+Jet background is vital for proper signal extraction
  - Separate rate parameters for **V+c, V+b, and V+light** processes (no W+b)
  - Additional rate parameter for $t\bar{t}$ background

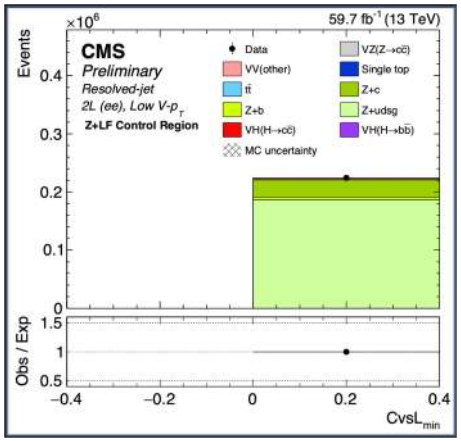

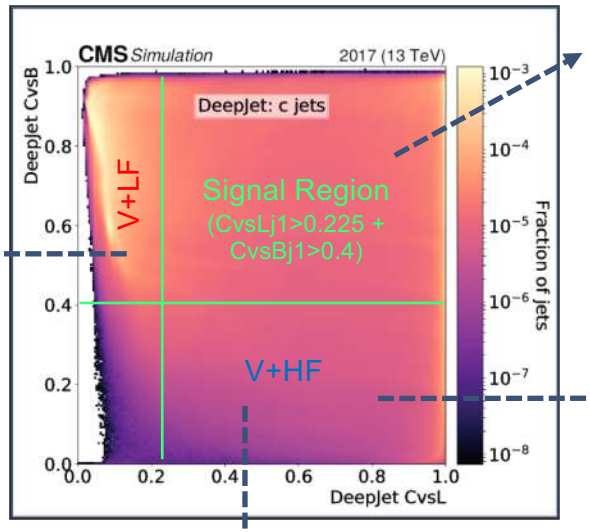

V+CC
Veto m(H)
region

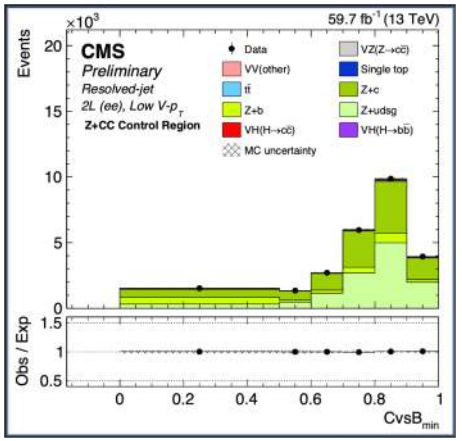

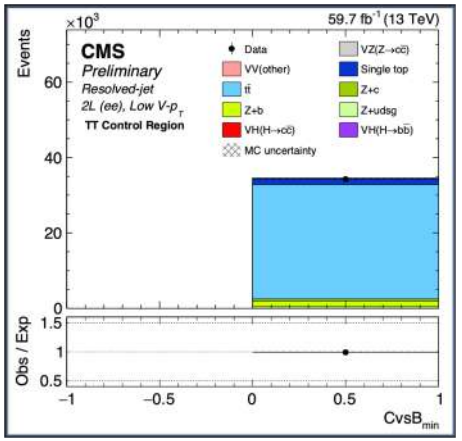

$t\bar{t}$
Invert Z mass (2L)
Require add jet (1L)*
Require add ℓ and jets (0L)

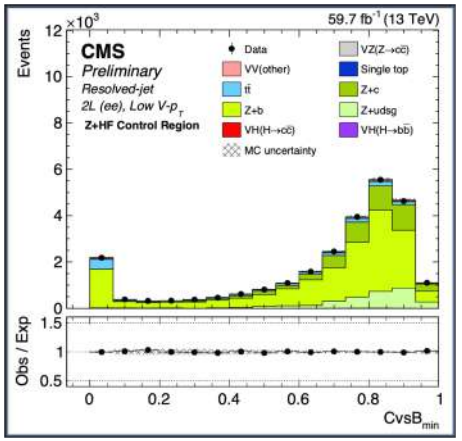

*1L: also require MET<170 GeV to keep orthogonal to 0L $t\bar{t}$ CR

Postfit plots – Signal regions - 2016

- Postfit distribution of the BDT discriminant obtained with the 2016 data
  - 7 Signal regions in each year: 2L(ee/μ) Low-p_T(V) and –High-p_T(V), 1L(e/μ) and 0L

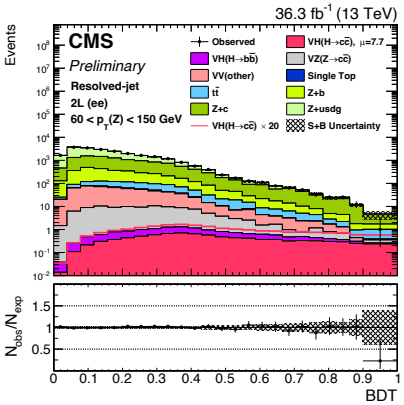

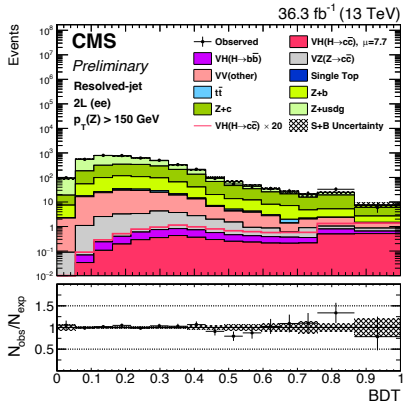

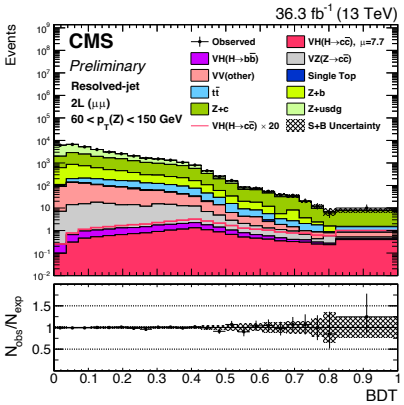

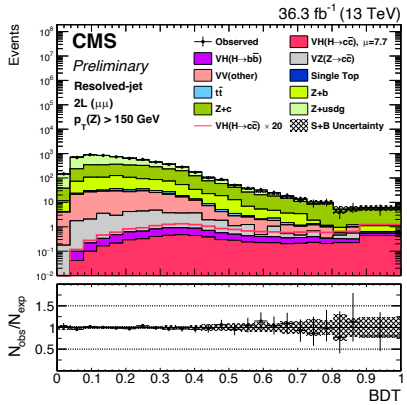

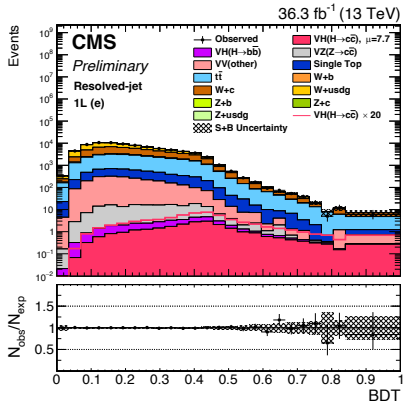

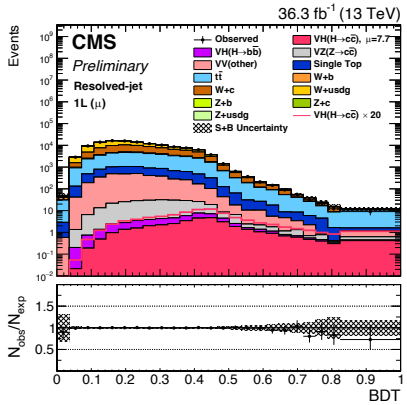

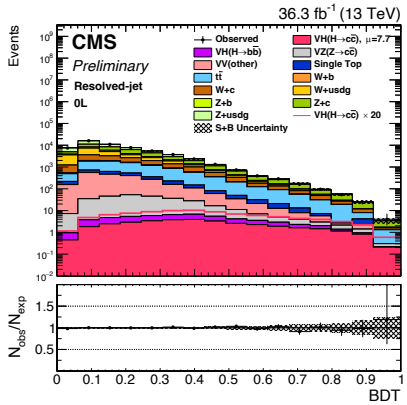

Postfit plots – Signal regions - 2017

- Postfit distribution of the BDT discriminant obtained with the 2017 data
  - 7 Signal regions in each year: 2L(ee/μ) Low-p_T(V) and –High-p_T(V), 1L(e/μ) and 0L

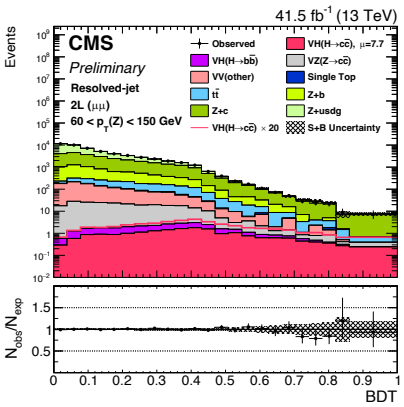

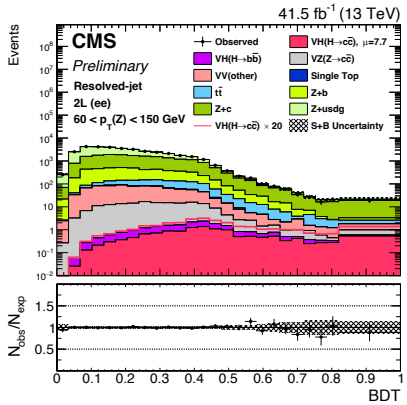

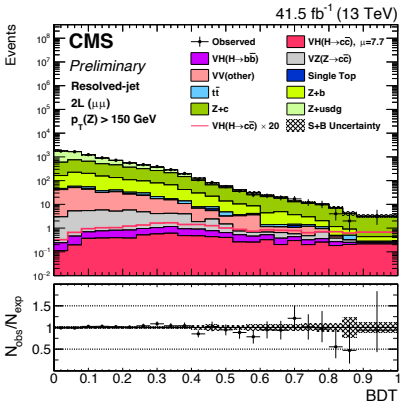

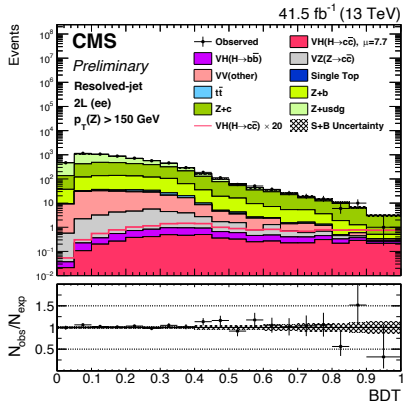

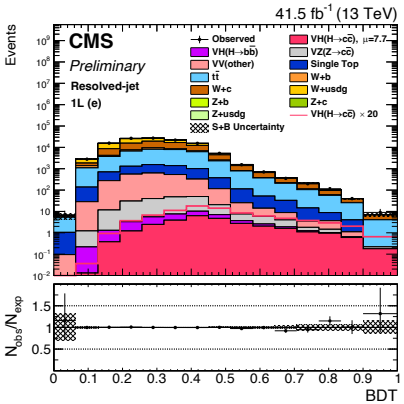

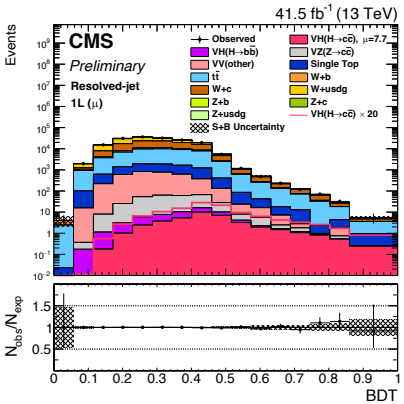

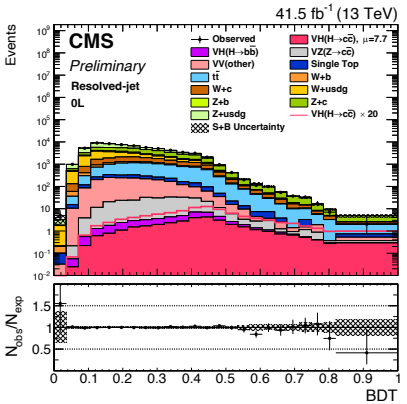

Postfit plots – Signal regions - 2018

- Postfit distribution of the BDT discriminant obtained with the 2018 data
  - 7 Signal regions in each year: 2L(ee/μ) Low-p_T(V) and –High-p_T(V), 1L(e/μ) and 0L

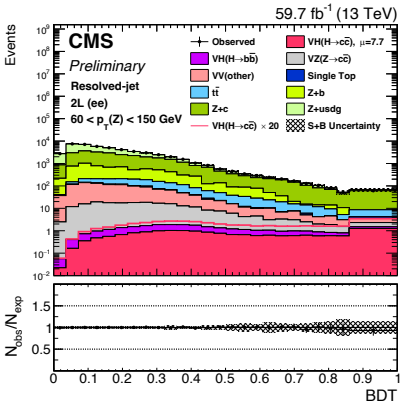

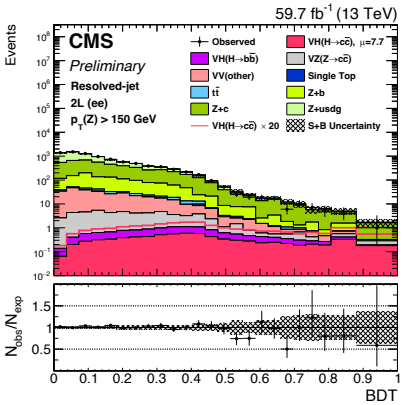

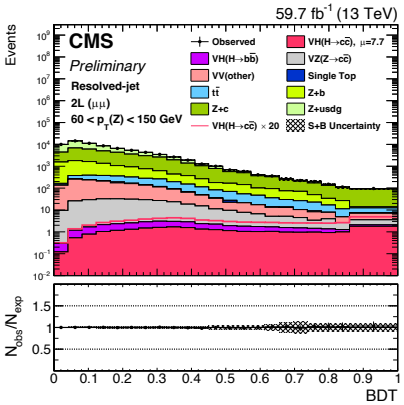

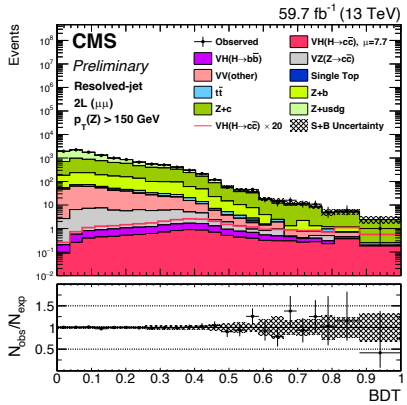

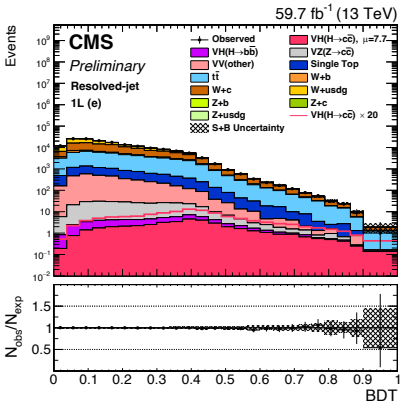

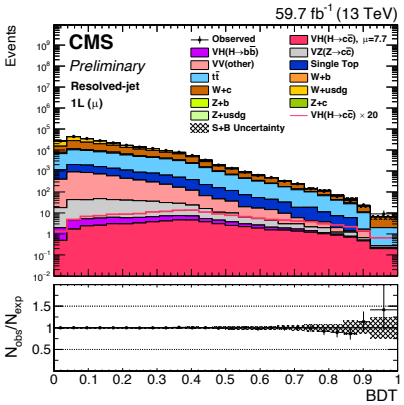

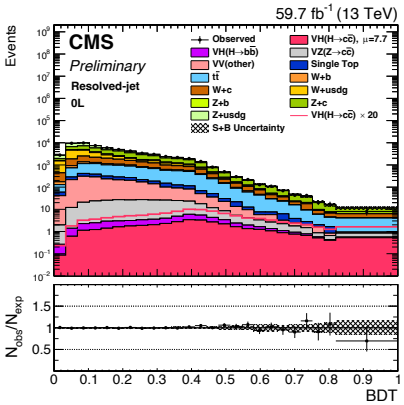

Resolved-jet topology - results

- Resolved-jet – all categories: **ordering the events by $\log_{10}(S/B)$**

VZ(cc)

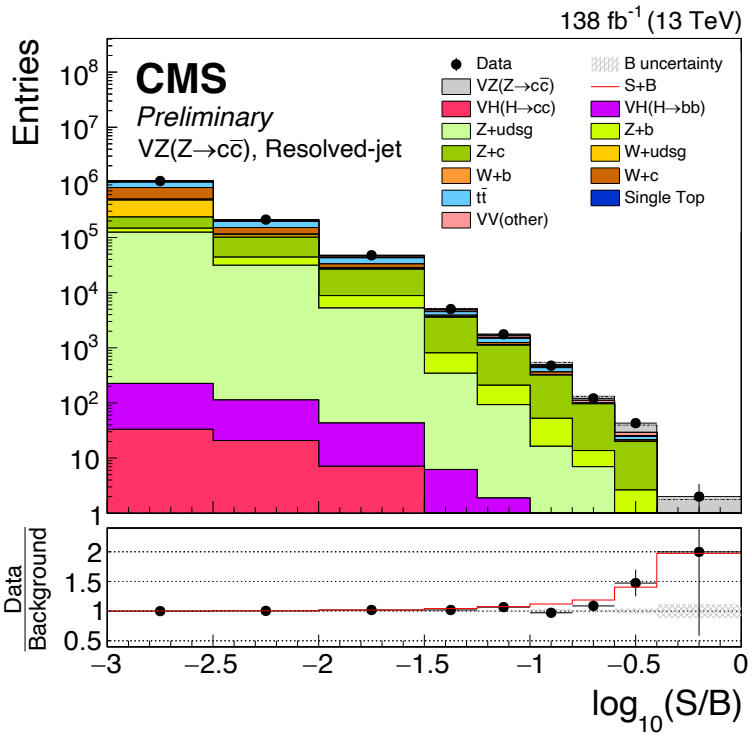

VH(cc)

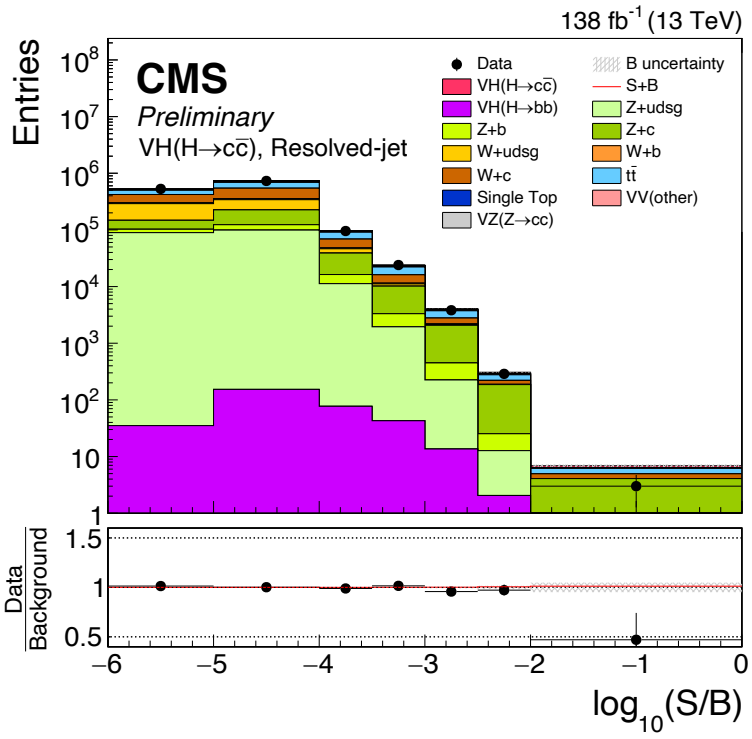

Projection at HL-LHC: Setup

- Extrapolation of the merged-jet analysis to HL-LHC with 3000 fb^{-1} data
- Modifications to the Run 2 analysis to allow for a simultaneous constraint on H → bb and H → cc
  - **addition of 3 categories enriched in H → bb decays**, selected with the ParticleNet bb-tagging discriminant
    - very small (1-2%) overlap of bb and cc categories – events assigned to a unique category
  - **large-R jet p_T threshold lowered from 300 GeV to 200 GeV** – increasing signal acceptance

- Systematic uncertainties adjusted according to the Yellow Report [CERN-2019-007]
  - theoretical uncertainties: reduced by half
  - most experimental uncertainties: scaled down with $\sqrt{\mathcal{L}}$
    - bb and cc tagging efficiencies: constrained by VZ(Z → bb) and VZ(Z → cc) events to ~3% and ~5%
    - misidentification of H → bb as H → cc: a prominent uncertainty on H → cc measurement at HL-LHC
      - assumed to be reduced from ~100% (Run 2) to 20% in the projection

A charming journey

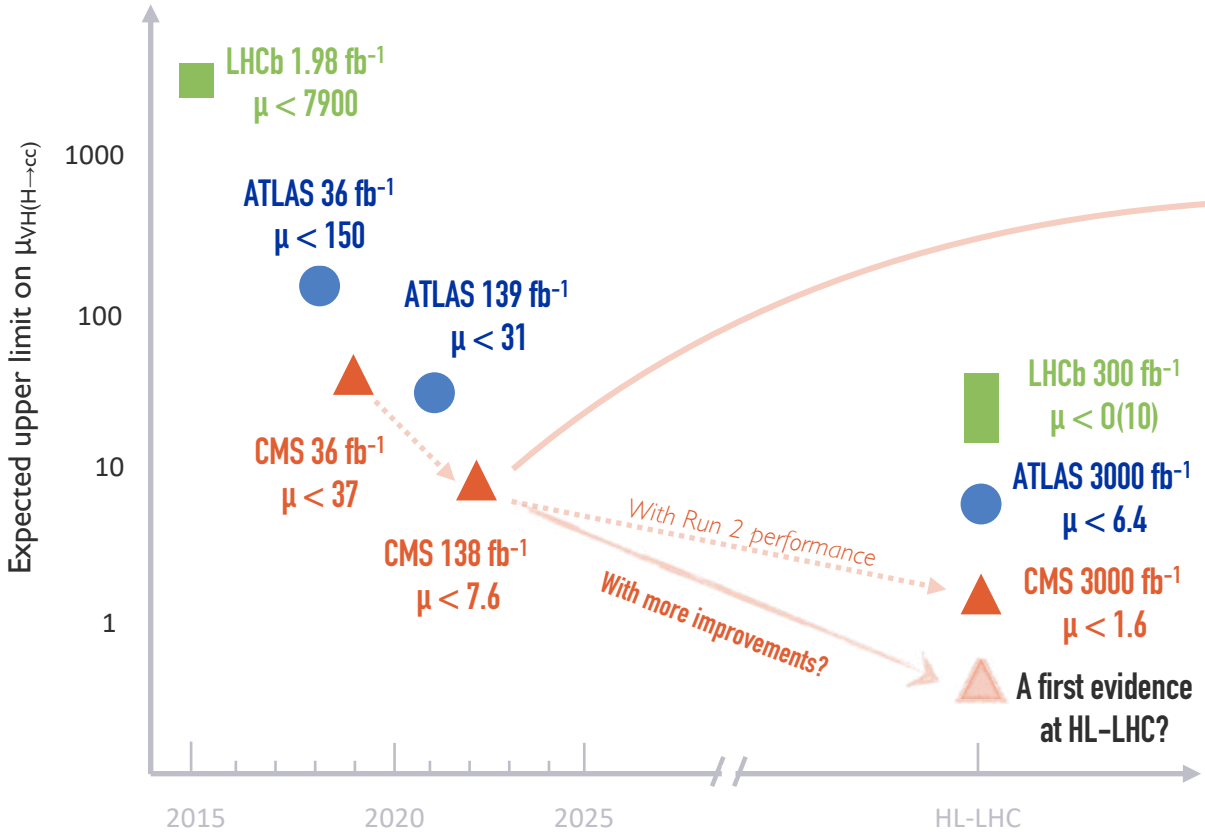

From $\mathcal{O}(1000)$ to $\mathcal{O}(100)$ to $\mathcal{O}(10)$ in ~5 years.
A combined effort and creativity from instrumentation, physics objects and analysis techniques!

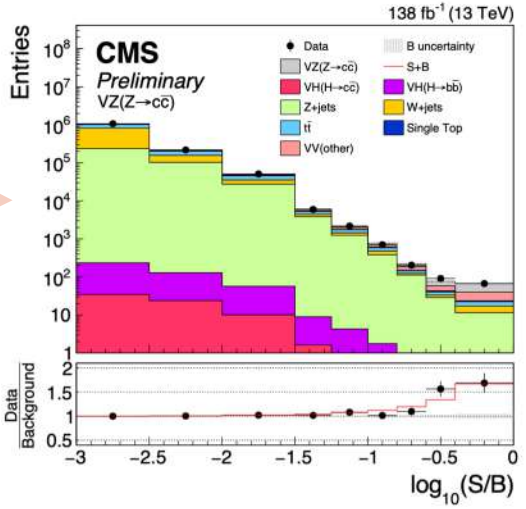

First observation of $Z \to cc$ at a hadron collider!
Opening a new era for future explorations.

- More channels: ttH(cc), VBF H(cc), indirect constraints, etc.
- Improvements in advanced analysis techniques (e.g., Deep Learning) and instrumentation (e.g., tracker)
- Reduction of systematic uncertainties: c-tagging, event modeling, theoretical uncertainties, …

A charming journey ahead!